KYOTO UNIVERSITY

GRADUATE SCHOOL OF GLOBAL ENVIRONMENTAL STUDIES

DOCTORAL THESIS

# Simulating the future of the Ifugao rice terraces through observations of the past

by:

**Ian Estacio**

A thesis submitted in partial fulfilment of the requirements for the degree of Doctor in Philosophy in Environmental Management

2023

# Abstract

The past century has seen global rapid land use/cover changes (LUCC) due to the need of accommodating the rapid population increase of human society. Mountainous agricultural landscapes around the world have all in common experienced agricultural abandonment and subsequently afforestation due to migration of rural farmers to the urban areas. As an example, in the heritage landscape of Ifugao rice terraces in the Philippines, agricultural occurs due to a combination of social drivers such as lack of farmland successors and environmental drivers such as lack of water supply. With this ongoing problem in the Ifugao rice terraces, it is important to formulate policies based on information of past changes, the driving factors, and the prediction of future status. Methods that utilize spatial data such as remote sensing, GIS, spatial regression, and agent-based modeling can provide holistic information for formulating policies.

This thesis aims to characterize the dynamics of the land cover in the Ifugao rice terraces to propose policies for the mitigation of agricultural abandonment. Specifically, the research aims to establish a Geomatics framework for informing environmental management, observe the past land cover transitions and paddy field dynamics, identify the spatial and non-spatial drivers of agricultural abandonment, and simulate the impact of policies on the future status of the agricultural landscape. The current research started with the analysis of the past land cover transitions and paddy field dynamics in the study area from 1990 to 2020. This was then followed by the development of a statistical model of agricultural abandonment that utilizes spatial and non-spatial drivers. Finally, Agent-Based Modelling was implemented to simulate the impact of combinations of socio-environmental policies to mitigate future agricultural abandonment.

Written as a position paper, Chapter 2 sets the general methodological workflow of the thesis by establishing a Geomatics framework that aims to holistically inform decision-making for environmental management. This framework is composed of three main tasks: data acquisition, spatial analysis, and Geosimulation. The framework can be utilized as an approach for utilizing spatial data of the environment with the purpose of "predicting the future through observations of the past". Two case studies of research projects that utilized the general Geomatics framework were presented to provide sample applications of the Geomatics

framework for aiding environmental management. Three implications of the Geomatics framework were discussed: the widening of the environmental application of Geomatics, the establishment of a methodological workflow for informing environmental management, and the enhancement of the collaboration between Geosimulation and other spatial science fields.

The analysis of past land cover transitions in Chapter 3 revealed that paddy fields turning into forests typically undergo a two-step process of transitioning first into low vegetation before transitioning into forests, which is unlike in previous land cover change studies in mountainous agricultural landscapes that observed the occurrence of afforestation due to abandonment of paddy fields. Transitions between low vegetation and forest were also observed to be regularly occurring at high rates, which may be attributed to the traditional practices of the local people such as tree-cutting and swidden farming. Analysis of paddy field dynamics showed that agricultural abandonment has been continuously occurring in the landscape. Although recultivation of paddy fields occurred from 2000 to 2010, permanent abandonment has increased again after this period. It was also found that the abundance of low vegetation cover has a significant inverse relationship with subsequent permanent abandonment of paddy fields, which coincides with previous studies showing that decreasing water yield from afforestation contributes to the abandonment of paddy fields.

To identify the spatial and non-spatial drivers of agricultural abandonment, a spatial statistical model was developed in Chapter 4 that integrates logistic and linear models in a single modeling framework to simulate LULC changes. The logistic model processes explanatory spatial variables to generate a probability map, while the linear model handles explanatory non-spatial variables to generate a global probability threshold. Results of the statistical modeling showed that slope, cosine aspect, quickflow, distance to town center, distance to road, world heritage site status, forest density, low vegetation density, and paddy field density were significant determinants of the local probabilities of agricultural abandonment while total forest area, five-year average precipitation, and average daily maximum temperature were significant determinants of the global probabilities of agricultural abandonment.

The impacts of combinations of socio-environmental policies to the spatial patterns of paddy fields were simulated by implementing agent-based modeling in Chapter 5. The simulation results showed that providing aid in restoring eroded terraces mitigates almost half of the agricultural abandonment. Meanwhile, increasing the ratio of youth valuing the terraces

and providing subsidy to farm households showed only a small impact on mitigating agricultural abandonment. Thus, it is recommended that the local government of Banaue should just focus on providing aid in restoring eroded terraces for effectively mitigating agricultural abandonment. The results of the simulations also imply that environmental drivers such as erosion have more effect on the agricultural abandonment than the social drivers such as lack of successors.

Chapter 6 synthesizes the research outputs of the previous chapters. The results of this thesis provide key information for mitigating the agricultural abandonment in the Ifugao rice terraces. First, the monitoring of past changes addressed the lack of accurate maps and quantification of the amount of abandonment. Second, the identification of significant drivers of agricultural abandonment in the Ifugao rice terraces provides landscape planners with an understanding of the phenomenon of agricultural abandonment. Lastly, simulations from the developed agent-based model identified the appropriate policies to implement for mitigating agricultural abandonment. The findings from this thesis provide new information for planning mountainous agricultural landscapes such as the consideration of the land-transition feedback loop that further promotes agricultural abandonment and the dynamics of farm succession and inheritance. Meanwhile, the methodological frameworks implemented can be adopted by other studies to provide solutions to environmental issues.

**Keywords:** Remote Sensing, GIS, Logistic regression, Spatial modeling, Agent-Based Modeling, Scenario simulation, Ifugao rice terraces, Mountainous agricultural landscape

# Table of Contents

# List of Figures

# List of Tables

# List of Abbreviations

| | |
|---|---|
| ABM | Agent-Based Model |
| ADP | Absolute Deviation Percentages |
| CA | Cellular Automata |
| CAP | Characterization and Parametrization framework |
| DEM | Digital Elevation Model |
| GA | Genetic Algorithm |
| GEE | Google Earth Engine |
| GIAHS | Globally Important Agricultural Heritage Systems |
| GIS | Geographic Information System |
| GNSS | Global Navigation Satellite Systems |
| HYSOG | Global Hydrologic Soil Groups |
| IRTCHO | Ifugao Rice Terraces Cultural Heritage Office |
| LiDAR | Light Detection and Ranging |
| LUCC | Land Use/Cover Change |
| NIR | Near Infrared |
| OA | Overall Accuracy |
| ODD | Overview, Design concepts, and Details |
| PA | Producer's Accuracy |
| PCA | Principal Components Analysis |
| POM | Pattern-oriented modeling |
| RF | Random Forest |
| ROC | Relative Operating Characteristic |
| SES | Socio-Ecological Systems |
| SRTM | Shuttle Radar Topography Mission |
| SWIR | Short-wave Infrared |
| UA | User's Accuracy |
| UNESCO | United Nations Educational, Scientific and Cultural Organization |

# Chapter 1:

# Introduction

## 1.1. Land cover change as a global phenomenon

Land use/cover change (LUCC) continuously occur on the surface of the earth as a result of complex interactions between socio-economic and environmental drivers (Geist et al., 2006; He et al., 2022; Mas et al., 2014; Mitsuda & Ito, 2011; Munroe & Müller, 2007). In the current age of globalization, LUCC typically occur as urban expansion where non-urban land use types are converted for urban use (Güneralp & Seto, 2013; Seto et al., 2011; van Vliet, 2019). Along with continuous urban expansion, globalization also drives the occurrence of other LUCC such as agricultural abandonment, deforestation, and reclamation (W. Cao et al., 2021; Hou et al., 2021; Phiri et al., 2019; van der Zanden et al., 2017; Wu et al., 2016; Xystrakis et al., 2017). As human society continuously interacts with the global environment to acquire its needs, hence forming perpetual socio-ecological systems (SES), it is expected that human activities will continuously cause impacts on the environment leading to recurring LUCC (X. Li et al., 2017; Synes et al., 2019).

However, with the modern ever-changing world, some LUCC may occur at an alarming rate, leading to various environmental consequences that can be detrimental if left in its current trend. For example, urbanization causes conversion of natural habitats leading to loss of biodiversity (McDonald et al., 2019), while increase in urban land use is projected to increase the hours of discomfort in cities (Vinayak et al., 2022; B. Yang et al., 2019) Agricultural abandonment has been shown to promote soil erosion (Cerdà et al., 2018) and decrease water yield (Soriano & Herath, 2018), which results to a feedback loop of further agricultural abandonment (Estacio et al., 2022). On the other hand, deforestation can decrease access to clean drinking water (Mapulanga & Naito, 2019), increase dry season fire (Butt et al., 2021), and induce global warming (Lawrence & Vandecar, 2014). Overall, changes in LUCCs cause alterations in ecosystem services leading to environmental problems (B. Li et al., 2016; Y. Liu et al., 2020; Wang et al., 2018; Zhang et al., 2019).

## 1.2. Deteriorating mountainous agricultural landscapes

Mountainous agricultural landscapes feature strong human-environment interactions that form socio-ecological systems, where local communities alter and nurture the environment while the environment provides food, resources, and livelihoods for the community (Aguilar et al., 2021; Y. Cao et al., 2013; Pôças et al., 2011; Tarolli & Straffelini, 2020). In addition to crops and wood, these landscapes also provide bundles of ecosystem services (Burkhard et al., 2015; Peng et al., 2019) such as water regulating services (Arnáez et al., 2015; Soriano & Herath, 2018). Some of these landscapes are also designated as Globally Important Agricultural Heritage Systems (GIAHS) such as the Hani Rice Terraces in China, Takachihogo-Shiibayama site in Japan, and Ifugao Rice Terraces in the Philippines (FAO, 2021). Hence, these landscapes also provide cultural identity (Tarolli et al., 2014; Tilliger et al., 2015) and opportunities for tourism (Terkenli et al., 2019; Tian et al., 2016).

As part of the direct interaction between the local community and the environment such as farming, fallowing, woodcutting, and tree planting, mountainous agricultural landscapes experience frequent transitions in land cover (Liang et al., 2020; Minta et al., 2018; Xystrakis et al., 2017). These changes can alter ecosystem services (Locatelli et al., 2017; Vidal-Legaz et al., 2013), hence it is vital to analyze the land cover changes in these landscapes for land use planning.

## 1.3. The Ifugao rice terraces: a world heritage in danger

The Ifugao Rice Terraces is a mountainous agricultural landscape in the Ifugao province, Philippines recognized for its five clusters of terraces being United Nations Educational, Scientific and Cultural Organization (UNESCO) world heritage sites (SITMo, 2008) (Fig. 1.1). Built with minimal equipment, largely manual (by hand), by the ancestors of the Igorot people, the public occasionally calls the terraces the "Eighth Wonder of the World." As a product of socioeconomic and environmental drivers, the rice terraces have become a critical part of the supporting ecosystems of Ifugao communities and beyond (Camacho et al., 2016; De Luna Habito & Ealdama, 2019).

Fig. 1.1 The Batad rice terrace cluster, one of the five inscribed world heritage cluster in the Ifugao rice terraces (photo taken from fieldwork)

The terraced landscape containing the five heritage clusters is commonly known as *Ifugao rice terraces* by the local people but is also interchanged as *Banaue rice terraces* by Filipinos (Cagat, 2018). However, this can is a misconception as the Banaue rice terraces refer only to the terraces in the municipality of Banaue. This interchange of name can be attributed to the popularity of the Banaue rice terraces as a tourism site. Meanwhile, the UNSECO actually refers to the world heritage landscape as *the Rice Terraces of the Philippine Cordilleras* (UNESCO, n.d.). The five clusters of terraces inscribed as world heritage sites are the following (Fig. 1.3):

1. The Nagacadan terrace cluster in the municipality of Kiangan,
2. The Hungduan terrace cluster that covers the whole municipality of Hungduan,
3. The Central Mayoyao terrace cluster in the municipality of Mayoyao,
4. The Bangaan terrace cluster in the municipality of Banaue, and
5. The Batad terrace cluster in the municipality of Banaue (Fig. 1.1).
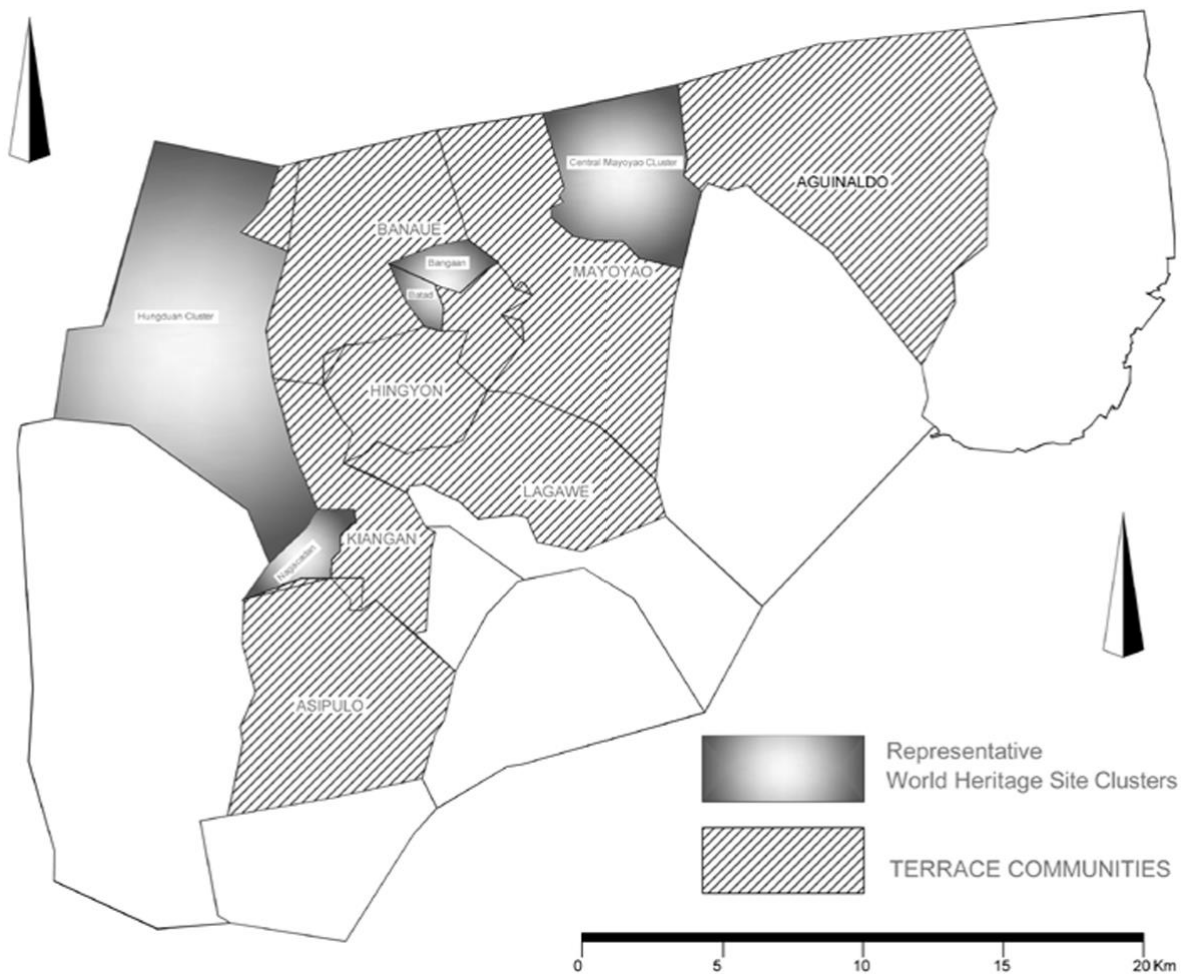
Fig. 1.2 A map showing the locations of the five inscribed heritage cluster in the Ifugao rice terraces (SITMo, 2008)

The landscape is classified as Climate Type III, one of the Corona's four climate types that are classified based on monthly rainfall. A place is classified as a Climate Type III if there is no pronounced maximum rain period. At the same time, the dry season lasts for about one to three months, starting at the earliest in December and ending at the latest in May (Ducusin et al., 2019; PAGASA, n.d.). Agriculture is mainly the source of sustenance and income of the local people in the Ifugao rice terraces, but the tourism industry also generates a large part of the local government's revenue (Calderon et al., 2009).

Soil types within the study area range from moderately-high runoff potential to high runoff potential. In conjunction with the high slopes, the soil makes the entire area susceptible to erosion. In fact, farmers have referred to the erosion of their agricultural lands as a critical

reason for abandoning their lands (Calderon et al., 2009). Scholars have also cited water availability as another critical cause of land abandonment, referring to an insufficient water supply from streams during the dry season (Calderon et al., 2009).

Aside from sowing, transplanting, and harvesting in the rice terraces, the local people also practice swidden farming, fallowing, wood cutting, and seedling planting (Aguilar et al., 2021; Camacho et al., 2016; Castonguay et al., 2016). Hence, the landscape undergoes frequent land cover transitions as part of the socio-ecological system in the landscape. With the rise of tourism and urbanization in the province, several people have emigrated, leaving some of the paddy fields permanently abandoned (Bantayan et al., 2012). In 2001, the Ifugao rice terraces was included in UNESCO's List of World Heritage in Danger due to increasing degradation and abandonment of the agricultural lands (UNESCO, n.d.). It has already been lifted from the list in 2012, but it still faces continuous abandonment in the present (FAO, 2018). Because of the rapid land cover changes and ongoing agricultural abandonment, the landscape of Ifugao rice terraces is ideal for investigating the socio-ecological system in a mountainous agricultural landscape.

As a case study, a watershed in Banaue municipality covering the Ifugao rice terraces was designated as a study area. (Fig. 1.3). A watershed was designated as the extent of analysis because of the assumption that hydrological processes in the landscape provide relations between land cover types (Soriano & Herath, 2018). For this study, the watershed being monitored is referred to as the Bangaan watershed. The Bangaan watershed has an area of 5,713 ha with the highest point being 2,111 m above mean sea level. The watershed mainly consists of forest areas, with other abundant land use types as shrublands, grasslands, rice field terraces, and swidden fields. Built-up areas are abundant mainly in the town center, with their sprawls scattered around the terraces (Acabado, 2012; McKay, 2003). In general, its topography widely varies, with an elevation range of 1,431 m and slopes reaching angles of 65°.
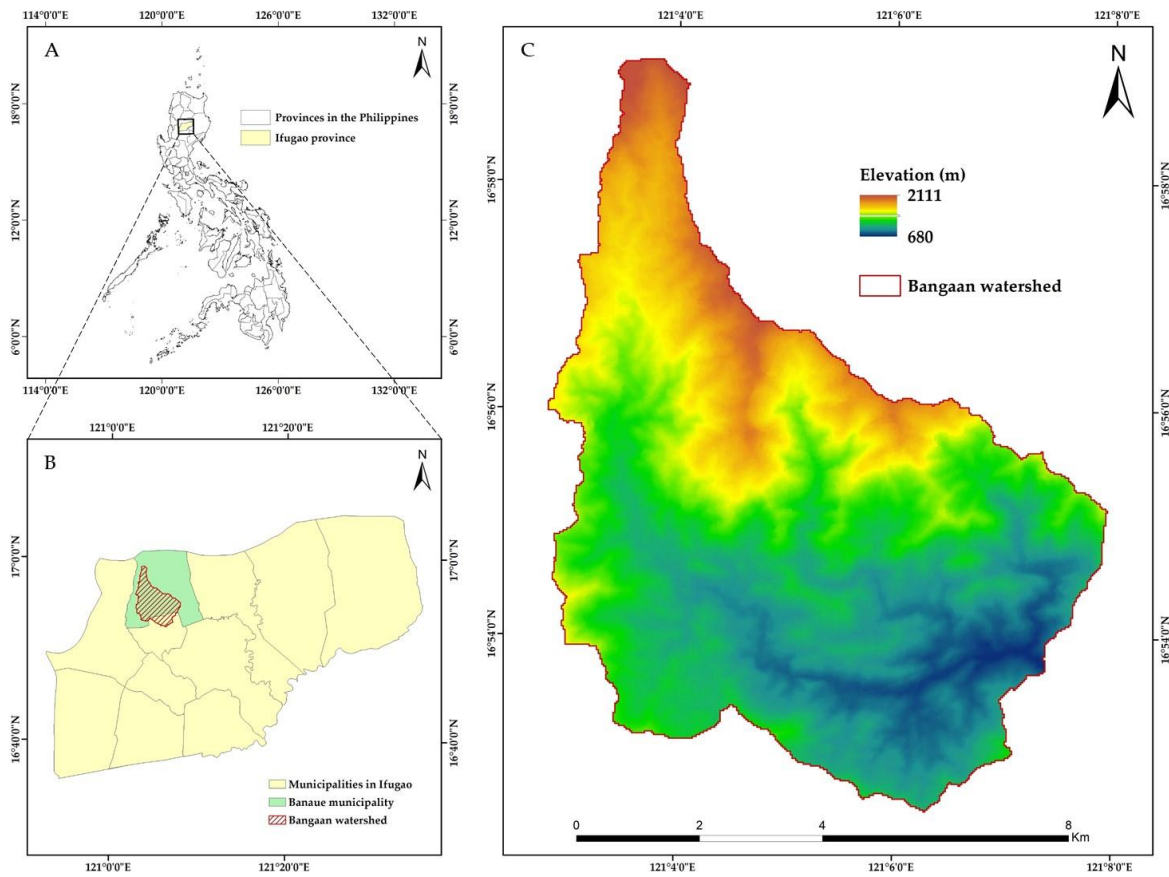
Fig. 1.3 The location of the Bangaan watershed: (A) The location of Ifugao province in the Philippines; (B) The location of the Bangaan watershed and Banaue municipality in the Ifugao province; (C) The topography in the Bangaan watershed.

## 1.4. Research motivations

As a landscape for five world heritage sites, it is imperative that the Ifugao rice terraces be conserved. Not only is it of significance to pass down this heritage to the future generations but the agricultural landscape also provides an abundance of ecosystem services that not only benefits the local Ifugao people but also downstream residents (Avtar et al., 2019; Soriano & Herath, 2018; Tilliger et al., 2015).

Although several estimates have been given for the land abandonment in the Ifugao rice terraces, there has not been any previous effort in mapping the agricultural lands to provide accurate values of the abandonment through time. It is important to produce maps of landscapes that are subject of environmental management not just for quantitative estimates but also for essential spatial analysis. At the same time, drivers of the abandonment may already be

6

understood based on interviews with farmers and environmental analysis in previous studies, but the combination of spatial factors that dictate the location of the abandoned fields is still unknown. Lastly, it is important that the results of monitored land cover changes and analysis of driving factors be used to provide informed decisions on making policies. An approach to accomplish this is to implement Agent-Based modeling that utilizes social-ecological inputs and processes to show emerging status of the agricultural lands.

On a global scale, the research on the Ifugao rice terraces will provide new information for studies of mountainous agricultural landscapes. As a unique socio-ecological system that features tight human-environment interactions and frequent land cover transitions, further research of these landscapes can provide new insights into planning and managing these landscapes. The thesis can thus aid in future landscape planning of mountainous agricultural landscapes.

Lastly, methodological frameworks that will be developed to obtain essential research outputs will provide novel approaches for informing environmental management actions and addressing environmental problems. As observations of the past trend, identification of driving factors, and simulation of the future status of the agricultural abandonment is planned to be implemented, it is expected that an abundance of spatial data will be utilized in this thesis. In general, this thesis will contribute to the advancement of Geomatics.

## 1.5. Research objectives

The main objective of this study is to analyze and understand the dynamics of agricultural abandonment in the mountainous agricultural landscape of Ifugao rice terraces by looking into its past trend, driving factors, and future status so that policies and management strategies can be proposed for its mitigation.

Addressing land cover changes such as agricultural abandonment should be realized through a multi-disciplinary and holistic approach. First, the magnitude and scope of the land cover change should be assessed by observing the past trend and analyzing the periodic transitions that occurred. The next step is to identify the drivers of these transitions so that the processes behind the land cover changes can be understood. Lastly, policies should be formulated to mitigate the land cover changes with the information of its future impacts. To achieve the main objective, the following specific objectives need to be attained:

1.  To establish a general Geomatics framework for informing environmental management through "predicting the future through observations of the past".

2.  To observe the land cover changes in the study area from 1990 to 2020 and analyze the dynamics of the paddy fields using remote sensing and GIS.

3.  To identify the spatial and non-spatial drivers of agricultural abandonment in the study area using spatial regression.

4.  To simulate the impacts of combinations of policies on the mitigation of agricultural abandonment in the study area by developing an Agent-Based Model (ABM).

## 1.6. Thesis Structure

This thesis is composed of six chapters (Fig. 1.4). Chapter 1 introduces the study by providing the background of the study, the case study, research motivations, and the research objectives. Chapter 2 proposes a general Geomatics methodological framework for informing environmental management that will be adopted for the whole thesis. Chapter 3 presents the observation of the past land cover changes in the study area and analysis of the paddy field dynamics. Chapter 4 builds on the observation results and identifies the spatial and non-spatial drivers of agricultural abandonment by developing a statistical model based on a combination of logistic and linear models. Chapter 5 utilizes data on the past changes and the driving factors to develop an ABM to simulate the impact of combinations of socio-environmental policies to mitigate future agricultural abandonment. Finally, Chapter 6 concludes the study by summarizing the discussions and synthesizing its implications for managing the Ifugao rice terraces, contributions to research on mountainous agricultural landscapes, and the methodological novelties.

| Dissertation chapter | Methods | Objectives |
|---|---|---|
| 1. Introduction | Research overview | Identification of the research problem |
| 2. A Geomatics framework for aiding environmental management | RRL and position paper writing | Proposing a Geomatics framework for informing environmental projects |
| 3. Observing the past dynamics of land cover changes | Remote sensing and GIS | Mapping of past land cover and agricultural abandonment |
| 4. Identifying the drivers of agricultural abandonment | Spatial Regression and GIS | Identification of driving factors of agricultural abandonment |
| 5. Simulating the future status of the cultural landscape | Agent-based Modeling and GIS | Simulation of effect of policies on future status of the agricultural lands |
| 6. Summary and conclusion | Research synthesis | Recommendation of policies and future research |

Fig. 1.4 Framework of the dissertation

# Chapter 2:

## A Geomatics framework for aiding environmental management

**The contents of this chapter have been submitted for peer-review under the**
***Geo-spatial Information Science* journal:**

Estacio, I., Onitsuka, K., & Hoshino, S. (under review). Predicting the future through observations of the past: Concretizing the role of Geosimulation for holistic geospatial knowledge. Geo-spatial Information Science.

## 2.1. Introduction

Simulations for predicting the future environment are already ubiquitous tools in the 21st century for informing decision-making in environmental management efforts. From predicting the global temperature, animal species distribution, and land cover changes, simulations have come a long way in providing useful accurate information of our future. In the early 2000s, a book *Geosimulation* was published by Benenson & Torrens (2006). In there, Geosimulation was defined to be *concerned with the design and construction of object-based high-resolution spatial models, using these models to explore ideas and hypotheses about how spatial systems operate, developing simulation software and tools to support object-based simulation, and applying simulation to solving real problems in geographic contexts.* A concise but shorter definition can be elicited from a later paper by Torrens (2006) where Geosimulation was stated *to be characteristic of models that handle massive quantities of geographic entities, each represented at an atomic (individual and independent) scale of consideration.* This being said, the availability of spatial data (or Geographic Information) is a vital part in Geosimulation as they provide the properties and attributes of the geographic entities in a model. Not to mention that only these spatial data provide the data used by the model but they are also used for calibrating and validating the Geosimulation model (Benenson & Torrens, 2004). We can therefore infer that there is a strong connection between Geosimulation and the fields of Remote Sensing and Geographic Information System (GIS); Remote Sensing and GIS provide the spatial information of the environment observed in the past while Geosimulation utilizes

these data to provide spatial predictions of the environment the future. In some sense, the utilization of spatial data to derive information about the Earth unifies these three fields. A term that encompasses this definition is *Geomatics*.

Based on the recent 2022 article "Proposal of Redefinition of the Terms Geomatics and Geoinformatics on the Basis of Terminological Postulates" (Zlatanova & Krawczyk, 2022), Geomatics was proposed to be defined as *the knowledge and ability to use information systems to integrate data about spatial objects and space-time phenomena relating to the Earth's surface, in order to perform spatial analyzes, forecast and visualize their state and changes*. This definition implies that Geomatics is a practice, in contrast with previous statements that Geomatics is a discipline. A 2009 definition is quite similar in this aspect which defines it as an approach, specifically *a systemic, multidisciplinary, integrated approach to selecting the instruments and the appropriate techniques for collecting, storing, integrating, modelling, analysing, retrieving at will, transforming, displaying and distributing spatially georeferenced data from different sources with well-defined accuracy characteristics continuity and in a digital format* (Gomarasca, 2009). Regardless of definition, it is quite agreeable that Geomatics, the utilization of spatial data, is used as a tool for understanding environmental issues so that informed decision-making can be carried out for environmental management actions.

However, as a tool for environmental management, Geomatics is well-known to be utilized only for the acquisition and analysis of spatial information and typically exclude the prediction of future conditions. Funded research projects supervised by professors in universities' Geomatics departments mainly ranged from the utilization of remote sensing techniques to acquire the spatial data of the environment and implementation of different spatial analysis in GIS to uncover relationships between spatial variables. Although studies that utilize Geosimulation may already be currently abundant, such studies are still lagging behind when compared to research done with remote sensing and GIS. This is an irony with the fact that the recent definition of Geomatics includes the forecasting of the state and changes on the Earth's surface. It is definitely the case that the role of Geosimulation is still not concreted in Geomatics, either in practice or as an approach. It is also worth mentioning that since that there has not been any concrete definition of Geomatics in the past decades and it was only recent that an effort has been made to formally define Geomatics terminologically (Zlatanova & Krawczyk, 2022), a general framework for integrating the different tasks encompassed by Geomatics—which includes forecasting—is still not established.

To establish and enhance the methodological repertoire of Geomatics, I posit that the role of Geosimulation for environmental management should be concreted. I write this chapter as a position paper with two main objectives. The first objective is to establish a general framework for Geomatics that positions the different spatial science disciplines along the workflow of data acquisition, spatial analysis, and Geosimulation. This proposed framework also brings forward the second objective which is to present Geomatics as an approach that can be used for "predicting the future through observations of the past".

In the following sections, I first define the different disciplines that Geomatics integrates itself into, which includes Geosimulation. I then propose a general Geomatics framework for unifying these disciplines, which in turn can establish Geomatics as an approach for decision-making in environmental management through "predicting the future through observations of the past". I then provide sample applications of using Geomatics for this approach by providing research projects that ranged from observation to simulation. I then offer my thoughts on the implications of establishing the Geomatics framework and concretizing the role of Geosimulation in Geomatics.

## 2.2. Definitions of disciplines that Geomatics integrates into

Several disciplines are concerned with the utilization or processing of spatial data. Hence, Geomatics willingly integrates itself into different fields (Zlatanova & Krawczyk, 2022). Such disciplines have their own sets of methodologies and end goals for tackling spatial data, thus each has its own role for aiding in informing environmental management actions. For the sake of establishing a Geomatics framework, I list down some of the disciplines that Geomatics mostly integrates into along with their roles in environmental management:

Remote Sensing: *the measurement of object properties on the earth's surface using data acquired from aircraft and satellites… therefore an attempt to measure something at a distance, rather than in situ* (Schowengerdt, 2007). Remote sensing is mostly used for observing the environment to acquire spatial data for analyzing environmental conditions. Currently, public or paid images from various satellite sensors can be utilized to acquire specific spatial information regarding environmental issues such as land degradation, pollution, urban heat island, or deforestation by considering the spectral signatures of features on the surface of the earth.

Global navigation satellite system (GNSS): *a worldwide position and time determination system that includes one or more satellite constellations, aircraft receivers and system integrity monitoring, augmented as necessary to support the required navigation performance for the intended operation* (ICAO, 2018). For data acquisition, geotagging is mainly used for determining and acquiring the 2D coordinates (or 3D if including the elevation) of a feature on earth. Hence, GNSS is used to 'spatialize' an object of interest so that it can be used for the subsequent spatial analysis.

Light Detection and Ranging (LiDAR): *a surveying method that utilizes a pulsed light source to illuminate a target object; by measuring the return time of the reflected light pulses, it is possible to calculate the object distance* (Kim et al., 2021). LiDAR can be classified as a type of remote sensing as it utilizes light pulses to sense objects and their characteristics. Hence, similar to the use of remote sensing for environmental management, LiDAR is used to acquire spatial data of features on the surface of the earth such as for 3d modeling and canopy analysis.

Geographic Information System (GIS): *computer assisted systems for the capture, storage, retrieval, analysis and display of spatial data* (Clarke, 1986). GIS and remote sensing usually go hand-in-hand, with remote sensing used for acquiring raster files and GIS used for storing, converting, and analyzing these spatial data. GIS also acts as a data processing method for other disciplines such as in spatial regression and cellular automata that involve raster files. For analyzing environmental issues, GIS can be used for extracting specific changes in environmental conditions and processing potentially significant explanatory variables such as topography, proximity, or meteorological variables.

Spatial regression: the estimation of *the cause-and-effect relationship between a response variable and one or more covariates* that *do account for spatial autocorrelation* (Okunlola et al., 2021; Srinivasan, 2015). Spatial regression is used for identifying the spatial explanatory variables that have significant correlation with a response variable. This is mostly used for identifying the spatial drivers of an environmental phenomenon such as land cover changes or urban heat island.

Cellular Automata (CA): *an arrangement of connected individual automata, arranged to form a partitioned space… static in their lattice space; they may diffuse information to neighbors, but they cannot alter their position* (Torrens, 2006). CA models usually integrate raster files derived from GIS and treat individual pixels as individual automata. Rules are then established that consider the attributes, states, and neighborhoods of such pixels to manifest

the physical processes in the environment. Simulations can then be implemented by repeating these rules in steps, hereby also changing the attributes, states, and neighborhoods of the pixels. Simulations of scenarios can also be implemented by changing the rules of the model or changing the input values in the pixels.

Agent-based modeling: can also be referred as multi-agent systems, a systems modeling approach where *a system is modeled as a collection of autonomous decision-making entities called agents* (Bonabeau, 2002). In contrast to CA, agents in an Agent-Based Models (ABM) can move in space. ABMs are also called bottom-up models as they simulate small-scale processes to forecast changes in the large-scale. Scenario simulations can be implemented through ABMs by modifying agents (whether their behavior, properties, or interaction) to see how these changes emerge into global changes. In the context of environmental management, Agent-Based Modeling is used to understand how policies that alter the processes between the environment and actors such as farmers, fishermen, or commuters, hereby showing the emergent changes to the environment.

## 2.3. The Geomatics framework
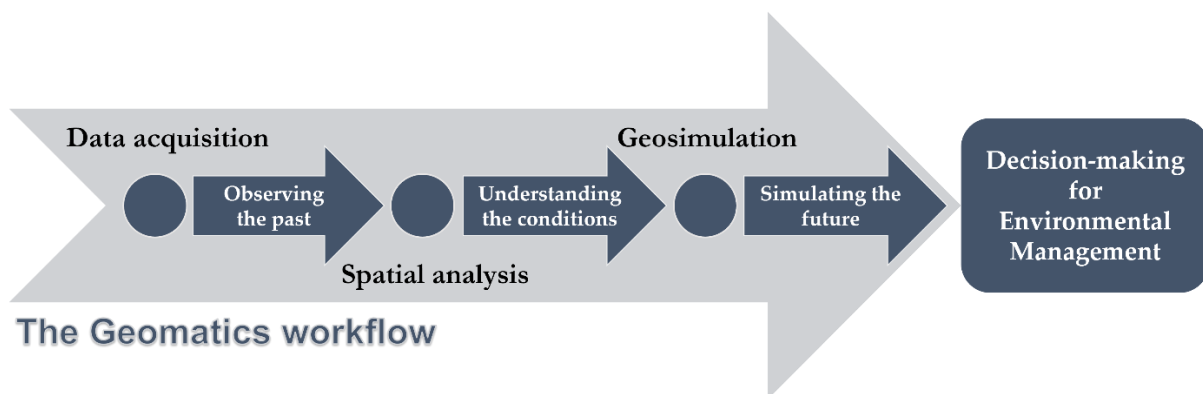


Fig. 2.1 The proposed Geomatics framework for informing decision-making for environmental management actions

Decision-making for addressing environmental problems and planning environmental management actions are usually informed through understanding the extent of damage caused by the environmental issue and understanding the drivers of this problem. However, decision-making can be informed more holistically if information on the effects of the proposed management actions can be understood. Thus, we propose a Geomatics framework where spatial information spanning from the past to the future is utilized for decision-making in environmental management (Fig. 2.1). In this framework, three main steps are followed in the chronological order of Data acquisition, Spatial analysis, and Geosimulation (Table 2.1).

The first step of the framework is acquisition of data. This mostly entails gathering of spatial data that provides information of spatially-varying variables that may be environmental, social, economic in nature. At the same time, non-spatial data can also be gathered to support later analysis of data. The goal of this step is to observe the magnitude and scope of the environmental problem in the past which can be for just one time stamp or through a time frame which can span decades. For this reason, remote sensing is ideal for usage as it can effectively gather data of the past as there is an abundance of satellite and aerial images that can be utilized. Field surveys can also be utilized in this step for data gathering, but it is mostly used in conjunction with remote sensing to validate generated maps. Methods in field surveys can vary and may include geotagging of land features using GNSS, field spectroscopy, or capturing photos using hand-held cameras or drones.

Table 2.1 The three main steps in the Geomatics framework along with their definitions and sample applicable techniques

| Step | Definition | Sample techniques |
|------|-----------|-------------------|
| Data acquisition | Application of k*nowledge of measuring techniques, of the use of remote sensing methods and GNSS, and knowledge of measurements' accuracy* (Zlatanova & Krawczyk, 2022) | Hyperspectral remote sensing, close-range photogrammetry, LiDAR, geotagging by GNSS |
| Spatial analysis | Utilization of *methods useful when the data are spatial... with the objective of solving some scientific or decision-making problem* (Goodchild & Longley, 1999) | Spatial regression, Network analysis, 3D analysis, Land cover change analysis |
| Geosimulation | Development of *models that handle massive quantities of geographic entities, each represented at an atomic (individual and independent) scale of consideration* (Torrens, 2006) | Cellular Automata, Agent-based modelling, hybrid spatial models |

The second step is spatial analysis which aims to answer relevant questions about the environmental problem to understand the conditions for it to occur. A main question usually answered to better understand the problem is to identify the driving factors of the environmental problem; For this part, spatial regression can be utilized to find explanatory variables that have significant correlations with a response variable representing the environmental problem. Network analysis is also a popular method to answer questions that involve consideration of connections of spatial features through a spatial network. 3D analysis is also gaining popularity as it considers the three-dimensional nature of spatial phenomena and can answer questions that involve heights of objects such as visibility analysis and volumetric analysis. By the end of this step, a better understanding of the relationships between spatial entities can be achieved.

The last step is Geosimulation which involves the development of models that captures the processes involving spatial entities in a system, thereby able to simulate the future conditions of the spatial entities by repeatedly running the processes in a loop. Geosimulation differentiates itself through other modeling and simulation paradigms through its extensive usage of spatial data such as raster and vector files for manifesting spatial entities. Geosimulation is an ideal last step for informing environmental management decisions as the effect of proposed policies can be simulated by altering the processes or entities in the model, thereby constructing scenarios that mimic the implementation of policies. In doing so, decision-makers can be informed of which policies or strategies are best to implement for addressing the environmental problem.

Table 2.2 Research projects utilizing Geomatics to inform environmental management actions

| Environmental Problem | Data acquisition | Spatial analysis | Geosimulation |
| --- | --- | --- | --- |
| Deterioration of blue carbon ecosystems | Multi-spectral remote sensing, LiDAR, drone mapping | Land cover change analysis, Suitability analysis | agent-based modeling, coupling with a hydrodynamic model |
| Urban Heat Island in cities | Multi-spectral remote sensing, drone mapping, geotagging by GNSS | Spatial regression, distance analysis | Micro-climate simulation, cellular automata, agent-based modeling |

By utilizing this three-step holistic approach that mainly involves spatial data, or we call it the Geomatics approach, formulating policies for mitigating environmental problems based on science-based information can be implemented.

## 2.4. Case examples

To provide empirical examples of research projects that adopt the Geomatics framework as a general methodological workflow, we discuss two completed research that aimed to provide solutions to environmental problems through the utilization of spatial data (**Error! Reference source not found.**). All of these projects followed a methodological workflow consisting of first acquiring spatial data using a combination of remote sensing and field survey techniques, then analyzing the spatial data using a combination of GIS techniques and other software, then implementing Geosimulation to simulate the future status of the environment. After the completion of the research, environmental management actions were recommended based on a combined knowledge of the magnitude of the problem, the conditions of the environment, and simulations of scenarios.

### 2.4.1. Deterioration of blue carbon ecosystems

Because of ongoing unsustainable practices in coastal areas as well as unmonitored coastal tourism, massive land cover changes have occurred in coastal ecosystems, specifically on the mangroves and seagrass areas. In 2018, a research program was funded by the Philippines' Department of Science and Technology with the name *Integrated Assessment and Modelling of Blue Carbon Ecosystems for Conservation and Adaptive Management (IAMBlueCECAM)*. This research program aimed to propose conservation and natural resource management actions for blue carbon ecosystems by producing an inventory of mangrove forests and seagrass habitats and simulating the dynamics in these ecosystems (United Nations ESCAP, n.d.). The research program is made up of ten component projects that all handle spatial data but work at different steps in the Geomatics framework. The first two projects utilized remote sensing to provide inventories of the mangrove and seagrass extents. One project worked on suitability models for spatial analysis. Meanwhile, four projects utilized Geosimulation techniques to elucidate blue carbon dynamics and associated ecosystem

services. Based on the synthesis of findings produced by the different projects, sustainable environmental management actions were presented to officials of respective government units.

### 2.4.2. Urban Heat Island in cities

Cities all experience the phenomenon Urban Heat Island (UHI), the increase in air temperature in urban areas relative to its surrounding natural areas. This phenomenon is caused by the combination of artificial materials and buildings in cities which eventually absorb and retain heat. UHI causes a variety of harmful impacts to people such as extreme discomfort, heat stroke, and a variety of illnesses. To mitigate the UHI in Philippines cities, the research project *Geospatial Assessment and Modelling of Urban Heat Islands in Philippine Cities (GUHeat)* was implemented to monitor the magnitude of the UHIs in different cities, relate this to with environmental factors, and utilize modeling techniques to simulate possible mitigation scenarios (PCIEERD, n.d.). In general, the research project also followed the Geomatics framework to implement a workflow spanning from data acquisition, spatial analysis, and Geosimulation. By the end of the project, research findings were presented to the cities' government officials such as the cooling effect of rivers, proper positioning of urban trees, and causes of local climate zones in cities.

## 2.5. Implications of the Geomatics framework

Adoption of the Geomatics framework for environmental management, thereby concretizing the role of Geosimulation in Geomatics, has several implications for future studies dealing with spatial data.

First, this will widen the application of Geomatics to include understanding the most probable future status of the environment based on scenarios. Conventionally, the environmental applications of Geomatics span only from the monitoring of spatial data of the environment to analyzing the relationships between these spatial data. Of course, understanding the past and present conditions of the environment may already be sufficient at times for providing insights on how to manage the environment. This is especially true in decision-making in a government level where information of the status of the environment and its causes is enough to signal intervening actions. However, understanding also the impacts of policies

on the future conditions of the environment can definitely provide a more holistically informed decision for drafting policies. This can be likened to how knowing that the climate has changed for the past decades brought awareness to people, but it is predictions of the future warming climate that triggered the worldwide actions from small to large-scale actors. Without a doubt, Geosimulation can provide valuable information for environmental management and concretizing the role of Geosimulation in Geomatics will make Geomatics a more holistic approach.

The second implication is a corollary of the first whereby a methodological workflow will be established that can be used as a generic template for implementation of research aiming to inform environmental management. This workflow will provide a straightforward approach that addresses both monitoring the past, understanding the causes, and predicting the future of an environmental problem. We posit that this methodological workflow will aid research projects in achieving more holistic findings that can easily be translated into policies.

Lastly, the Geomatics framework will enhance the collaboration between Geosimulation and the other spatial science disciplines such as Remote Sensing and GIS. This would stimulate an environment where more novel methodological approaches can be developed that would cover at least a combination of Geosimulation and either remote sensing or GIS. Currently, the remote sensing and GIS disciplines are strongly connected and a huge chunk of remote sensing studies already include a spatial analysis section. The connection between GIS and Geosimulation can also be deemed quite well established. Several cellular automata and agent-based models have been developed which utilize outputs from spatial regression or suitability mapping. The agent-based modeling software *GAMA (GIS Agent-based Modeling Architecture)* has also been developed that provides easy utilization of raster and vector files in developing ABMs (Taillandier et al., 2019). However, compared to combined remote sensing and GIS studies, combined Geosimulation and GIS studies are still relatively scarce. Once Geosimulation is concretized in Geomatics, more GIS-Geosimulation studies can be expected to flourish.

## 2.6. Conclusion

The latest definition of Geomatics is the knowledge and ability for analyzing and forecasting spatial phenomena. However, the role of forecasting is still not effectively utilized

when spatial data is used for informing environmental management actions. As a call to concretize the role of Geosimulation in Geomatics, we propose a Geomatics framework that spans from data acquisition, spatial analysis, and Geosimulation. This Geomatics framework can also be adopted as a methodological workflow for informing decision-making in environmental management with its capability of "predicting the future through observations of the past". To provide examples of the usage of the Geomatics framework as a workflow, we presented case studies that aimed to inform environmental management actions through utilization of spatial data.

We also discussed the possible implications of adopting the Geomatics framework: the widening of the environmental application of Geomatics, the establishment of a methodological workflow for informing environmental management, and the enhancement of the collaboration between Geosimulation and other spatial science fields. We hope that we were able to demonstrate the benefits of concretizing the role of Geosimulation in Geomatics. We write this paper mainly to advocate the adoption of this framework as the implications stated above will only manifest if it is disseminated. The quickest way to achieve this is if educational curriculums in Geomatics adopt this framework. We believe that this new perspective in Geomatics will bring value in teaching the environmental applications of Geomatics. Another way for this framework to be adopted is if spatial scientists utilize it in their research. We thus also invite researchers to utilize or enhance this framework to advance the practice of Geomatics.

# Chapter 3:

## Observing the past dynamics of land cover changes

## 3.1. Introduction

Land cover transitions in mountainous agricultural landscapes have previously been analyzed through the utilization of remote sensing technologies such as satellite and aerial images (Aguirre-Gutiérrez et al., 2012; Minta et al., 2018; Pôças et al., 2011; Xystrakis et al., 2017). However, analysis of land cover transitions in these studies was limited as the time-intervals between land cover maps were more than ten years or inconsistent. This limits the analysis of land cover transitions as it may not have captured rapid land cover transitions that have occurred in shorter time spans. Previous analysis may have missed a step before observed transitions or may have mistaken retransitions to former land covers as no changes.

Apart from undergoing regular transitions in land cover, mountainous agricultural landscapes have also been observed to undergo agricultural abandonment due to socio-economic and environmental drivers such as high cultivation cost in steep conditions and lack of available water in high elevations (Gellrich, Baur, Koch, et al., 2007; Gellrich & Zimmermann, 2007; Hou et al., 2021; Minta et al., 2018; Modica et al., 2017; Xystrakis et al., 2017). It is important to monitor the rate of permanent abandonment to maintain cultural ecosystem services (Tilliger et al., 2015) and prevent erosion (Londoño et al., 2017; Tarolli et al., 2014). However, as fallowing is a common practice in these landscapes, previous monitoring studies may have misclassified fallowing as permanent abandonment (Pôças et al., 2011; Xystrakis et al., 2017). Transitions from agricultural land to other land cover type were generally classified as agricultural abandonment and may have missed out on the fallowing

process.

As a consequence of agricultural abandonment, afforestation has also been widely observed to occur in mountainous agricultural landscapes (Gellrich, Baur, Koch, et al., 2007; Gellrich & Zimmermann, 2007; Kobler et al., 2005). Forest growth was shown to decrease water yield (García-Ruiz & Lana-Renault, 2011; Soriano & Herath, 2018; Ziegler et al., 2004), which also acts as a catalyst for further land abandonment. This implies a feedback loop between afforestation and agricultural abandonment, where the increase of occurrence of one phenomenon also increases the occurrence of the other phenomenon (Soriano & Herath, 2018). Previous studies have shown that proximity from forest areas increases the likelihood of agricultural abandonment (Bolliger et al., 2017; Gellrich, Baur, & Zimmermann, 2007; Pazúr et al., 2020). However, there haven't been previous studies that show that the total area or abundance of forest cover also increases the magnitude of agricultural abandonment. This is important in landscape planning with the purpose of conserving agricultural lands.

This study aims to analyze the dynamics of rapid land cover transitions and permanent agricultural abandonment in the mountainous agricultural landscape of Ifugao rice terraces in the Philippines. Specifically, this study aims to answer the following three questions: (1) What rapid land cover transitions are prominent in the Ifugao rice terraces landscape? (2) What is the frequency of permanent abandonment, fallowing, first-time cultivation, and recultivation in the landscape? And (3) Is permanent agricultural abandonment related to abundance of other vegetation types in the landscape? To answer these research questions, time-series land cover mapping and transition analysis in consistent five-year intervals were implemented in Google Earth Engine (GEE). A framework for analyzing paddy field dynamics from land cover maps was developed. Lastly, regression analysis was implemented to analyze correlation between vegetation abundance and subsequent permanent agricultural abandonment.

## 3.2. Methods

### 3.2.1. Datasets

For this study, GEE was used as the source for most datasets. GEE is an online platform that provides an abundance of geospatial data and automatic cloud-based computations for handling data (Gorelick et al., 2017). GEE is especially useful for spatial-temporal analysis

because of the automated process of extracting time-series images and generating image composites. GEE was also utilized for analyzing the land cover transitions and paddy field dynamics.

Landsat 5 and Landsat 8 Level 2, Collection 2, Tier 1 image collections were used as the main data for mapping the land cover in the Bangaan watershed from 1990 to 2020. These Landsat images were already geometrically and atmospherically corrected and cross-calibrated among different sensors, so they are suitable for decadal time series land cover change applications (Wulder et al., 2016). Shuttle Radar Topography Mission (SRTM) Version 3.0 Digital Elevation Model (DEM), which was released in 2013 and has a 30 m spatial resolution, was used for generating the shapefile of the Bangaan watershed and for training classification models.

Aside from GEE, other software were also utilized for generating and exploring needed dataset. The shapefile of the Bangaan watershed was derived by using the SRTM DEM as input in the Arc Hydro tools in ArcGIS. Arc Hydro uses a straightforward approach in generating watersheds in a specified region by using a DEM to compute water flow, define streams, and generate catchments (Djokic et al., 2011). High-resolution images from Google Earth were used for the creation of training samples and validation of land cover images. Google Earth has been widely used alongside GEE to refer to high-resolution images for time-series mapping purposes (W. Cao et al., 2021; Zhou et al., 2019).
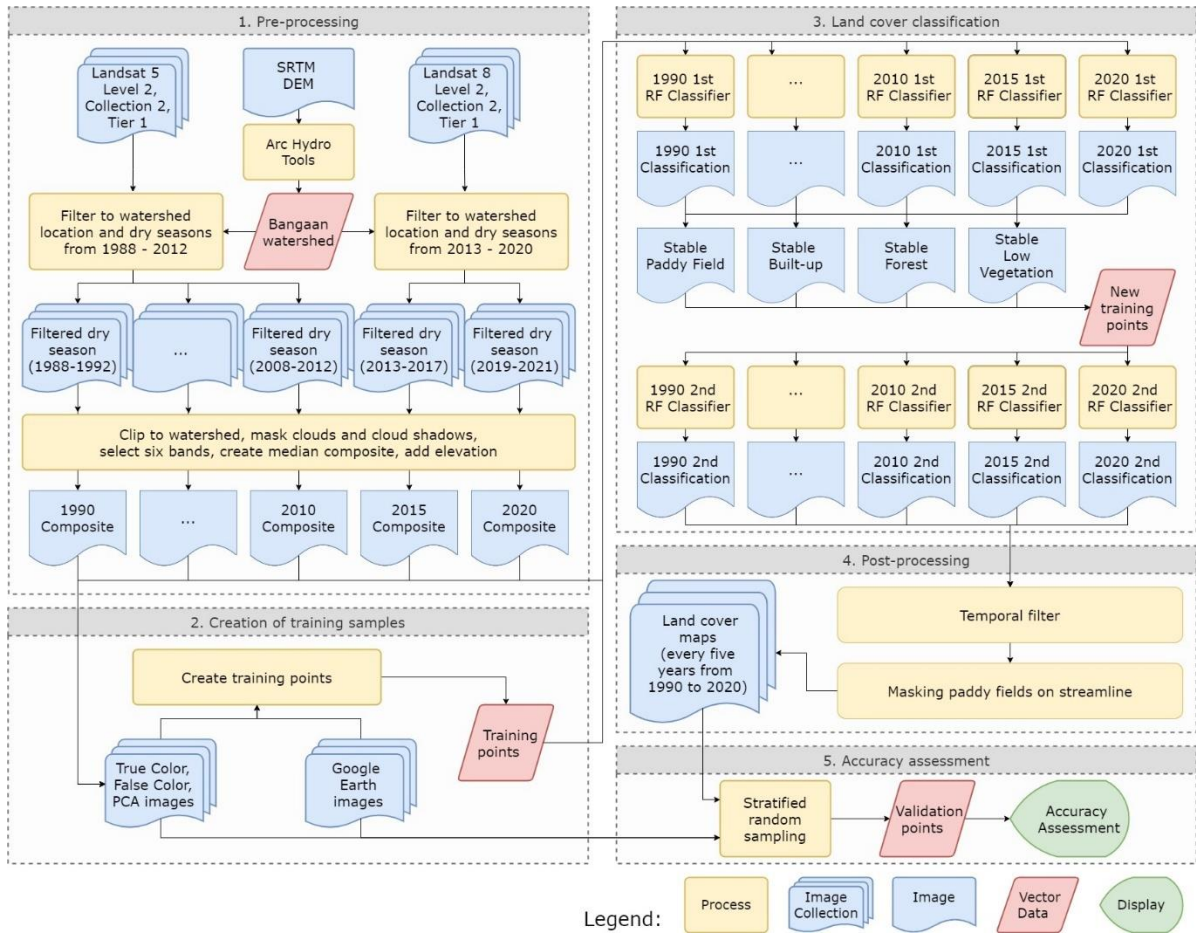
Fig. 3.1 The framework for mapping the land cover at the Bangaan watershed from 1990 to 2020 using a combination of Google Earth Engine, Google Earth. and ArcGIS. RF = Random Forest

## 3.2.2. Mapping

The framework for mapping the land cover from 1990 to 2020 includes pre-processing, creation of training samples, land cover classification, post-processing, and accuracy assessment (Fig. 3.1). The procedures were implemented mostly in GEE and supplemented by ArcGIS and Google Earth.

### 3.2.2.1. Pre-processing

Landsat image collections were spatially filtered to images overlapping with the location of the Bangaan watershed and temporally filtered to images captured during the dry

season, set from December 1st of a previous year to May 31st of a subject year. The dry season in the Ifugao province was used as the intra-annual period as this coincides with the transplanting and growth stage of the rice in the rice terraces (SITMo, 2008), where flooding can be detected in paddy fields (Dong et al., 2015). The images were temporally grouped into collections of five-year time period for creating an image composite, with the target years as the middle years (e.g., for the year 2000, an image collection was created with images spanning from the years 1998 to 2002). Image composition has been widely used in previous studies to take into account phenology of vegetation (Chen et al., 2017; Kollert et al., 2021; Praticò et al., 2021) or agricultural cycle (Dong et al., 2015). A five-year period was used as making image collections from single year or three-year periods cannot produce a whole composite after implementing cloud and shadow masking. Also, a five-year interval between land cover maps was deemed appropriate for land cover transition analysis. Collections that have images from 1988 to 2012 were derived from the Landsat 5 satellite while images from 2013 to 2021 were derived from the Landsat 8 satellite; Landsat 7 images were not used because of the inconsistency produced by the scan-lines. For the case of year 2020, the three-year period 2019–2021 was used because the year 2021 can only be the used as latest year.
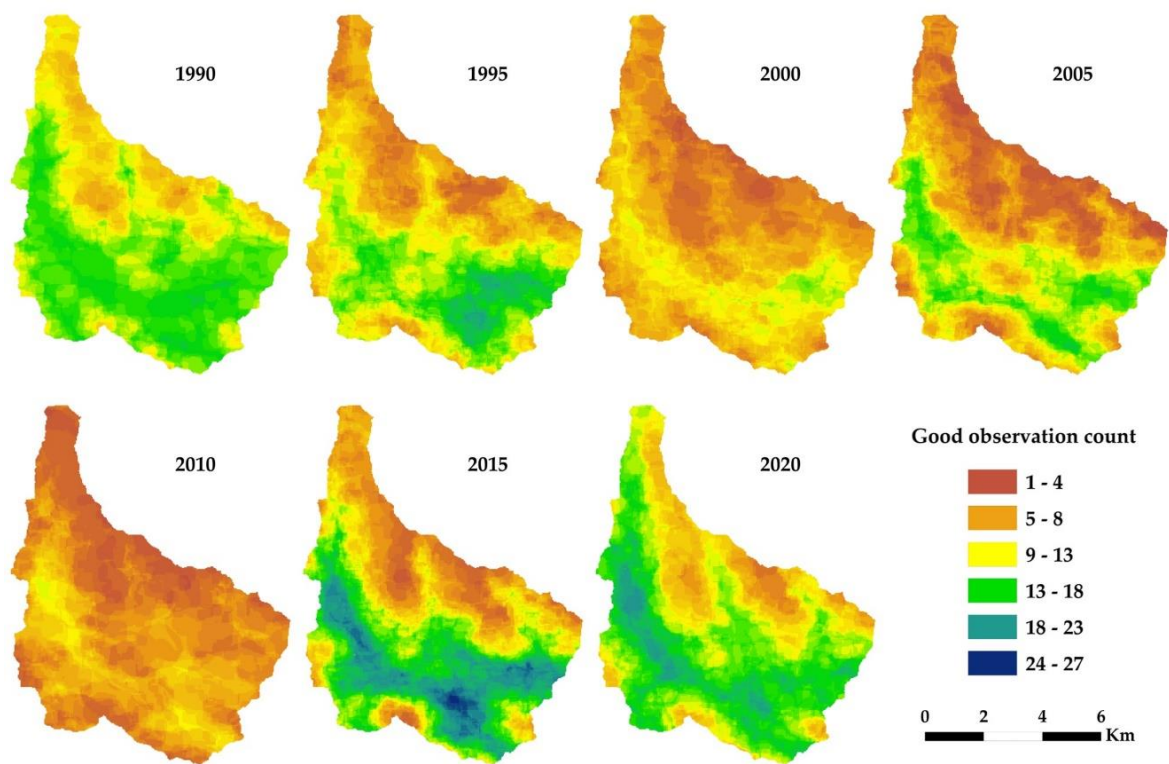


Fig. 3.2 The spatial distribution of good observation count per time period

The images from the dry-season multi-year collections were clipped to the shape of the watershed. Clouds and cloud shadows were masked for every image by utilizing the available pixel quality attributes generated from the CFmask algorithm (Foga et al., 2017). The spatial distribution of good observation counts per pixel showed consistent low counts in the higher mountainous areas, indicating more pixels are being masked which may be due to terrain shadows (Fig. 3.2). The respective Blue, Green, Red, Near Infrared (NIR), Short-wave Infrared 1 (SWIR1), and Short-wave Infrared 2 (SWIR2) bands of Landsat 5 and Landsat 8 were selected as these are the common bands between the two Landsat sensors, hence leaving out the other bands. A median function was implemented for each image collection to derive the image composite per target year (Alencar et al., 2020). A median function was used to get average pixel values during the dry period but at the same time ignore possible outlier values in paddy field areas such as fields that is not in the transplanting stage which may produce values close to low vegetation. Lastly, an elevation band derived from the SRTM DEM was added to each yearly composite, making each composite have seven bands for training the classifications models (Blue, Green, Red, NIR, SWIR1, SWIR2, and elevation). Before adding the elevation band, grains of misclassified pixels occurred in areas where there were terrain shadows, hence had low good observation count because of shadow masking. Coincidentally, these areas were in the higher parts of the mountain where there was only forest cover as training points, hence adding an elevation band easily removed the misclassified pixel grains. Seven image composites were produced, representing the years 1990, 1995, 2000, 2005, 2010, 2015, and 2020.

### 3.2.2.2. Creation of training samples for land cover classification

Based on a field visit and previous studies on the Ifugao rice terraces, land usages in the landscape were identified (Table 3.1). These land usages were compared to high-resolution images in Google Earth and true color and false color images from the generated Landsat composites for identification. Spectral signatures of the different land usages in Landsat images were inspected and it was found that some of these land usages have low spectral separability (e.g., grassland and caneland cannot be differentiated). Also, not all land usages can be identified with confidence by image interpretation using Google Earth and Landsat images, which is important for creating training and validation samples. When choosing the land cover

types to be classified for subsequent land cover transition analysis, the following were considered: (1) Transitions involving paddy field and forest land cover types are the most important as based on previous studies, agricultural abandonment leads to afforestation, and afforestation promotes agricultural abandonment through decrease in water yield; (2) Obtaining high accuracies for generated land cover maps is a priority to obtain reliable land cover transition analysis. From these considerations, the land cover types chosen for image classification were paddy field, low vegetation, forest, and built-up (Table 3.1) as these land cover types have high spectral separability and can be differentiated with confidence using Google Earth and Landsat images. Some land use transitions may be missed (e.g., transitions between grassland and swidden field), but this is deemed acceptable for the current research as dynamics involving paddy field and forest were prioritized. Water was not included as there were no lakes due to the study area being in a mountainous area, while the streams did not cover much area (only around 20 pixels per image composite). The small area of water was instead addressed in the post-classification section.

Table 3.1 Description and land usage of each land cover type

| Land cover type | Description | Land usage (Acabado, 2012) |
| --- | --- | --- |
| Paddy field | Flooded terraced land for cultivation of semiaquatic crops such rice or taro | Pond-field |
| Low vegetation | Dry land with vegetation of low density such as lands with sparse trees or lands filled with grass or vegetables | Grassland, Caneland, Swidden, Drained field |
| Forest | Land with high, woody, and compacted trees | Woodlot, Forest |
| Built-up | Land with artificial surfaces such as concrete, asphalt, or aluminum | House terrace, Roads, Buildings |

| High-resolution image | Landsat PCA image |

Sample reference points: ● Paddy Field ◆ Low Vegetation ⬠ Forest △ Built-up
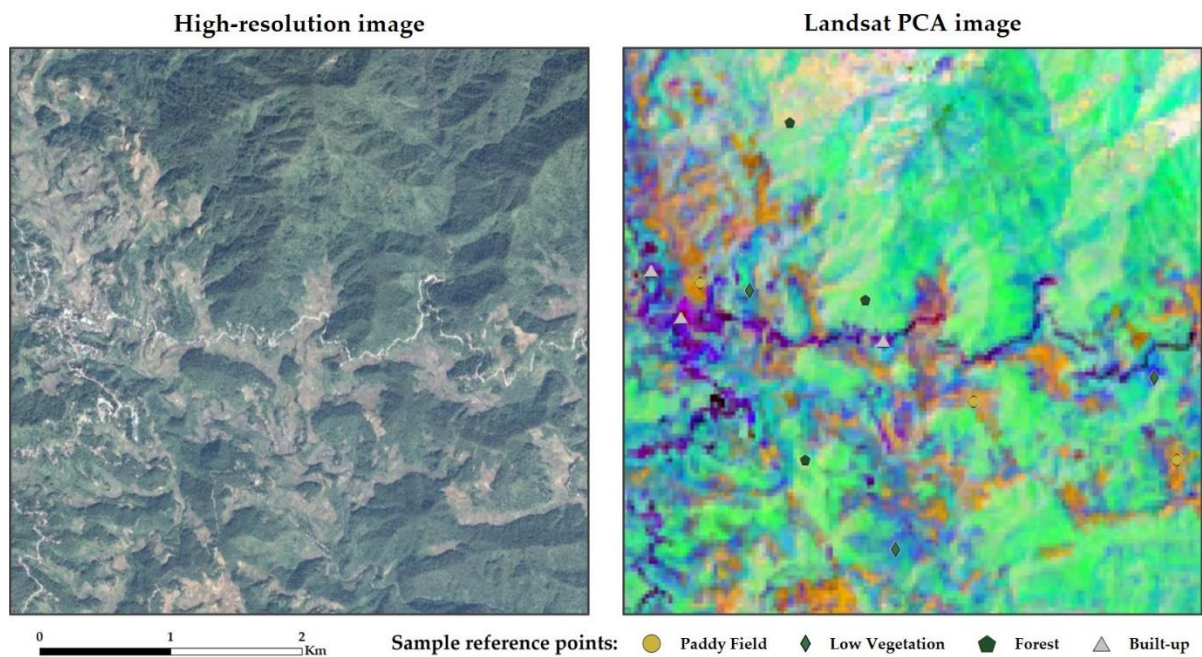
Fig. 3.3 Comparison between a 2015 high-resolution image from Google Earth and a 2015 Landsat Principal Component Analysis (PCA) image in a terraced area in the Bangaan watershed. Reference points indicate the landcover type in relation to the visualizations in the high-resolution image and PCA image.

After choosing the land cover types to classify, 600 training samples (150 points per land cover type) were created based on Google Earth high-resolution images, Landsat true color, false color, and Principal Components Analysis (PCA) images. Principal Component Analysis is a dimensionality-reduction method applied in remote sensing that linearly transforms a multi-band image to generate a new image with less correlated bands, with the first band covering the maximum variance in the data space (Lei et al., 2008; Munyati, 2004). PCA is useful for identifying land cover types through visualization as the first three bands can capture most of the variance in the image's spectral values. PCA images aided in differentiating the different land cover types, especially between built-up and low vegetation areas (Fig. 3.3). High-resolution images in Google Earth were only available from the years 2010 to 2020, so Landsat image interpretation were mostly used for creating the samples. However, Google Earth images from 2010 onwards also helped in sampling previous years as it confirmed low vegetation cover that were previously paddy fields due to the forms of the terraces. As the pixel size of Landsat images is larger than the pixel size of Google Earth images (which can reach sub-meter level accuracy), sampling was limited to one point per Landsat pixel, with Google

Earth image pixels within the Landsat pixel used as supplement for interpreting the land cover type of the sample point.

*3.2.2.3. Land cover classification*

Two rounds of pixel-based supervised classification were employed to generate the land cover maps (Alencar et al., 2020). In the first round of classification, the 600 training samples per target year were used to train a Random Forest classifier model (Breiman, 2001). Random Forest is a machine learning classifier that *combines several randomized decision trees and aggregates their predictions by averaging* (Biau & Scornet, 2016). It aims *to form an ensemble of classification and regression tree(CART)-like classifiers* to classify remote sensing images (Gislason et al., 2006). In this study, the parameter for the number of trees in the Random Forest model was calibrated according to coherence of generated land cover maps to actual images in Google Earth Engine until the parameter was set to 100. The other parameters in the model were set as default (number of variables per split = square root of number of variables, min leaf population = 1, bag fraction = 0.5, max nodes = no limit). After the first round, the authors noticed that some areas in the classified images have inconsistent classification through the years. This may be due to the fact that the spectral signatures gathered from the training samples may have been insufficient to train consistent Random Forest models through the years. To address this, the authors decided to adopt two-rounds of classification by Alencar et al. (2020). In the second round, the initial seven generated land cover images were used to produce a new set of training points. If a land cover type occurred in a pixel for at least five years (e.g., 1990, 2000, 2005, 2015, and 2020), a point was placed in that pixel with the classification of the subject land cover type and was treated as a training point for the years the land cover type occurred. This procedure produced a minimum of 13,000 training samples per year. After the second classification, the maps produced looked more consistent, which will aid in land cover transition analysis.

*3.2.2.4. Post-classification*

To further improve the accuracies of the land cover images, two post-classification procedures were applied: temporal filter and masking misclassified paddy fields on the

streamline. Temporal filtering is a post-processing technique which reclassifies the land cover types in time-series land cover maps to correct the transitions between land cover types. Meanwhile, masking in the context of post-processing is used when a portion or feature in a classified land cover map exhibits misclassification. By identifying the feature associated with this misclassification, masking can be implemented to correct the misclassified land cover type.

Generated classified images showed some grains which were obviously misclassified. As these grains of misclassification will affect the land cover transition analysis, temporal filters were implemented (Alencar et al., 2020). Transition rules were applied on land cover images based on the assumption that some transitions are improbable to occur in the mountainous agricultural landscape (Table 3.2). For example, built-up land cover type occurring between periods of paddy fields is highly improbable and may be caused by misclassification. These transition rules were applied to the land cover images, starting from the earliest year (1990) until the last year (2020), then repeated two times.

Table 3.2 Transition rules for the temporal filter. P = Paddy field; L = Low vegetation; F = Forest; B = Built-up.

| ID | Rules | Correction |
|----|-------|------------|
| *First-year rules* | | |
| 1 | B-P-P | P-P-P |
| 2 | B-F-F | F-F-F |
| *Between-years rules* | | |
| 3 | P-B-P | P-P-P |
| 4 | P-F-P | P-P-P |
| 5 | B-P-B | B-B-B |
| 6 | B-F-B | B-B-B |
| 7 | B-L-B | B-B-B |
| 8 | F-P-F | F-F-F |
| 9 | F-B-F | F-F-F |
| 10 | L-B-L | L-L-L |
| *Last-year rules* | | |
| 11 | B-B-P | B-B-B |
| 12 | B-B-F | B-B-B |
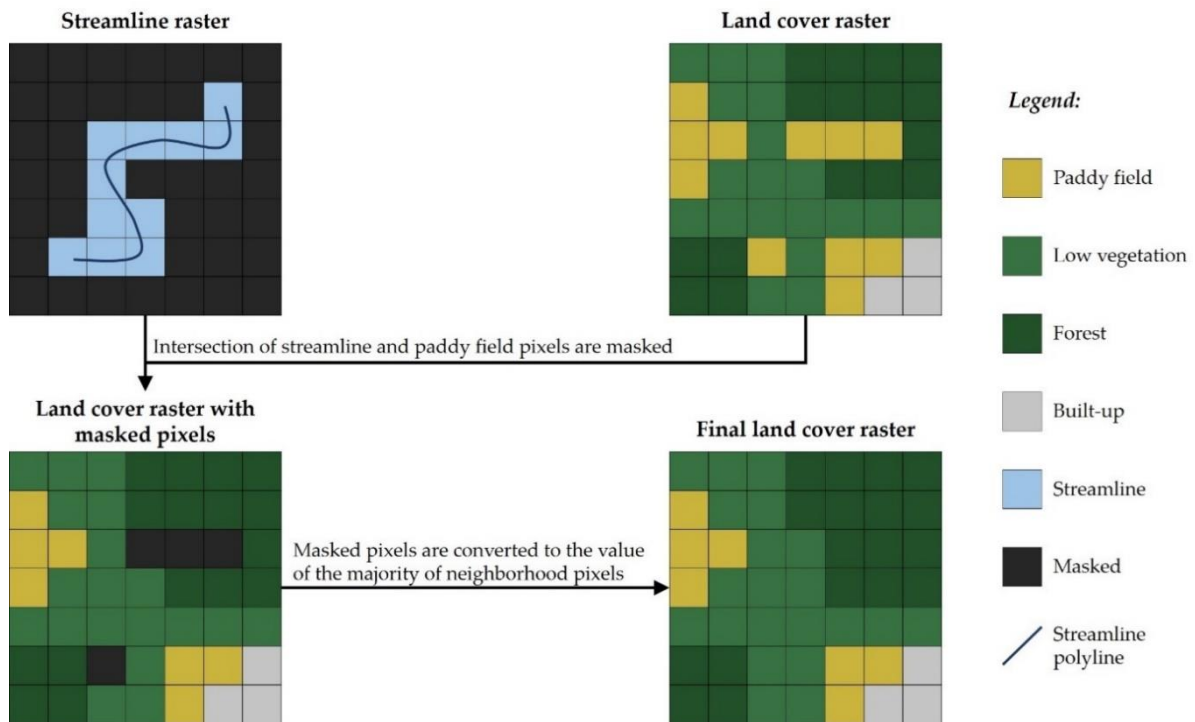
Fig. 3.4 Illustration of masking misclassified paddy field pixels on a streamline.

It was also observed that some pixels along the streamlines were misclassified as paddy fields. This may be explained with the water along streamlines being mistaken as the flooding in the paddy fields. To address this, misclassified paddy field pixels on the streamline were masked and converted to neighboring land cover types (Fig. 3.4). A polyline shapefile of the streamline was first digitized using high-resolution images as reference, then converted to raster. Paddy field pixels that intersected with streamline pixels were considered misclassified and were masked. These masked pixels were then converted to the land cover type of the majority in the square neighborhood pixel.

### 3.2.2.5. Accuracy assessment

The accuracies of the final land cover maps were assessed using validation points sampled using stratified random sampling (W. Cao et al., 2021). After generating the final land cover maps, 300 validation points were generated per target year, with the number of points per land cover type in proportion to the land cover type's area. The generated validation points were assigned a reference data by referring to Google Earth high-resolution images and Landsat true color, false color, and PCA images. Meanwhile, classifications in the generated land cover

map were extracted into the validation points as classification data. Using the validation points, the Producer's and User's accuracies of each land cover type and the Overall accuracy of each land cover map were determined to assess the land cover maps.

### 3.2.3. Analysis of dynamics of land cover transitions and paddy field abandonment

From the generated land cover maps, relational and conditional raster operations were implemented to analyze land cover transitions, paddy field dynamics, and the relationship between vegetation cover abundance and paddy field abandonment.
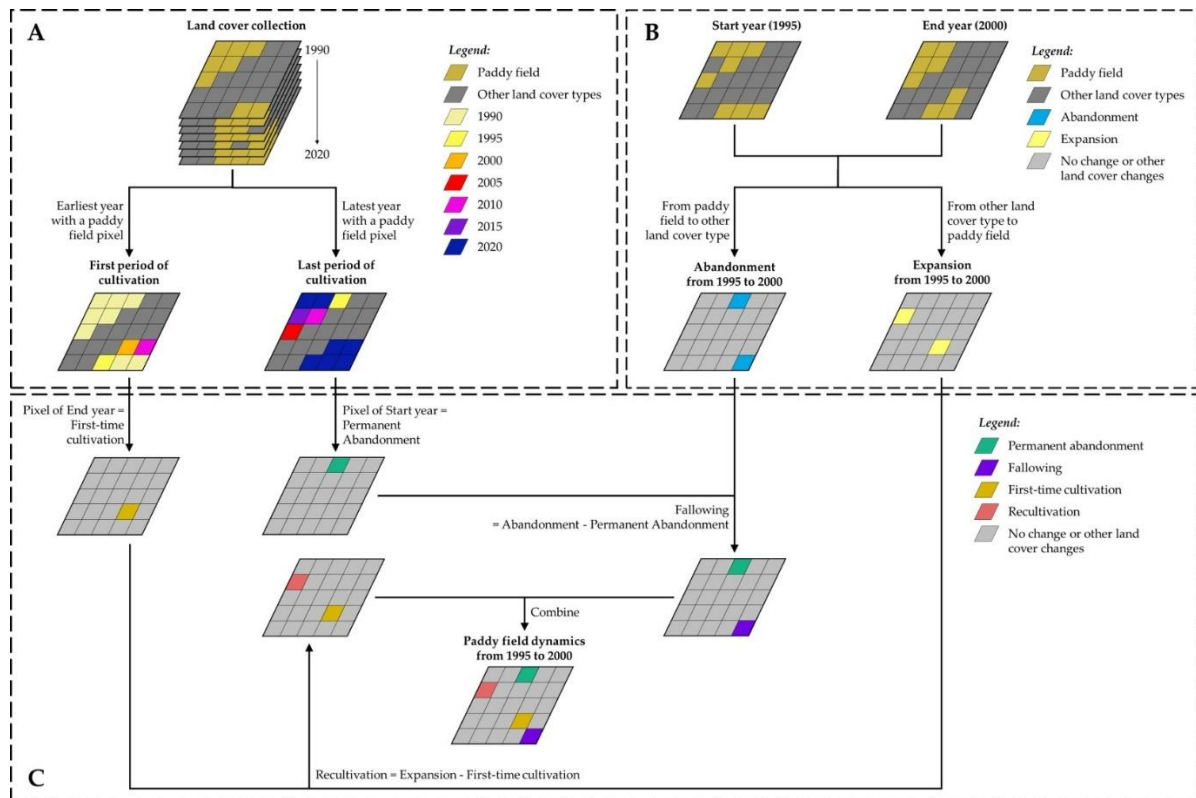


Fig. 3.5 The framework for analyzing paddy field dynamics for the study period 1990–2020: (A) Generating a raster showing the first period of cultivation and a raster showing the last period of cultivation; (B) Generating rasters of abandonment and expansion for each five-year period; (C) Generating a raster of paddy field dynamics which shows permanent abandonment, fallowing, first-time cultivation, and recultivation.

*3.2.3.1. Land cover transitions*

For each five-year interval between land cover maps, the transitions between land cover types were analyzed. For example, if a pixel was classified as Paddy Field in 2000 and Low Vegetation in 2005, the pixel was classified as a "Paddy Field to Low Vegetation" transition in the 2000–2005 land cover transition map. The total area for every transition type was computed to determine the abundant transitions in the watershed (Aguirre-Gutiérrez et al., 2012; Pôças et al., 2011; Zhu & Woodcock, 2014).

*3.2.3.2. Paddy field dynamics*

Based on the time-series land cover maps, a three-part framework for analyzing temporal dynamics of paddy fields was developed (Fig. 3.5).

The first part deals with deriving maps showing the years cultivation was first and last practiced (Fig. 3.5A). The 'First period of cultivation' map was generated by identifying the earliest year a paddy field was identified in a pixel. For example, given a pixel from land cover maps spanning from 1990 to 2020, if the first year a paddy field was detected is year 2000, the value in the 'First period of cultivation' map for the respective pixel is '2000'. On the other hand, the 'Last period of cultivation' map was generated by identifying the last year a paddy field was identified in a pixel. For example, given the same pixel, if the last year a paddy field was detected is year 2015, the value of the pixel in 'Last period of cultivation' map is '2015'.

The second part deals with deriving maps showing abandonment and expansion of paddy fields for every five-year period (Fig. 3.5B). Abandonment maps were generated by treating transitions from paddy field as 'Abandonment'. For example, given a pixel in 2000 and 2005 land cover maps, if the pixel transitioned from a paddy field, the pixel is classified as 'Abandonment' in the 1995–2000 Abandonment map. On the other hand, expansion maps were generated by treating transitions to paddy field as 'Expansion'. For example, given a pixel in 2000 and 2005 land cover maps, if the transition is going into a paddy field, the pixel is classified as "Expansion" in the 1995–2000 Expansion map

The third part combines the results of the first and second parts and derives maps showing the dynamics of paddy fields for every five-year period (Fig. 3.5C). First, 'Abandonment' pixels in an Abandonment map are inspected. If an 'Abandonment' pixel for a

period coincides with a pixel that has a value of the period's ending year in the 'Last period of cultivation' map, the pixel is identified as "Permanent abandonment". For example, in the 1995–2000 Abandonment map, if an 'Abandonment' pixel coincides with a '2000' pixel from the 'Last period of cultivation' map. the pixel will be classified as "Permanent Abandonment". On the other hand, if an abandonment pixel does not coincide with a pixel that has a value of the period's ending year in the 'Last period of cultivation' map, it is classified as 'Fallowing'. For example, if an abandonment pixel from the same 1995–2000 Abandonment map does not coincide with a '2000' pixel from 'Last period of cultivation', the pixel will be classified as "Fallowing". After inspecting 'Abandonment' pixels, 'Expansion' pixels in an Expansion map are inspected next. If an 'Expansion' pixel coincides with a pixel that has a value of the period's starting year in the 'First period of cultivation' map, the pixel is identified as 'First-time cultivation'. For example, in the 1995–2000 Expansion map, if an 'Expansion' pixel coincides with a '1995' pixel from the 'First period of cultivation' map, the pixel will be classified as 'First-time cultivation'. On the other hand, if an 'Expansion' pixel does not coincide with a pixel with a value of the period's starting year in the 'First period of cultivation' map, it is classified as 'Recultivation'. For example, if an 'Expansion' pixel from the same 1995–2000 land cover transition map does not coincide with a '1995' pixel from 'First period of cultivation', the pixel will be classified as "Recultivation".

Through this developed three-part framework, the temporal dynamics of permanent abandonment, fallowing, first-time cultivation, and recultivation were analyzed.

*3.2.3.3. Relationship between vegetation cover abundance and paddy field abandonment*

To analyze the relationship between the abundance of vegetation land cover types (low vegetation and forest) to the permanent abandonment of paddy fields, regression analysis was implemented. The areas of the vegetation land cover types were each treated as an explanatory variable while the subsequent permanent abandonment was treated as the response variable. Since abandonment pixels in the 2015–2020 period were all classified as permanent abandonment (recultivation still cannot be confirmed), only periods from 1990 to 2015 were considered in the regression analysis. Regression analysis was implemented using the Analysis ToolPak in Microsoft Excel.

## 3.3. Results

## 3.3.1. Land cover change from 1990 to 2020

Table 3.3 Confusion matrices of the land cover maps generated every five years from 1990 to 2020. UA = user's accuracy, PA = producer's Accuracy, OA = overall accuracy

| Year | Classification | Reference | | | | UA (%) |
|------|----------------|-------------|----------------|--------|----------|--------|
| | | Paddy Field | Low Vegetation | Forest | Built-up | |
| 1990 | Paddy Field | 26 | 0 | 2 | 0 | 92.86 |
| | Low Vegetation | 0 | 68 | 2 | 0 | 97.14 |
| | Forest | 2 | 2 | 189 | 0 | 97.93 |
| | Built-up | 1 | 0 | 0 | 8 | 88.89 |
| | PA (%) | 89.66 | 97.14 | 97.93 | 100.00 | OA = 97.00 |
| 1995 | Paddy Field | 28 | 2 | 0 | 0 | 93.33 |
| | Low Vegetation | 1 | 65 | 0 | 0 | 98.48 |
| | Forest | 1 | 1 | 194 | 0 | 98.98 |
| | Built-up | 0 | 0 | 0 | 8 | 100.00 |
| | PA (%) | 93.33 | 95.59 | 100.00 | 100.00 | OA = 98.33 |
| 2000 | Paddy Field | 27 | 0 | 0 | 0 | 100.00 |
| | Low Vegetation | 0 | 65 | 5 | 0 | 92.86 |
| | Forest | 0 | 3 | 191 | 0 | 98.45 |
| | Built-up | 0 | 0 | 1 | 8 | 88.89 |
| | PA (%) | 100.00 | 95.59 | 96.95 | 100.00 | OA = 97.00 |
| 2005 | Paddy Field | 27 | 1 | 0 | 0 | 96.43 |
| | Low Vegetation | 0 | 71 | 1 | 0 | 98.61 |
| | Forest | 1 | 3 | 187 | 0 | 97.91 |
| | Built-up | 0 | 0 | 0 | 9 | 100.00 |
| | PA (%) | 96.43 | 94.67 | 99.47 | 100.00 | OA = 98.00 |
| 2010 | Paddy Field | 29 | 0 | 0 | 0 | 100.00 |
| | Low Vegetation | 0 | 54 | 3 | 0 | 94.74 |
| | Forest | 1 | 2 | 203 | 0 | 98.54 |
| | Built-up | 0 | 0 | 0 | 8 | 100.00 |
| | PA (%) | 96.67 | 96.43 | 98.54 | 100.00 | OA = 98.00 |
| 2015 | Paddy Field | 26 | 0 | 0 | 0 | 100.00 |
| | Low Vegetation | 1 | 60 | 0 | 0 | 98.36 |
| | Forest | 0 | 4 | 201 | 0 | 98.05 |
| | Built-up | 0 | 0 | 0 | 8 | 100.00 |
| | PA (%) | 96.30 | 93.75 | 100.00 | 100.00 | OA = 98.33 |
| 2020 | Paddy Field | 21 | 2 | 0 | 1 | 87.50 |
| | Low Vegetation | 1 | 57 | 1 | 0 | 96.61 |
| | Forest | 0 | 3 | 205 | 0 | 98.56 |
| | Built-up | 0 | 0 | 0 | 9 | 100.00 |
| | PA (%) | 95.45 | 91.94 | 99.51 | 90.00 | OA = 97.33 |
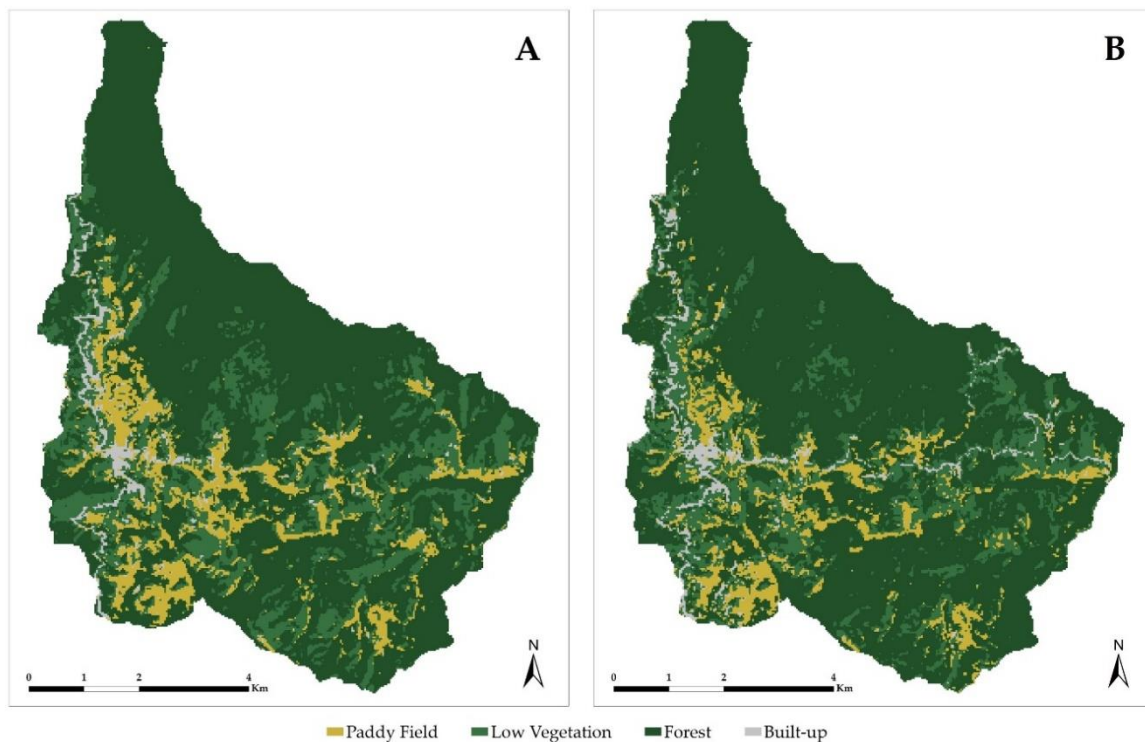
Fig. 3.6 The land cover of the Bangaan watershed at the start and end of the three-decade time period: (A) The land cover map in 1990; (B) The land cover map in 2020.

Time-series land cover maps from 1990 to 2020, in five-year intervals, were produced. The minimum overall accuracy of the land cover maps was 97.00% (for the years 1990 and 2000), the minimum producer's accuracy was 89.66% (Paddy field for year 1990), and the minimum user's accuracy was 88.89% (Built-up for the years 1990 and 2000) (Table 3.3). These accuracies indicated that the land cover maps produced were accurate and reliable to be used for land cover transition analysis. The high accuracies of the maps may be attributed to the large number of training samples from the second round of classification and the post-classification procedures.

From 1990 to 2020, paddy fields and low vegetation covers in the Bangaan watershed experienced net loss in area (Fig. 3.6). The paddy fields in the terraces experienced the most decrease in area, where it only retained 60% of its original cover and expanded only to other land cover by 17%, having only 77% of net area from 1990 (Table 3.4). Low vegetation only retained 60% of its original cover and expanded by 28%, having 88% of net area from 1990. On the other hand, forest and built-up covers experienced net gains in area. Forests retained 93% of its original cover, and expanded by 14%, having a net area of 107% from 1990. Built-

up, although retaining only 59% of its original cover, expanded to other areas by 65%, having a net area of 114% from 1990.

All land cover types also underwent both increases and decreases in area (Fig. 3.7). Paddy fields experienced a decrease in area of 113 ha from 1990 to 2000. It experienced a slight increase of 37 ha in the following ten years from 2000 to 2010 before experiencing a decrease of 69 ha from 2010 to 2020. Forests experienced almost alternating increases and decreases in area, but it notably experienced a sharp increase of 304 ha in the 2005–2010 period. Same with the forests, low vegetation cover experienced almost alternating changing trends, but on the other hand, experienced a sharp decrease of 303 ha in the 2005–2010 period. Built-up was relatively stable, with the highest magnitude of change at 30 ha (increase) in 2015–2020.
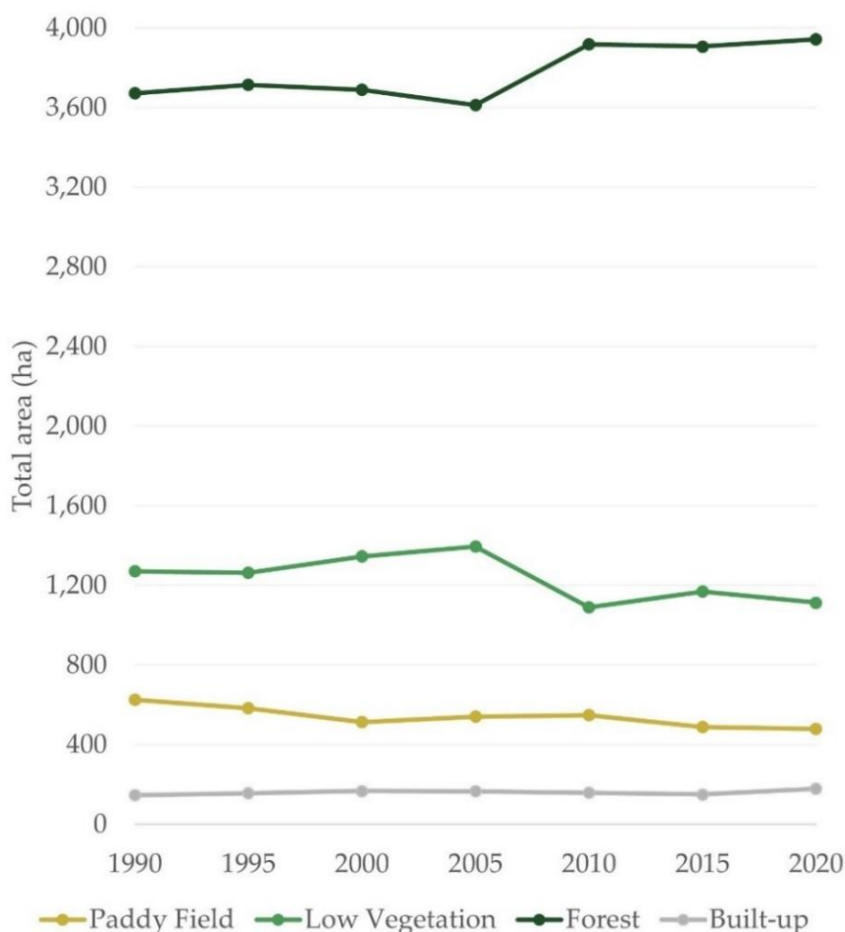


Fig. 3.7 Trend in total area of the four land cover types in the Bangaan watershed from 1990 to 2020

Table 3.4 The overall retained areas, reduction, and expansion of the land cover types from

1990 to 2020. Percentage is ratio with the 1990 land cover type area

| Land cover type | Retained areas | | Total reduction | | Total expansion | |
|---|---|---|---|---|---|---|
| | (ha) | (%) | (ha) | (%) | (ha) | (%) |
| Paddy field | 374 | 60 | 252 | 40 | 105 | 17 |
| Low vegetation | 761 | 60 | 511 | 40 | 352 | 28 |
| Forest | 3,418 | 93 | 253 | 7 | 524 | 14 |
| Built-up | 85 | 59 | 60 | 41 | 94 | 65 |
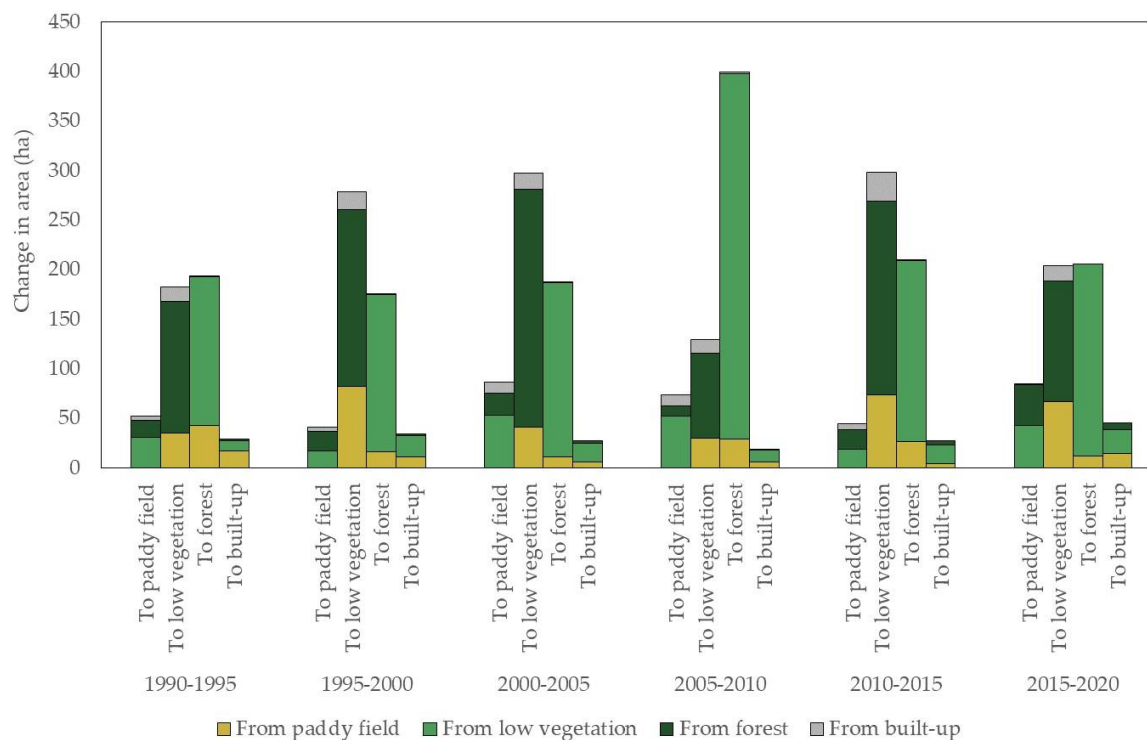


Fig. 3.8 The magnitudes of transitions between the four land cover types in the watershed for each five-year period. The total area of a color per period indicates the total transition from a land cover type while the total area of a column indicates the total transition into the land cover type.

### 3.3.2. Land cover transitions

When the net area of a land cover type changes, a transition between land cover types occurs (Fig. 3.8, Fig. 3.9). For most land cover transitions that occurred, low vegetation acted as a dominant transition source and transition outcome; the other land cover types (Paddy field, Forest, Built-up) mostly transitioned from and into low vegetation. It appears that low vegetation acts as an intermediary land cover for transitions. In the three-decade study period,

most transitions occurred between paddy fields, low vegetation, and forest; there was only a relatively small amount of change in built-up per period compared with the other land cover types. From a spatial perspective, the same areas in the study area experienced multiple transitions in the three-decade period, such that first-time transitions were almost followed later on by another transition.
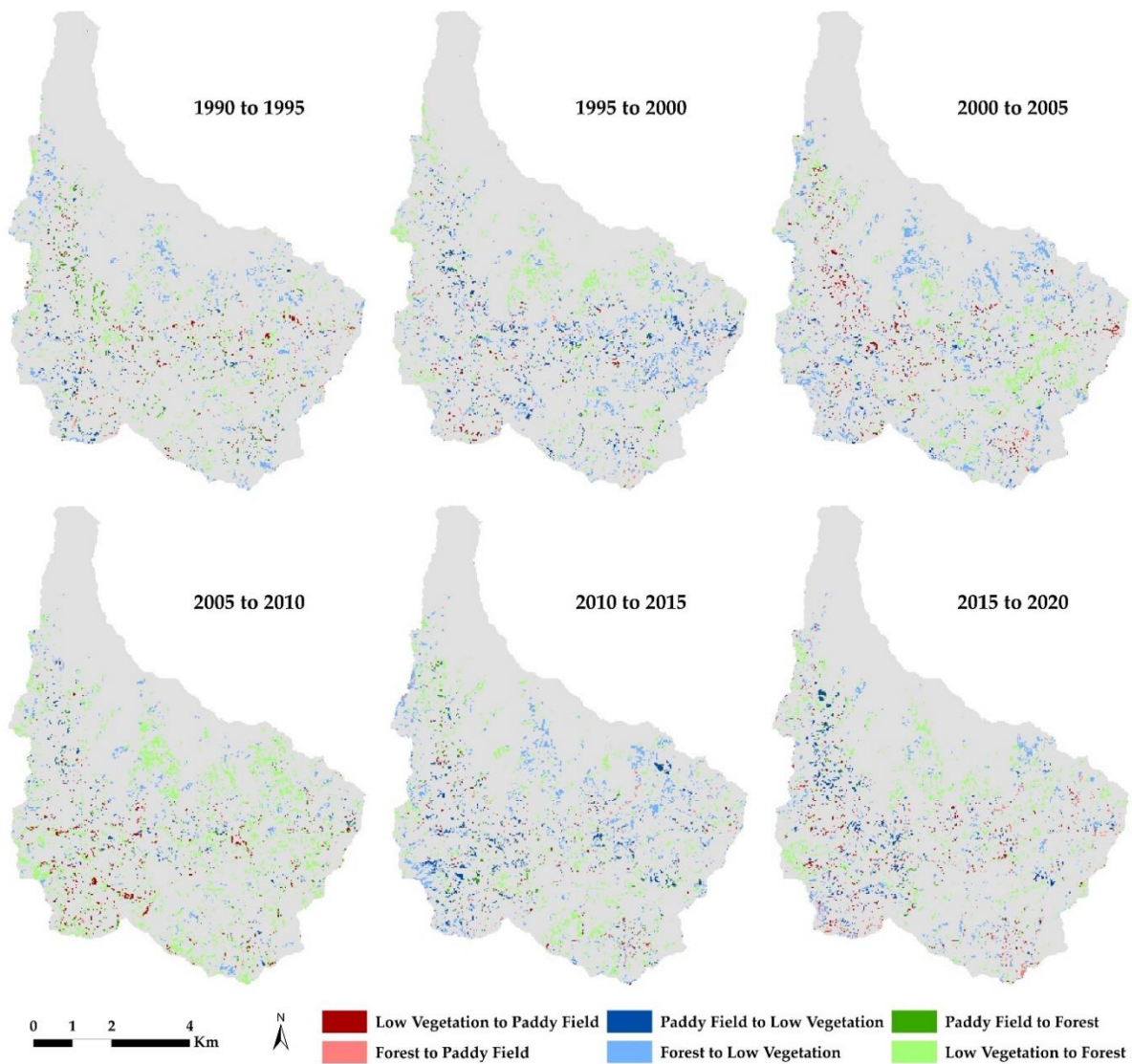


Fig. 3.9 Spatial pattern of land cover transitions between paddy field, low vegetation, and forest for each five-year period from 1990 to 2020. Built-up was not included in the visualization because of relatively low magnitude of change

Throughout the three-decade study period, "from low vegetation to forest" and "from

forest to low vegetation" transitions were constantly the largest transitions in the landscape. Forest and low vegetation covers regularly interchanged between each other at large and almost alternating rates. Forest transitioned more to low vegetation in the 1995–2000, 2000–2005, and 2010–2015 periods, while low vegetation transitioned more to forest in the 1990–1995, 2005–2010, 2015–2020. Notably, there was a relatively large transition of 369 ha from low vegetation to forest in the 2005–2010 period, making up 70% of the total expansion of forest and 72% of the total reduction of low vegetation in the three-decade study period.

For most periods, transitions from paddy fields (agricultural abandonment) exceeded transitions to paddy fields (agricultural expansion). For the periods 2000–2005 and 2005–2010, agricultural expansion exceeded agricultural abandonment by 28 ha and 8 ha, respectively. However for all other periods, agricultural abandonment exceeded expansion in average by 36 ha. This greater rate of agricultural abandonment compared with expansion may be accounted for the overall net decrease of paddy fields through the three-decade study period.
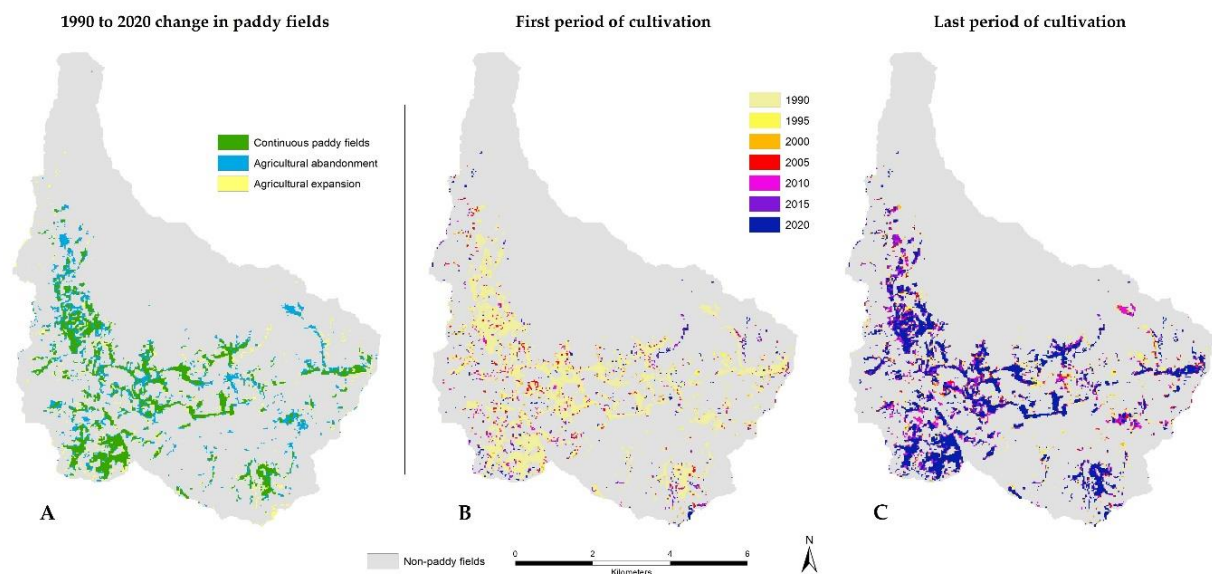


Fig. 3.10 Spatio-temporal patterns of paddy field cultivation from 1990 to 2020: (A) The overall land cover change in paddy fields in the three-decade period; (B) The period when an area was first cultivated; (C) The period when an area was last cultivated.

*3.3.3. Dynamics of paddy fields*

Maps of the first and last period of cultivation in the paddy fields showed different years when agricultural expansion and abandonment were abundant (Fig. 3.10B and C). In the periods from 1990 to 2020, first-time cultivations occurred at a rate of 36 ha per five-year period, with no period having a notable magnitude (Fig. 3.11). On the other hand, permanent abandonment occurred at an average of 61 ha per five-year period, almost double the area of first-time cultivations. Notably, the years of 2010 and 2015 had the highest area of permanent abandonment at 88 ha and 94 ha, respectively. Overall, from 1990 to 2020, the areas permanently abandoned exceeded the areas newly cultivated, making the total area of paddy fields lower by 2020 (Fig. 3.10A).

Analysis of the dynamics of paddy fields also confirms the regular occurrence of fallowing and recultivation in the landscape (Fig. 3.11). From 1990 to 2015, the area of fallowed paddy fields was constantly decreasing, indicating that the practice of fallowing has been decreasing. Fallowing had relatively high occurrence between 1990 and 2000 at an average of 52 ha per five-year period compared with the occurrence between 2000 and 2010 at an average rate of 20 ha per five-year period. It should be noted that there were no fallowed areas in the 2015–2020 period as future recultivation cannot be determined. Meanwhile, recultivation varied for every period. In the 2000–2005 period, recultivation increased by 416% compared to the value in the 1995–2000, indicating that large-scale agricultural expansion occurred in this period. It should also be noted that there were no recultivated areas in the 1990–1995 period as previous fallowing cannot be determined.
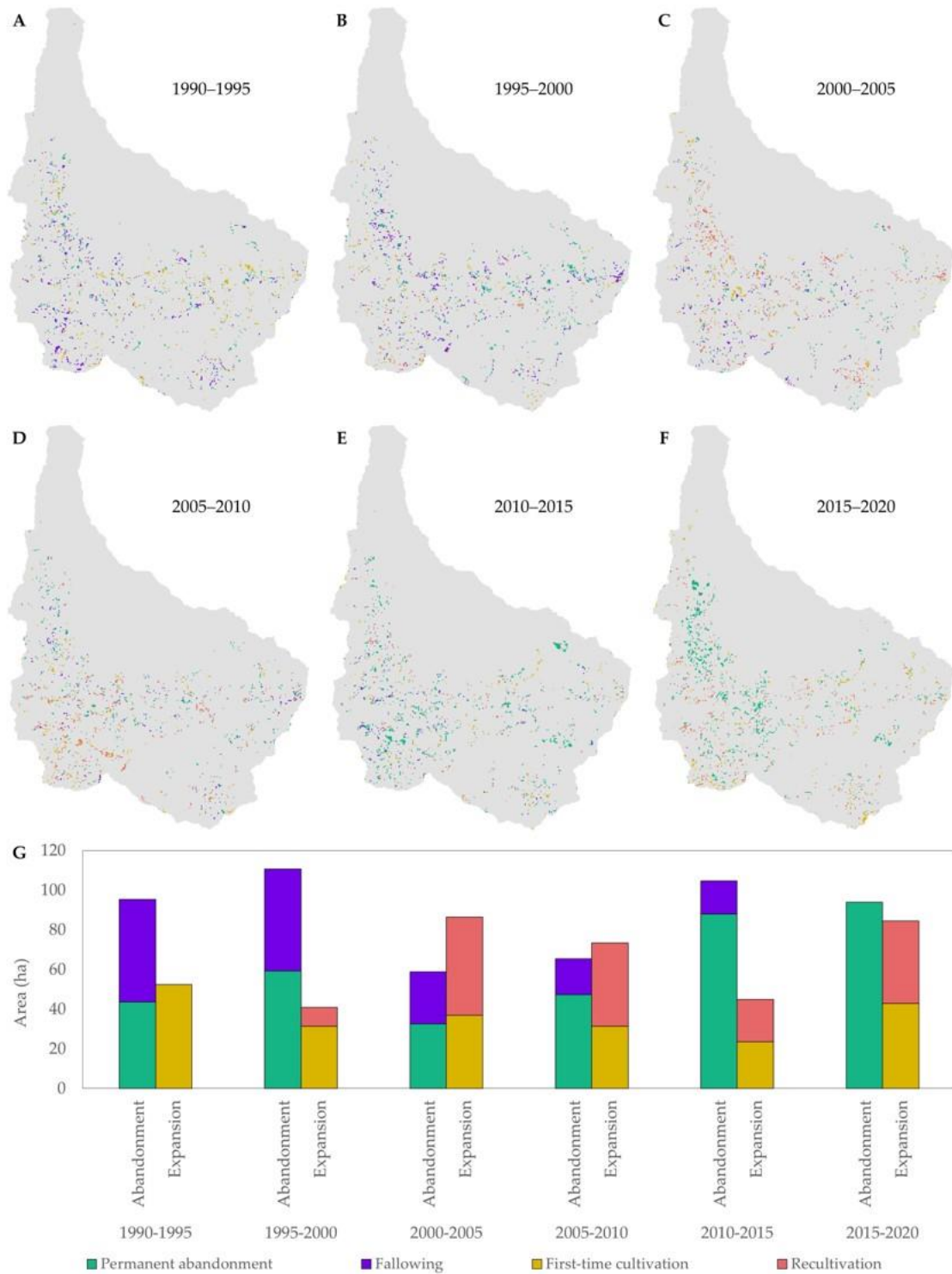
Fig. 3.11 Dynamics of paddy fields for every five-year period from 1990 to 2020: The spatial distribution of paddy field dynamics in (A) 1990–1995; (B) 1995–2000; (C) 2000–2005; (D) 2005–2010; (E) 2010–2015; (F) 2015–2020; (G) Magnitude of changes for each period. The total area of a column indicates the total agricultural abandonment or expansion per period.
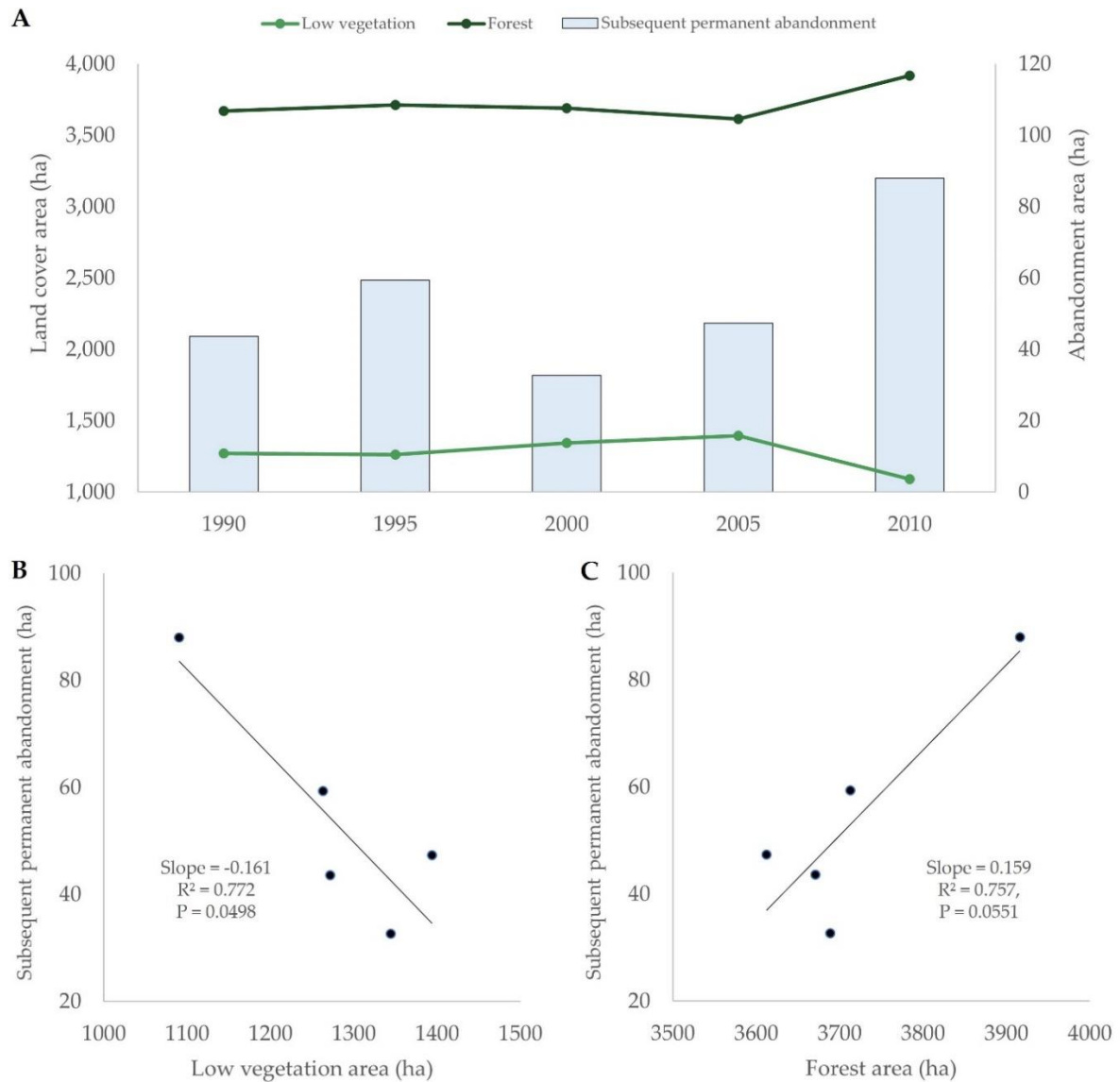
Fig. 3.12 Relationship between abundance of vegetation land cover types and permanent abandonment of paddy fields from 1990 to 2020: (A) The temporal variation of low vegetation area, forest area, and subsequent permanent paddy field abandonment; (B) Correlation between low vegetation area and subsequent permanent abandonment; (C) Correlation between forest area and subsequent permanent abandonment.

### 3.3.4. Relationship of vegetation abundance to paddy field abandonment

Total area of low vegetation cover had a significant inverse relationship with subsequent permanent abandonment of paddy fields (Slope = $-0.161$, $R^2 = 0.772$, $P = 0.0498$) (Fig. 3.12B). In general, higher areas of low vegetation led to lower rates of permanent paddy

field abandonment (Fig. 3.12A). For forests, total area had a direct relationship with subsequent permanent abandonment (Slope = 0.159, $R^2$ = 0.757, P = 0.0551) (Fig. 3.12C), with higher forest areas leading to higher rates of permanent paddy field abandonment.

## 3.4. Discussion

### 3.4.1. Land cover transitions

Analysis of land cover transitions in consistent five-year intervals showed that the mountainous agricultural landscape of Ifugao rice terraces undergo frequent rapid transitions. Transition maps also showed that the same areas experienced multiple transitions throughout the three-decade study period. Regularity of land cover transitions is in line with studies on agroecosystems in mountainous agricultural landscapes (Aguilar et al., 2021; Liang et al., 2020). These agricultural systems are examples of socio-ecological systems where humans interact with agricultural lands, forests, and other land cover types, and in turn cause the regular transitions in land cover in these landscapes.

Specifically in the Ifugao rice terraces, the farmers practice slash-and-burn for the swidden fields which converts forest cover into low vegetations cover (Avtar et al., 2019). Swidden fields when left alone are then converted to woodlot, which may cause afforestation (Herzmann et al., 1998; Serrano & Cadaweng, 2005). Tree cutting for woodcarving or fuel and planting of seedlings are also common practices in the area. (Camacho et al., 2016). The occurrence of these traditional practices may explain the frequent transition between forest to low vegetation. However, in the past decades, local people doing these practices have decreased due to emigration and lack of successors (Calderon et al., 2009; Dizon et al., 2012). The decrease of occurrence of these practices may have driven the long-term decrease of low vegetation, especially in the 2005–2010 period.

Previous studies have established that agricultural abandonment in mountainous agricultural landscapes consequently result to afforestation (Gellrich, Baur, Koch, et al., 2007; Gellrich & Zimmermann, 2007; Kobler et al., 2005). These studies however have only observed the long-term changes in the landscape. The land cover transition analysis in this study revealed that typically a two-step transition process occurs between agricultural abandonment and afforestation. Low vegetation acts as an intermediary land cover type for

transitions between paddy field and forest. Hence, paddy fields first transition into low vegetation cover before transitioning into forests.

Low vegetation being an intermediary land cover for transitions may also explain its large variation in changes through the three-decade time period. Low vegetation regularly undergoes multiple transitions hence is vulnerable to changes in total area. Grassland, being one of the land use types under low vegetation land cover, may also be a reason for the large changes observed in this study.. Xystrakis et al. (2017) observed that grassland is a dynamic land cover and large changes in area occurred in all periods of their study. Along with grassland, swidden fields are also dynamic land use types, with active periods spanning two to five years and fallows periods of up to five years (Camacho et al., 2016).

*3.4.2. Paddy field dynamics*

Farmers in the Ifugao rice terraces traditionally practice fallowing of paddy fields to allow the land to recover, hence cultivation of paddy fields are always in a cycle of continuous cultivation, a period of fallowing, then recultivation (Herath et al., 2015). This agricultural cycle in turn lead to the observed dynamics in paddy fields and the regular transitions from and to paddy fields.

Along fallowing and recultivation, permanent abandonment and first-time cultivation of paddy fields have also been observed, with permanent abandonment having a much greater average rate than first-time cultivations, evident by the total area of the paddy fields being much lower in the year 2020 than in 1990. In the periods from 1990 to 2000, large rates of permanent abandonment were observed. This observation is in line with historical accounts as in 2001, the Ifugao rice terraces was put in UNESCO's List of World Heritage in Danger due to increasing abandonment and degradation in the rice fields (UNESCO, n.d.). After this declaration, the Philippine government established the Ifugao Rice Terraces Cultural Heritage Office (IRTCHO) in 2003 that oversaw the conservation of the rice terraces and the drafting of a 10-year master plan (Calderon et al., 2009). Based on the master plan, projects were implemented for water management, agricultural management, watershed management, hazard management, transport development, spatial restructuring and tourism development, cultural enhancement, and livelihood development (UNESCO, 2005). In the periods from 2000 to 2010, it was observed that first-time cultivation and recultivation rates occurred at rates much higher

than previous occurrences, hence signifying that such implemented projects were successful in restoring parts of the terraces. Consequently, the Ifugao rice terraces was removed from the List of World Heritage in Danger in 2012 (UNESCO, n.d.). However, the problem of agricultural abandonment still persisted after (FAO, 2018), as was observed in the large area of permanent abandonment observed from 2010 to 2020.

As with the case of Ifugao rice terraces, agricultural abandonment has also been observed to occur in other mountainous agricultural landscapes (Gellrich, Baur, Koch, et al., 2007; Gellrich & Zimmermann, 2007; Xystrakis et al., 2017). In fact, a review by MacDonald et al. (2000) found that most mountainous landscapes around Europe have experienced widespread abandonment after World War II. Modica et al. (2017) have also observed dynamics of fallowing and recultivation in the terraced landscape of Costa Viola in Italy using photo interpretation. The study found that some of the terraces that were active at the start and end of the study period were once abandoned during the period. At the same time, some of abandoned terraces were also active at some point, indicating that dynamics of fallowing, recultivation, permanent abandonment, and first-time cultivation also occurred in other mountainous agricultural landscapes. In all of these studies, agricultural abandonment occurred in such landscapes due to socio-economic factors such as high cultivation costs in steep areas and migration to lowland areas. As the world undergoes modernization, the difficult cultivating conditions in mountainous agricultural landscapes create lower wages which prompt farmers to seek better working and living conditions. This situation leads to the abandonment of agricultural lands, which through time leads also to natural afforestation.

*3.4.3. Relationship between vegetation abundance and permanent paddy field abandonment*

The results showed a significant inverse relationship between abundance of low vegetation cover and subsequent permanent abandonment of paddy fields. Studies have shown that forest regeneration leads to a decrease in water yield (García-Ruiz & Lana-Renault, 2011; Soriano & Herath, 2018). Forest cover decreases the water yield because forest canopy intercepts water and exotic trees decrease low flow, the stream of water during dry season (Bonnesoeur et al., 2019). Grasslands in high elevations also have water yield 40% greater than tree plantations (Bonnesoeur et al., 2019). As a consequence, a higher low vegetation cover and lower forest cover in the landscape indicate higher water recharge. As water scarcity is one

of the factors for terrace abandonment in the Ifugao rice terraces (Calderon et al., 2009; Camacho et al., 2016), a higher area of low vegetation cover and lower area of forest cover would also indicate a lower rate of permanent paddy field abandonment.

### 3.4.4. Implication for landscape planning

Overall, the abundance of low vegetation and forest cover forms a feedback loop with permanent abandonment of the paddy fields (Soriano & Herath, 2018) (Fig. 3.13). As part of the socio-ecological system in the Ifugao rice terraces, traditional practices of the local farmers regularly alter the paddy field, low vegetation, and forest covers in the mountainous agricultural landscape. These practices have been sustainable for several generations as the condition of the terraces can be retained. However, due to a variety of driving forces such as emigration, lack of successors, and water scarcity, permanent abandonment of paddy fields occurs (Calderon et al., 2009; Camacho et al., 2016; Dizon et al., 2012). Permanent abandonment of paddy fields leads to transitions into low vegetation cover, which later on transitions into forest cover. Increase of forest cover or afforestation alters the hydrological balance in the watershed, decreasing the water resources for the paddy field. This decrease in water resources again causes permanent abandonment which starts the feedback loop, making the condition of the terraces in the mountainous agricultural landscape unsustainable to be retained. Based on this mechanism in the Ifugao rice terraces, the Local Government Unit (LGU) should look into developing policies to mitigate both the social and environmental driving factors to maintain the Ifugao rice terraces.

For the social factors, different programs and policies have already been initiated by the LGU to maintain the farmers in the terraces. A sustainable financing mechanism has been proposed where payment from tourists is to be optimized and allocated to farmers to prevent emigration (Calderon et al., 2009). A program was also initiated where wood carving and fabric weaving were promoted to farmers when it is agricultural off-season to increase income and motivate them to still engage in agriculture (Agoot, 2018). A school has also been established called "School of Living Traditions" that teaches the culture of the Ifugao indigenous community and promotes the maintenance of the rice terraces to the younger generation (Dulnuan, 2014).
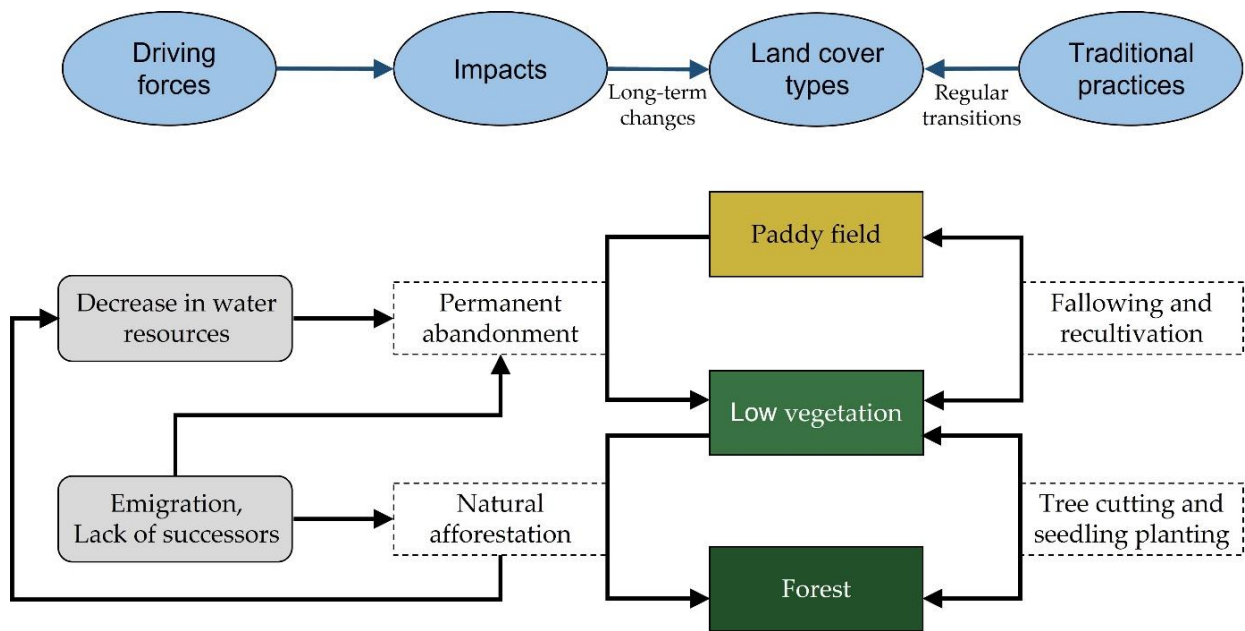
Fig. 3.13 Overview of the land cover processes occurring in the mountainous agricultural landscape. Land cover processes are either regular transitions caused by traditional practices and long-term changes caused by driving forces. The driving forces and the resulting impacts form a feedback loop that will continue to decrease the area of paddy fields and low vegetation, and increase the area of forests (modified from Soriano and Herath, 2018).

To maintain the water supply, the status of the paddy fields should be prioritized. Afforestation starts with the permanent abandonment of paddy fields, hence maintaining the paddy fields prevents further increase of forests, which will maintain the water supply. To maintain the paddy fields, the social problems stated before should first be addressed to prevent further abandonment. This implies that mitigating the social driving factors also help in mitigating the environmental driving factors. Maintaining the population of agricultural practitioners also maintains the area of low vegetation cover.

The LGU should also take into account the trade-offs in ecosystem services brought by changing land cover. The decrease of paddy field and low vegetation covers and increase in forest cover brings an increase in other ecosystem services such as carbon sequestration and habitat quality (S. Yang et al., 2018). Analyzing the ecosystem trade-offs should also be done hand-in-hand with analyzing sustainability of the different aspects in the mountainous agricultural landscape such as economic, environmental, and social aspects. In the end, the local community should benefit with drafted policies as they are the ones interacting with the landscape.

*3.4.5. Advantages of the mapping and analysis frameworks*

As was implemented by Alencar et al., (2020), two rounds of image classification were implemented. The first round used training samples extracted from image interpretation to create land cover classification images from Random Forest models. The second round of classification used recurring land cover types from the initial classified images to train a second batch of Random Forest models. Applying a second classification model where the training points were extracted from recurring land cover locations provided more training samples which provided more spectral signatures for training the Random Forest models. This procedure produced more accurate land cover maps which made the land cover transition analysis reliable.

The developed framework for analyzing paddy dynamics provided an in-depth analysis of the spatio-temporal patterns of fallowing and recultivation in paddy fields based on land cover maps. The approach for analyzing paddy field dynamics was able to uncover periodic dynamics of permanent abandonment, fallowing, first-time cultivations, and recultivation. This analytical framework can be applied not only in mountainous agricultural landscapes but also in agricultural lands in general where dynamics of cultivation need to be monitored. These data provide a more detailed view on farmer actions and how cultivation patterns can cause changes in land cover. In the future, these data on farmer actions can be related with social and environmental factors to determine the drivers for these cultivation patterns.

## 3.5. Conclusion

Due to modifications by local people and challenges from globalization, mountainous agricultural landscapes tend to undergo frequent land cover changes which includes agricultural abandonment and afforestation. Hence, it is important that transitions in land cover and dynamics of paddy fields are analyzed to draft information-based policies for the management and conservation of these cultural landscapes. The current study utilized the quick cloud-computing capability of Google Earth Engine to map five-year interval land cover maps in a mountainous agricultural landscape (Ifugao rice terraces, Philippines) from 1990 to 2020 then analyzed the land cover transitions and paddy field dynamics. Unlike in previous land cover change studies in mountainous agricultural landscapes that observed the occurrence of

afforestation due to abandonment of paddy fields, analysis of land cover transitions in this study revealed that paddy fields turning into forests typically undergo a two-step process of transitioning first into low vegetation before transitioning into forests. Transitions between low vegetation and forest was also observed to be regularly occurring at high rates, which may be attributed to the traditional practices of the local people such as tree-cutting and swidden farming. To the best of the author's knowledge, this is the first study to observe temporal dynamics in paddy fields such as permanent abandonment, fallowing, first-time cultivation, and recultivation based on time-series land cover maps. This framework of analysis can be used for analyzing patterns of cultivation in agricultural landscapes to bring informed decisions on the management of these landscapes. Analysis on the long-term changes in the landscape showed that agricultural abandonment has been continuously occurring in the landscape. Although government efforts have been successful in recultivating the paddy fields from 2000 to 2010, permanent abandonment have increased again after this period. It was also found that the abundance of low vegetation cover has a significant inverse relationship with subsequent permanent abandonment of paddy fields, which coincides with previous studies showing that decreasing water yield from afforestation contributes to the abandonment of paddy fields. Given the continuous abandonment of paddy fields in the landscape, planning of the conservation of the terraces should also consider the abundance of other vegetation cover types aside from existing social driving factors. In the future, analysis of the change in ecosystem services due to the observed land cover transitions will aid in land use planning of the landscape. In-depth study of the driving factors for the observed paddy field dynamics is also worth investigating. Lastly, the mapping and analysis frameworks applied in this study can be utilized in future temporal land cover change analysis. The mapping framework that utilized two rounds of classification to generate more training samples can provide more coherent time-series land cover maps. Meanwhile, the analysis framework that explains the temporal dynamics of cultivation in agricultural lands can be used to elucidate farmer actions in relation to spatial drivers.

# Chapter 4:

## Identifying the drivers of agricultural abandonment

## 4.1. Introduction

Land use/cover change (LUCC) continuously occur on the surface of the earth as a result of complex interactions between socio-economic and environmental drivers (Geist et al., 2006; He et al., 2022; Mitsuda & Ito, 2011). In the current age of globalization, LUCC typically occur as urban expansion where non-urban land use types are converted for urban use (Güneralp & Seto, 2013; Seto et al., 2011; van Vliet, 2019). Along with continuous urban expansion, globalization also drives the occurrence of other LUCC such as agricultural abandonment, deforestation, and reclamation (W. Cao et al., 2021; Hou et al., 2021; Wu et al., 2016; Xystrakis et al., 2017). As human society continuously interacts with the global environment to acquire its needs, hence forming perpetual socio-ecological systems (SES), it is expected that human activities will continuously cause impacts on the environment leading to recurring LUCC (X. Li et al., 2017; Synes et al., 2019). These LUCCs cause alterations in ecosystem services that can lead to multifaceted environmental problems (B. Li et al., 2016; Y. Liu et al., 2020; Wang et al., 2018; Zhang et al., 2019). Thus, it is imperative that future LUCC based on current trends can be projected so that planners will have the technical information to devise counter-interventions to mitigate the escalation of subjected LUCCs.

For simulating the future status of land, several LUCC models and tools have been developed in previous research (T. Liu & Yang, 2015; Ren et al., 2019; Verburg et al., 2019). LUCC models can be placed along a spectrum of pattern-based to process-based model types (Ren et al., 2019), On one end of the spectrum, the process-based models, which adopt "bottom-

up" approach, simulate the behavior and interactions of system actors to predict the emergent spatial patterns of land cover. These models are useful for simulating scenarios based on management policies, thus they can act also as decision models. However, development of process-based models is limited by the availability of empirical resources and the ability to capture the significant system processes, hence most of the time cannot achieve high land cover prediction accuracy (T. Liu & Yang, 2015; Ren et al., 2019). On the other hand, pattern-based models, which adopt a "top-bottom" approach, map future land cover based on historical patterns by utilizing statistical or machine learning approaches (Boavida-Portugal et al., 2016). The advantage of such models is that future land cover maps can be simulated with relatively more available data even with lack of knowledge of the processes of the LUCC. Within statistical approaches, a demand-allocation approach is implemented where Markov chains compute the demand or quantitative data of LUCC while logistic models compute the allocation of the quantitative data into a map through probability maps. A limitation of this purely statistical approach is that only spatial drivers can be incorporated, but in reality, non-spatial drivers have significant effects in the quantity of LUCC. To address this limitation, hybrid models have also been developed which, like pattern-based models, adopt a demand-allocation approach but integrates process-based models to represent the demand component so that non-spatial drivers can be incorporated to project LUCC. For example, System Dynamics has been used in several studies to represent how aggregated system structures affect the quantity of LUCC (Dang & Kawasaki, 2017; Mao et al., 2014; Xu et al., 2016). Previous studies have also incorporated Agent-based models (ABM) to incorporate the decision making in an SES (D. Liu et al., 2020; Mustafa et al., 2017; Tang & Yang, 2020).

Although there already exist hybrid models that can incorporate non-spatial drivers to project future LUCC, two limitations can be found in the usage of these models. First, as much as current hybrid models can accept various non-spatial variables as inputs, it is possible that the variables being used by a specific model may not be significant drivers of an LUCC being studied. For example, agricultural abandonment is a multifaceted global phenomenon that is driven by various drivers depending on the social, economic, and environmental settings of a landscape (Gellrich & Zimmermann, 2007; Osawa et al., 2016; Pazúr et al., 2020). It is thus necessary that in projecting the future agricultural abandonment in a study area, the significant spatial and non-spatial drivers be first identified so that they can all be incorporated in a simulation model. Second, development of a model that incorporate all the significant drivers

of an LUCC model requires capturing the complexity of the interactions and feedbacks of all these drivers in a socio-ecological system (T. Liu & Yang, 2015; Ren et al., 2019). However, modeling of these systems requires the participation of experts and stakeholders which possess the empirical knowledge regarding the SES in hand and a skilled modeler that can devise a model structure to incorporate this empirical knowledge. For planning purposes, the participation of such knowledgeable and skilled personnel is mostly not feasible. For simple prediction purposes such as projecting LUCC brought by changes in some driving factors, a more general statistical model which can also incorporate non-spatial drivers can be useful. Looking into the spectrum of process-based to pattern-based models of LUCC, there has not been a previously developed statistical pattern-based model that can incorporate non-spatial drivers.

In order to propose a method of identifying both the significant spatial and non-spatial drivers of LUCC and simplifying the projection of future LUCC, this study presents a statistical model of LUCC which integrates both a logistic model based on spatial explanatory variables and a linear model based on non-spatial explanatory variables. Specifically, the proposed statistical model simulates LUCC by mapping a probability map and a global probability threshold through the logistic model and linear model, respectively. By comparing each pixel in the probability map with the global probability threshold, the true-or-false occurrence value of LUCC in every pixel is mapped. To test the statistical model's capability in simulating LUCC maps, the model was applied in simulating the agricultural abandonment in the Ifugao rice terraces in the Philippines, where a UNESCO World Heritage site is situated. The accuracies of the simulated maps were assessed by comparing the simulated maps with actual maps of agricultural abandonment using map comparison accuracy measures.

## 4.2. Model description

In pattern-based and hybrid models of LUCC, a logistic model is used to act as an allocation component which produces a probability map (also called suitability map) of occurrence of an LUCC (Gellrich, Baur, Koch, et al., 2007; Hu & Lo, 2007). A logistic model is expressed as a function of the form

$$P(u, v, t) = \frac{1}{1+e^{-\left(a_0 + \sum_{i=1}^{m} a_i x_i(u,v,t)\right)}} = \frac{1}{1+e^{-(a_0 + a_1 x_1 + a_2 x_2 + \cdots + a_m x_m)}} \qquad \text{(Eq. 4.1)}$$

where $P$ is the probability of the LUCC to occur at a pixel of indices $(u, v)$ at a time period $t$ and has a range from 0 to 1 where a higher value indicates a higher likelihood of LUCC occurrence, $x_i(i = 1,2,\ldots,m)$ is a spatial explanatory variable that varies through space and time, and $a_i(i = 0,1,\ldots,m)$ is a parameter estimated from logistic regression, where $a_0$ is the intercept and $a_1$, $a_2$, …, $a_m$ are the respective coefficients of the spatial explanatory variables $x_1$, $x_2$, …, $x_m$ (Cheng & Masser, 2003; Shu et al., 2020). Logistic regression, which estimates the parameters of the logistic model, is implemented by denoting a binary variable $Z$ as a dependent variable, where Z takes only values of 1 or 0, a value of 1 denoting the LUCC occurred while 0 denoting the LUCC did not occur. However, as the logistic model only produces values of probability that ranges from 0 to 1, the logistic model in the form of Equation 4.1 does not produce the spatial pattern of occurrences of LUCC but instead produces just the spatial pattern of probability. Hence, for the simulation of future LUCC, a demand module is incorporated which produces quantitative data based on non-spatial explanatory variables (T. Liu & Yang, 2015; Ren et al., 2019). Different types of demand modules have been utilized such as System dynamics (Dang & Kawasaki, 2017; Mao et al., 2014; Xu et al., 2016), and Agent-based Modeling (Tang & Yang, 2020).

A workaround from computing a quantitative data of LUCC is to implement thresholding of probability values in a probability map. Thresholding is implemented by assigning a global probability threshold $P_{threshold}$ and using the following equation to compute for the LUCC occurrence $Z$:

$$Z(u, v, t) = \begin{cases} 1, & P(u, v, t) > P_{threshold}(t) \\ 0, & P(u, v, t) \leq P_{threshold}(t) \end{cases} \qquad \text{(Eq. 4.2)}$$

Equation 4.2 indicates that the occurrence of LUCC in a pixel is based on the comparison of the pixel's probability value with a global $P_{threshold}$ at period $t$ with the probability value in a pixel, where the lower is the $P_{threshold}$, the higher is the chance that the LUCC will occur in the pixel. Thus the $P_{threshold}$ acts as a global model parameter that increases or decreases the likelihood of LUCC in a map, hereby affecting the quantitative value of LUCC in an inversely proportional manner. This also implies that different probability threshold values will produce different simulated maps which will have different accuracies when compared to actual maps of LUCC. Hence, an optimal probability threshold exists where the difference between

simulated and actual maps will be at a minimum and accuracy will be maximized. Previous studies implemented different strategies to find the optimal thresholding values such as through parametric methods (Sandnes, 2011) or by optimizing an objective function (H. Li et al., 2020). In the study, an optimal probability threshold value was determined by implementing an optimization routine with the objective to find the $P_{threshold}$ that maximizes the similarity statistic between simulated and actual LUCC maps.
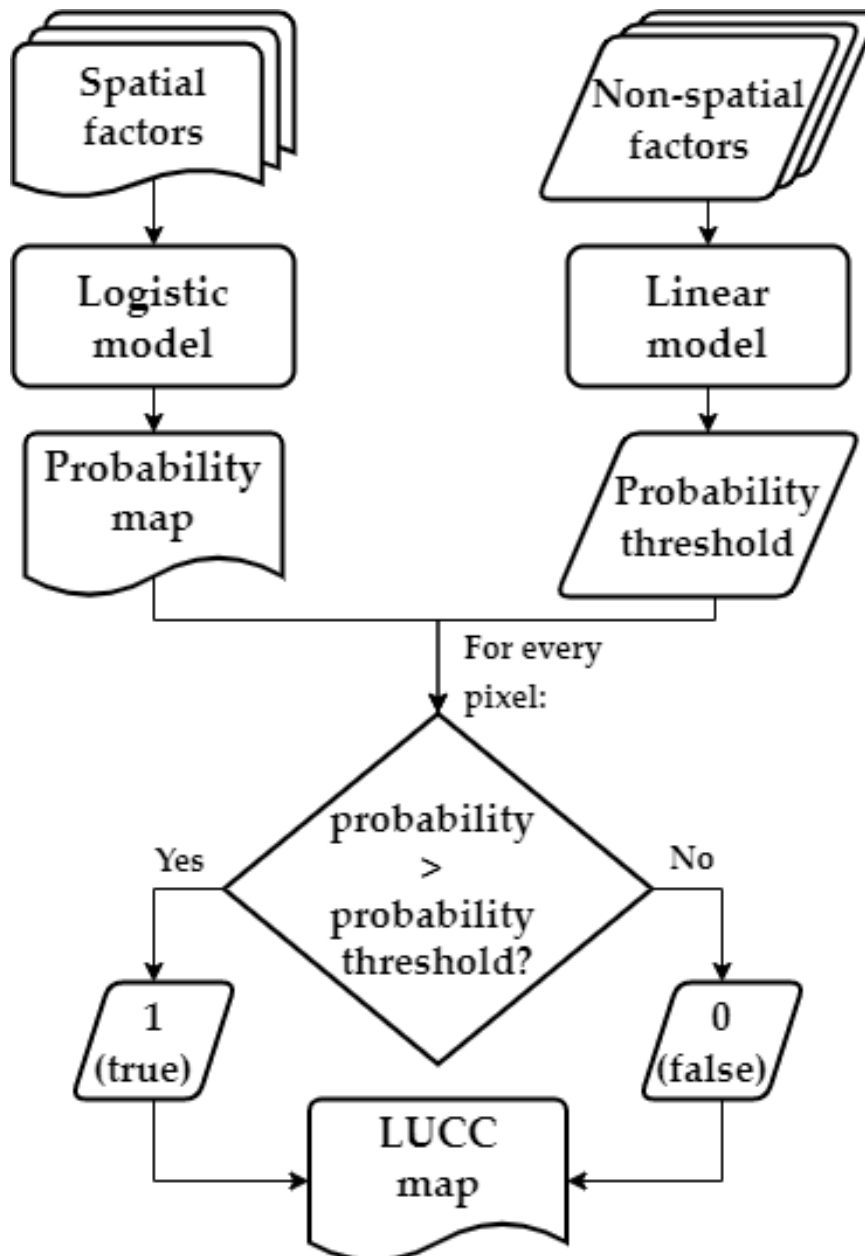


Fig. 4.1 The conceptual framework of the statistical model for simulating maps of LUCC based on spatial and non-spatial factors

The probability of LUCC, $P$, was related to spatial explanatory variables because it is spatial in nature. On the other, the $P_{threshold}$ is a global variable that is constant throughout a study area, thus it is a non-spatial in nature and can be related to non-spatial explanatory variables. To relate the global probability threshold to non-spatial explanatory variables, a linear model is utilized in the form

$$P_{threshold}(t) = b_0 + \sum_{j=1}^{n} b_j y_i(t) = b_0 + b_1 y_1 + b_2 y_2 + \cdots + b_n y_n \qquad \text{(Eq. 4.3)}$$

where $P_{threshold}$ is the global probability threshold value for converting a probability map at time period $t$ into an LUCC map, $y_i (j = 1,2, \ldots, n)$ is a non-spatial explanatory variable that varies through time, and $b_i (j = 0,1, \ldots, n)$ is a parameter estimated from linear regression, where $b_0$ is the intercept and $b_1$, $b_2$, …, $b_n$ are the respective coefficients of the non-spatial explanatory variables $y$, $y_2$, …, $y_n$. To produce the linear model in Equation 4.3, linear regression is implemented where the dependent variable is $P_{threshold}$ values through time and the explanatory variables are non-spatial drivers, variables that are constant through the mapping area but varies through time. Based on accuracy statistics of the linear regression, variables that are found significant for explaining the variation in quantities of LUCC through different periods will be added to the linear model.

Based on equations 4.1, 4.2, and 4.3, this study developed a statistical model which incorporates a logistic model and a linear model for simulating LUCC at pixel $(u, v)$ at time period $t$ with the form:

$$Z(u,v,t) = \begin{cases} 1, & \frac{1}{1+e^{-\left(a_0 + \sum_{i=1}^{m} a_i x_i(u,v,t)\right)}} > b_0 + \sum_{j=1}^{n} b_j y_j(t) \\ 0, & \frac{1}{1+e^{-\left(a_0 + \sum_{i=1}^{m} a_i x_i(u,v,t)\right)}} \leq b_0 + \sum_{j=1}^{n} b_j y_j(t) \end{cases} \qquad \text{(Eq. 4.4)}$$

The left side of Equation 4.4, which comes from the logistic model, dictates the local probabilities of LUCC by producing a probability map based on spatial drivers (Fig. 4.1). The right side of the equation, which comes from the linear model, dictates the global probability of LUCC by computing for a global probability threshold based on non-spatial drivers. By comparing every pixel in the probability map with the global probability threshold, an LUCC map will be produced.
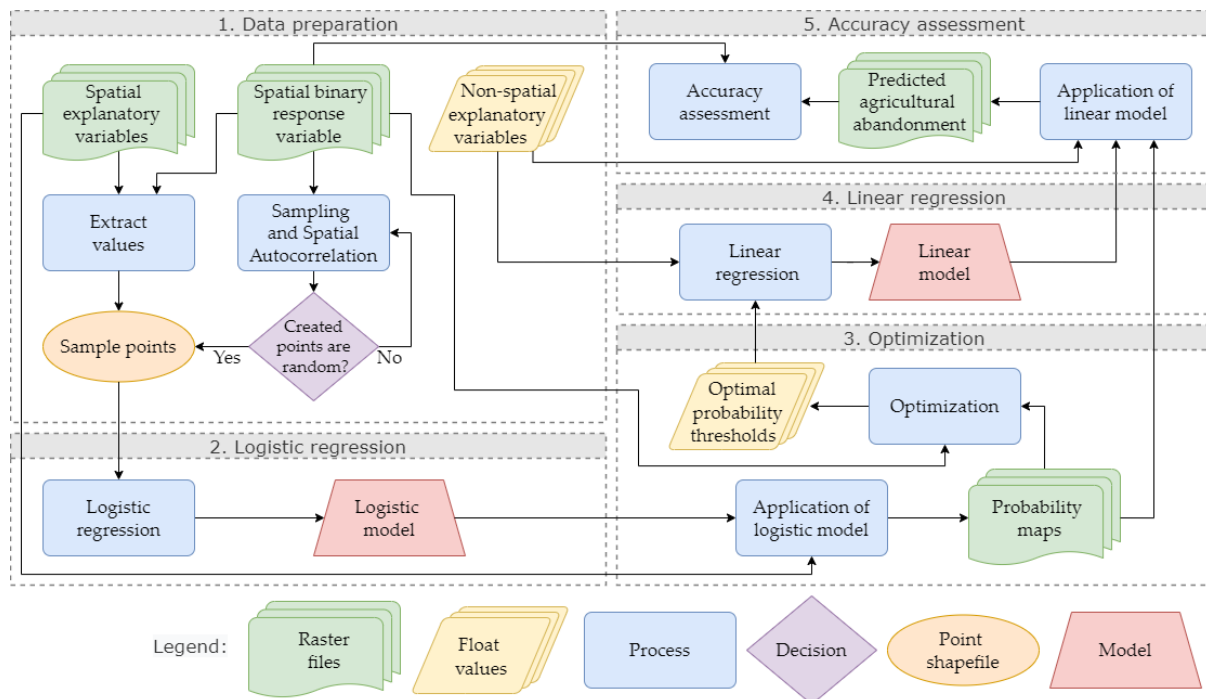
Fig. 4.2 Workflow of the modeling process in five main steps

## 4.3. Methods

The methodological workflow was implemented in five main steps (Fig. 4.2). First, GIS techniques were utilized to prepare spatial and non-spatial data. Second, logistic regression was implemented based on point samples of the binary response variable and spatial explanatory variables to produce a logistic model. Third, optimization based on a Genetic Algorithm (GA) was implemented to find the optimal global probability threshold for every probability map produced by the logistic model. Fourth, linear regression was implemented based on values of the optimal global probability threshold response variable and non-spatial explanatory variables to produce a linear model. Lastly, the accuracies of the simulated maps were assessed by comparing it to the actual maps of agricultural abandonment.

### 4.3.1. Data preparation

Four types of data were prepared for the statistical modeling of agricultural abandonment: Raster files of LUCC binary response variable, vector files of sample points, raster files of spatial explanatory variables, and tables values of non-spatial explanatory

variables.

### 4.3.1.1. Preparation of the LUCC binary response variable

Binary maps of continuously cultivated and permanently abandoned paddy fields were prepared using Geographic Information System (GIS) analysis (Fig. 4.3). First, land cover maps that include a class for paddy field were prepared by acquiring maps of the Ifugao rice terraces from 1990 to 2015 (in five-year intervals) derived by a previous research that utilized Landsat satellite images (Estacio et al., 2022). The class of paddy field was extracted from the acquired land cover maps and reclassified to the value of 0 (indicating false for the subsequent logistic regression). Alongside the land cover maps, maps showing dynamics of the paddy field from 1990 to 2015 such as permanent abandonment, fallowing, first-time cultivation, and recultivation were also acquired (Estacio et al., 2022). The class of permanent abandonment was extracted from these maps and reclassified to the value of 1 (indicating true for the subsequent logistic regression). Using map algebra in ArcGIS, a raster file of paddy field for a year (e.g., 1990) and a raster file of permanent abandonment for the subsequent period (e.g., 1990–1995) were added together to create a single raster file showing permanently abandoned paddy fields (1) and continuously cultivated paddy fields (0). In total, five binary response maps were produced from 1990 to 2015, one for each five-year period.

### 4.3.1.2. Creation of sample points

It is imperative that samples of the binary response variable are not spatially autocorrelated of each other, else sampling bias will arise. Hence, proper point sampling is needed to achieve a spatial autocorrelation which denotes that points are not clustered or dispersed, but random. For a class in the binary response map (0 or 1), random sampling was implemented using the Create Random Points tool in ArcGIS by specifying a 'minimum allowed distance' (starting at 60 m). Depending on the number of points generated by the tool, points are randomly removed or added until 150 points were generated each for permanently abandoned paddy fields and continuously cultivated paddy fields, for a total of 300 points per binary response map. The Spatial Autocorrelation tool was implemented to assess the randomness of the produced points. If the z-score is between -1.65 and 1.65, the points were

considered random. Else if the z-score does not fall between this range, random sampling was reimplemented by increasing the minimum allowed distance and creating random points until the spatial autocorrelation test states that the points are already random. For all binary response maps, sample points achieved a z-score within the desired range and a maximum magnitude of Moran's I of 0.027, meaning that the spatial autocorrelation between points is low and that the points are considered random (Cheng & Masser, 2003; Xiao et al., 2015).
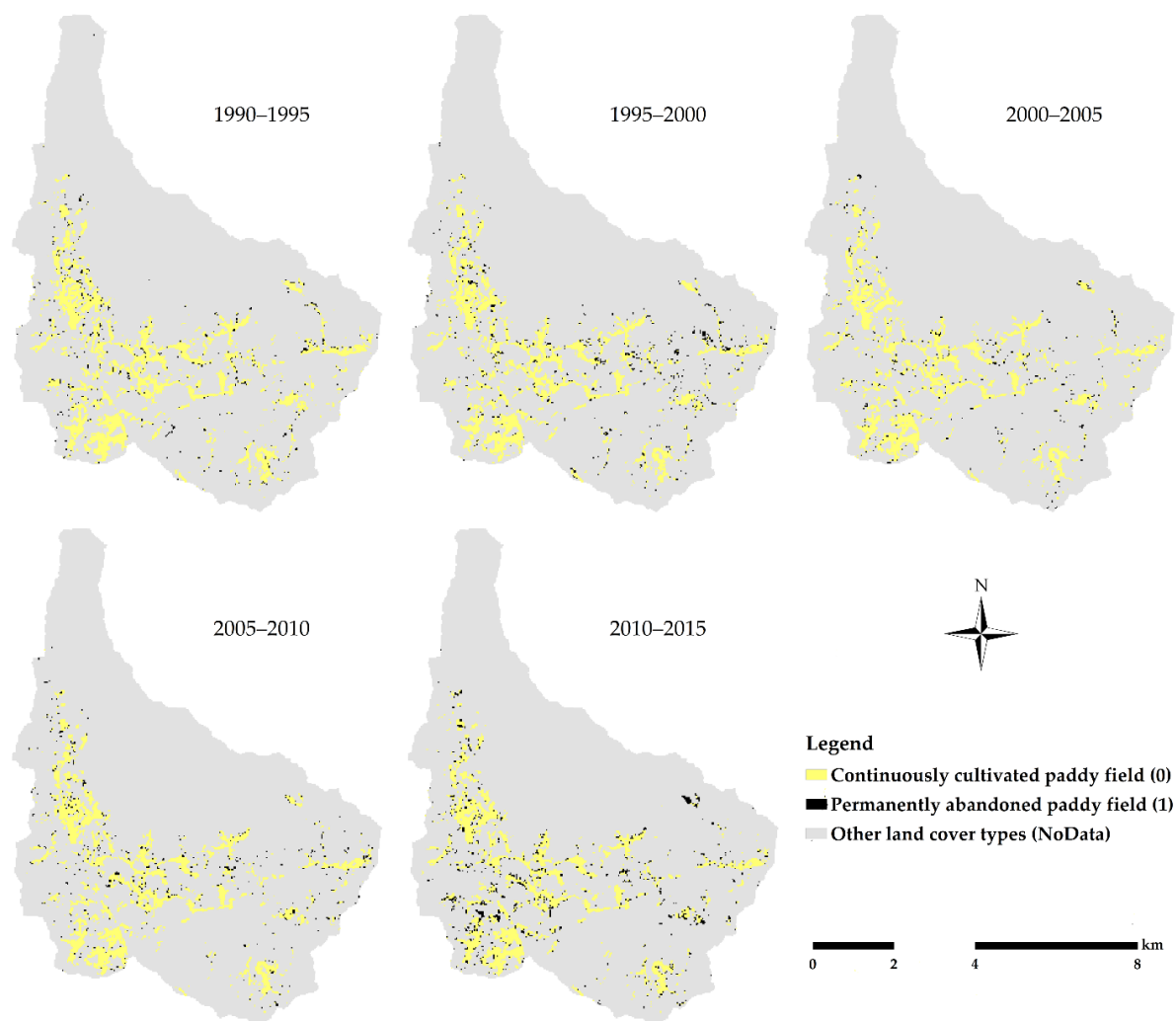


Fig. 4.3 Spatial distribution of the continuously cultivated and permanently abandoned paddy fields through five-year periods from 1990 to 2015

Table 4.1 List of spatial explanatory variables included in the logistic regression to model probability maps of permanent agricultural abandonment

| Category | Variable (unit) | Nature | Data source | Method |
|---|---|---|---|---|
| Topography | Elevation (m) | Continuous | SRTM 3.0 DEM | - |
| | Slope (°) | Continuous | SRTM 3.0 DEM | Slope tool in ArcGIS |
| | Sine aspect | Continuous | SRTM 3.0 DEM | Aspect tool in ArcGIS |
| | Cosine aspect | Continuous | SRTM 3.0 DEM | Aspect tool in ArcGIS |
| Productivity | Soil type | Binary | Global Hydrologic Soil Groups (HYSOGs250m) | - |
| | Quickflow (mm) | Continuous | Land cover (Estacio et al., 2022), HYSOGs250m, WorldClim global climate data | InVEST software |
| Accessibility | Distance to stream (m) | Continuous | Land cover (Estacio et al., 2022), HYSOGs250m, WorldClim global climate data | InVEST software, Euclidean tool in ArcGIS |
| | Distance to town center (m) | Continuous | Google Earth image | Digitization of town center, Euclidean tool in ArcGIS |
| | Distance to road (m) | Continuous | OpenStreetMap | Euclidean tool in ArcGIS |
| | Distance to tourist hotspot (m) | Continuous | Google Earth image | Digitization of tourist hotspot, Euclidean tool in ArcGIS |
| Political restriction | World heritage site status | Binary | Google Earth image | Digitization of area of world heritage site |
| Spatial configuration | Forest density (Circle, 150 m diameter, mean) | Continuous | Land cover maps (Estacio et al., 2022) | Neighborhood statistics, Bivariate analysis |
| | Low vegetation density (Square, 90 m width, mean) | Continuous | Land cover maps (Estacio et al., 2022) | Neighborhood statistics, Bivariate analysis |
| | Built-up density (Circle, 330 m diameter, max) | Continuous | Land cover maps (Estacio et al., 2022) | Neighborhood statistics, Bivariate analysis |
| | Paddy field density (Square, 90 m width, mean) | Continuous | Land cover maps (Estacio et al., 2022) | Neighborhood statistics, Bivariate analysis |

*4.3.1.3. Preparation of spatial explanatory variables*

Based on previous studies on the abandonment of mountainous agricultural landscapes (Nainggolan et al., 2012; Pazúr et al., 2020; Xystrakis et al., 2017) and also subjected to data availability, spatial explanatory variables were selected and prepared for logistic regression (Fig. 4.4, Table 4.1). The variables were categorized based on the categories of LUCC drivers reviewed by Mitsuda & Ito (2011), resulting in five categories of variables: topography, productivity, accessibility, political restriction, and spatial configuration.

Topography determines the form and shape of the land surface. Topography can dictate the flow of supply of resources and is an important indicator of landscape connectivity (Pe'er et al., 2006). Topography can also dictate the suitability for cultivation, thus is an important indicator in agriculture. To prepare the topography variables, a Digital Elevation Model (DEM) of 30 m spatial resolution generated from the Shuttle Radar Topography Mission (SRTM) Version 3.0 was acquired from Google Earth Engine (Gorelick et al., 2017). Slope, Aspect, and Raster Calculator tools were used to derive the topography variables.

Productivity indicates factors that affect the potential productivity of a paddy field for agricultural yield (Mitsuda & Ito, 2011). For example, the type of soil can affect the agricultural productivity of land as it directly affects the growth of crops. For preparing the soil type, maps from the Global Hydrologic Soil Groups (HYSOGs250m) of the Oak Ridge National Laboratory (ORNL) Distributed Active Archive Center (DAAC) were used. Furthermore, erosion or landslide also affect productivity as eroded land in mountainous landscapes cannot be used for cultivation unless restored back to its terraced state (Calderon et al., 2009). To indicate the susceptibility of a land to erosion, quickflow, which is the amount of water that flows on land during or shortly after a rain event was used. The spatial distribution of quickflow was mapped using the Seasonal Water Yield model in the InVEST (Integrated Valuation of Ecosystem Services and Tradeoffs) suite (Benra et al., 2021). InVEST is an open-source software composed of different models that can be used to map certain ecosystem services.
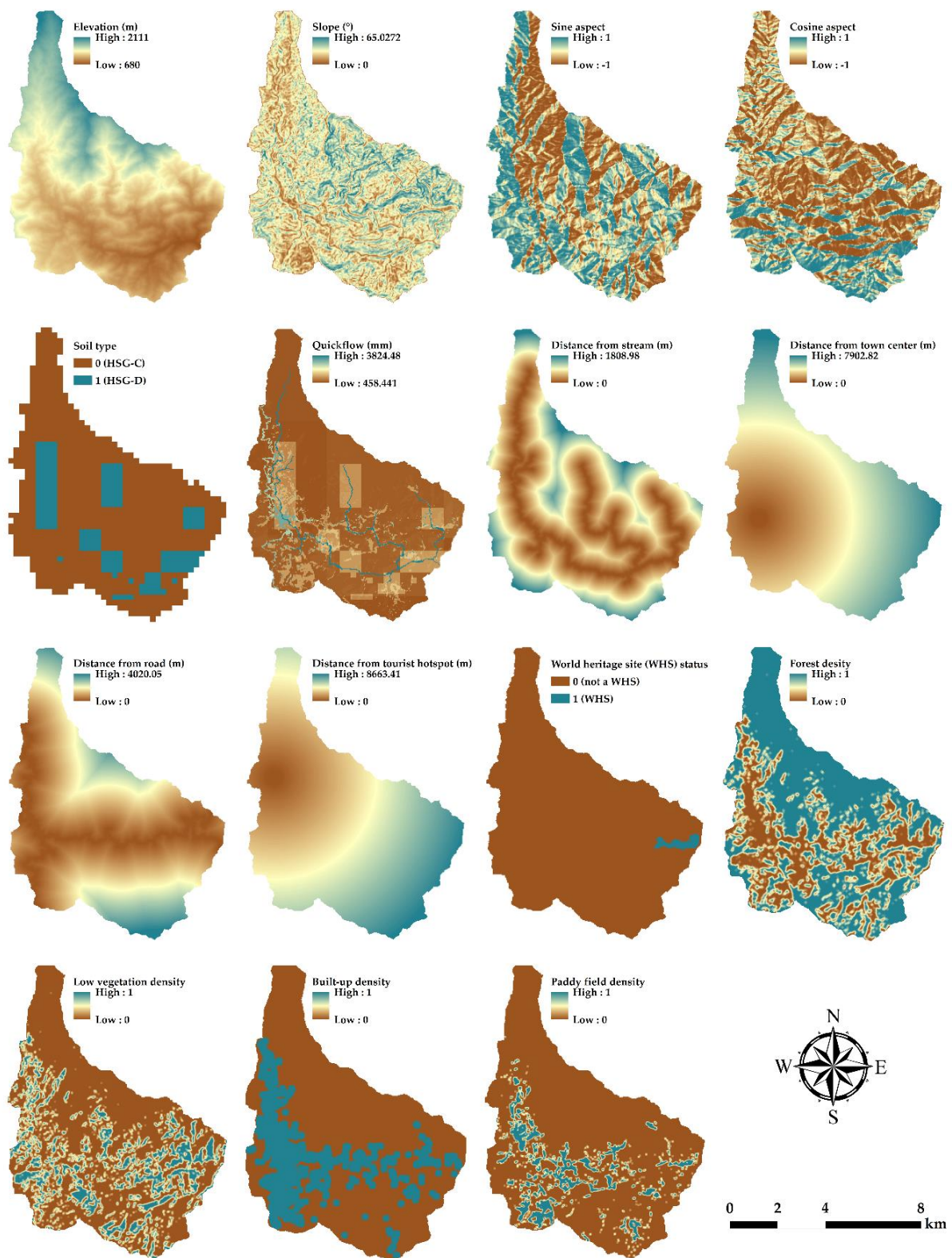
Fig. 4.4 Raster layers of spatial explanatory variables included in the logistic regression
(sample layers for the year 2000)

Accessibility factors, represented by the distance from an agricultural land to a particular place, indicate the accessibility of services (transportation or health care), supplies (water or food), or opportunities (work or tourism). To represent accessibility, four variables were prepared; distance to steam which represents accessibility to water; distance to town center which represents accessibility to services, supplies, and jobs, distance to road which represents accessibility to transportation, and distance to tourist hotspot (the Viewpoint place in Ifugao) which represents accessibility to tourists. All variables were processed using the Euclidean tool in ArcGIS.

Political restriction determines if an area is a conservation site due to a special status imposed by the government. In the study area, the status of a terrace cluster as a World Heritage was selected as a political restriction factor. Using high-resolution images in Google Earth Engine, the clusters of the Bangaan world heritage site was delineated and converted to a binary raster file.

Spatial configuration denotes the pattern of the neighborhood where LUCC occurs such as the density of neighboring land cover types. Based on the acquired land cover maps, variables indicating the density of a particular land cover within a neighborhood were prepared: forest density, low vegetation density, built-up density, and paddy field density. As the definition of neighborhood varies based on the shape, diameter length, and aggregation statistics of the neighborhood, different neighborhood types were first tested for each land cover type using a bivariate analysis. First, the Focal Statistics tool was used to map different land cover densities by considering different neighbor neighborhood types. Multiple raster files were produced by using different combinations of neighborhood shape (varied between circle or rectangle), diameter length (varied from 90 m to 390 m, in 60 m increments), and aggregation statistics (varied between mean or maximum). Second, preliminary bivariate logistic regression was implemented for each land cover density raster file where land cover density was treated as an explanatory variable and the binary agricultural abandonment variable was treated as the response variable. Lastly, after deriving the statistics for each logistic regression, the land cover density with the lowest p-value was chosen as the neighborhood configuration for the particular land cover type. For example, for forest density, the bivariate analysis showed that the mean number of forest pixels within a circle neighborhood of 150 m radius has the highest significance in explaining the variation in agricultural abandonment (neighborhood configurations for the other density variables are shown in Table 4.1).

After preparing the raster files of all spatial explanatory variables, their values were extracted into the created sample points so that each point has a binary value of agricultural abandonment occurrence alongside values of the spatial explanatory variables.

## 4.3.1.4 Preparation of non-spatial explanatory variables

Previous models of LUCC have incorporated non-spatial drivers such as economic, social, and environment variables to set quantitative data of LUCC (D. Liu et al., 2020; Mao et al., 2014; Xu et al., 2016). In the same sense, non-spatial drivers were selected and prepared, subjected to data availability, to produce a linear model of the global probability threshold of agricultural abandonment in the study area (Table 4.2). These non-spatial variables were categorized into three: land cover, demography, and environment.

Land cover refers to the total area of a particular land cover type in the watershed. Previous studies have shown that the total area of vegetation cover types has a correlation on agricultural abandonment due to changing water yield (Estacio et al., 2022; Soriano & Herath, 2018). Values of land cover area in the starting years of every five-year period were derived from the acquired land cover maps.

Demography refers to the size and structure of the population in Banaue (the municipality encompassing the watershed). Migration of local people into the lowlands has been cited as a factor for abandonment (Calderon et al., 2009; Castonguay et al., 2016), hence the change in demography can be a significant explanatory factor for agricultural abandonment. Demographic data were acquired from publicly available administrative data in the Philippines.

Lastly, climate refers to the weather over the study area during a particular period. Even though climatic variables such as temperature and precipitation may vary through space, as the study area is a small-scale area (with maximum length of approximately15 km), the spatial resolution of acquired historical climatic variables cannot capture the spatial variation in the study area, hence climate variables were treated as non-spatial variables that vary through time due to climate changes. Climate data were acquired from the Climate Change Knowledge Portal (CCKP).

Table 4.2 List of non-spatial explanatory variables included in the linear regression to model global probability thresholds of permanent agricultural abandonment

| Category | Variable (unit) |
|---|---|
| Land cover | Paddy field total area (m$^2$) |
| | Low vegetation total area (m$^2$) |
| | Forest total area (m$^2$) |
| | Built-up total area (m$^2$) |
| Demography | Average household size |
| | Number of households |
| | Household Population |
| Climate | Precipitation – annual mean (mm) |
| | Precipitation – 5-year smooth (mm) |
| | Mean Temperature – annual mean (°C) |
| | Mean Temperature – 5-year smooth (°C) |
| | Min Temperature – annual mean (°C) |
| | Min Temperature – 5-year smooth (°C) |
| | Max Temperature – annual mean (°C) |
| | Max Temperature – 5-year smooth (°C) |

*4.3.2. Logistic regression of LUCC binary response variable with spatial explanatory variables*

To identify the significant spatial drivers of agricultural abandonment, logistic regression was implemented using the 1500 samples points of binary response variable and spatial explanatory variables gathered from 1990 to 2015. The accuracy of the resulting logistic model was assessed using Pseudo R-square and ROC (Relative Operating Characteristic) values. If the Pseudo R-Square is greater than 0.2, the produced logistic model for the respective period was deemed to be of good fit to be used to explain the significance of each spatial driver to the occurrence of agricultural abandonment (Hu and Lo, 2007). Logistic regression was implemented using R 3.3.0.

*4.3.3. Derivation of optimal probability threshold by optimization*

The next step is to derive the optimal probability thresholds for the probability maps of every period. First, probability maps for every period were generated using the produced logistic model, utilizing the spatial explanatory variables for every period. Optimization was then implemented using a Genetic Algorithm (GA) to find the probability threshold that will yield the highest Fuzzy Kappa statistic between a simulated map and an actual map. Fuzzy

Kappa is a statistic for comparing the similarities between two maps based on local neighborhood, and is closer to how human observers compare maps (Drogoul et al., 2016; Visser & De Nijs, 2006). Hence, optimizing the probability threshold based on maximizing the fuzzy kappa statistic is akin to finding a simulated map with the least difference between an actual map. It should be noted that Fuzzy simulation, another accuracy statistic, was not used because an end-state land use/cover map is used as input in this statistic, and a map simulated in this step is an LUCC (land use/cover change). A Genetic Algorithm, which is a population-based search algorithm that aims to find the best solution, was set with the following parameters: population = 7, generations = 5, crossover = 0.7, mutation = 0.1 (Katoch et al., 2021; Mirjalili, 2019). After implementing the GA, optimal probability thresholds for each period were obtained. Coding of the GA was implemented in the GAMA platform (Taillandier et al., 2019).

### 4.3.4. Linear regression of optimal probability thresholds with non-spatial explanatory variables

To relate the variation of the global probability thresholds with non-spatial explanatory variables, multivariate linear regression was implemented to create a linear model. First, as several non-spatial explanatory variables were prepared, different combinations of variables were tested for the linear regression. For every combination, the P-value of every non-spatial explanatory variable was checked for its significance (if $P < 0.05$). The significance F of the model was also checked for is significance (if $F < 0.05$), which indicates that the linear model fits the data better than a model with no explanatory variables. Once all the P-values and significance F in a combination of variables are significant, the adjusted R-squared of the model was recorded. After testing different combinations of variables, the combination with the recorded highest adjusted R-squared was chosen as the non-spatial explanatory variables of the linear model of global probability threshold. Linear regression was implemented using the Data Analysis tools in Microsoft Excel.

*4.3.5. Accuracy assessment of modeled maps*

Using the produced linear model where non-spatial explanatory variables and probability maps were used as inputs, binary maps of agricultural abandonment for every period were simulated. To assess the accuracy of the simulated agricultural abandonment maps and the reliability of the statistical model, the simulated maps were compared with its respective actual maps by computing for the Fuzzy Kappa and Absolute Deviation Percentages (ADP) statistics. Unlike Fuzzy Kappa statistic which computes similarities based on local neighborhood, ADP is a global indicator that computes the differences between maps based on the quantity of each land cover class (Truong et al., 2016). Using the two statistics, along with visual comparison of the actual and simulated maps, the accuracy of the model was assessed if it can be used for LUCC simulation.

## 4.4. Results

*4.4.1. Logistic regression of agricultural abandonment with spatial explanatory variables*

Logistic models for each five-year period from 1990 to 2015 produced by the logistic regression achieved a minimum Pseudo-R squared value of 0.202 and a minimum AUC ROC of 0.793 (Table 4.3), suggesting that all produced logistic models were of good-fit and can be used for explaining the significant drivers of agricultural abandonment in the rice terraces. In four of the five periods, slope was highly significant ($P < 0.01$) in influencing agricultural abandonment, with higher slope values indicating higher probabilities of abandonment. Paddy field density was also significant for three periods ($P < 0.05$), where paddy fields with low density of neighboring paddy fields have higher chances of abandonment. Cosine aspect was highly significant for two periods ($P < 0.01$), where negative estimates indicate that sloping fields facing south is more likely to experience abandonment than fields facing north, while fields facing east and west are not affected. Other variables were found to be significant for only one period such as quickflow, world heritage site status, forest density, and low vegetation density.

Table 4.3 Coefficients of significant spatial variables and accuracy statistics for the logistic models of every period

| Spatial variables (standardized) | 1990–1995 | 1995–2000 | 2000–2005 | 2005–2010 | 2010–2015 |
|---|---|---|---|---|---|
| (Intercept) | ns | ns | ns | ns | ns |
| Elevation | ns | ns | ns | -0.712* | ns |
| Slope | 0.495** | 0.678*** | ns | 0.446** | 0.430** |
| Sine aspect | ns | ns | ns | ns | ns |
| Cosine aspect | ns | -0.663*** | ns | -0.419** | ns |
| Soil type | ns | ns | ns | ns | ns |
| Quickflow | ns | 0.503** | ns | ns | ns |
| Distance to stream | ns | ns | ns | ns | ns |
| Distance to town center | ns | ns | ns | ns | ns |
| Distance to road | ns | ns | ns | ns | ns |
| Distance to tourist hotspot | ns | ns | ns | ns | ns |
| World heritage site status | ns | ns | -0.606** | ns | ns |
| Forest density | ns | 0.588* | ns | ns | ns |
| Low vegetation density | ns | 0.609* | ns | ns | ns |
| Built-up density | ns | ns | ns | ns | ns |
| Paddy field density | -0.954** | ns | -1.081*** | -0.729* | ns |
| | | | | | |
| Accuracy: Pseudo R-squared | 0.253 | 0.342 | 0.267 | 0.228 | 0.202 |
| Accuracy: AUC ROC | 0.824 | 0.866 | 0.829 | 0.810 | 0.793 |

ns: P > 0.05 (insignificant)

*: 0.01 ≤ P < 0.05

**: 0.001 ≤ P < 0.01

***: P < 0.001

Logistic regression based on 1500 samples from all periods produced a logistic model with Pseudo-R squared value of 0.225 and AUC ROC of 0.804, indicating that this model was also of good fit (Table 4.4). Similar to the logistic models of each period, slope and paddy field density were the most significant drivers of agricultural abandonment in the general logistic model (P < 0.001). The next set of significant variables are cosine aspect, quickflow, and low vegetation density (P < 0.01), which were significant in at least one period in the periodic logistic models. Other significant drivers were distance to town center, distance to road, world heritage site status, and forest density (P < 0.05). It is worth noting that even though both of the accessibility variables, distance to town center and distance to road, were not significant in any of the periods, the general logistic model determined that these accessibility variables were significant factors of agricultural abandonment from 1990 to 2015. This implies that the

significant explanatory variables in the general logistic model affect the overall variability in occurrence of agricultural abandonment in the whole 25-year period, and do not necessarily have to be significant for a particular five-year period.

Table 4.4 Coefficients of significant spatial variables and accuracy statistics for the logistic model for all periods

| Spatial variable (unit) | Coefficients | Standard error | Z | P-value |
|---|---|---|---|---|
| (Intercept) | ns | ns | 0.338 | 0.653 |
| Elevation (m) | ns | ns | -0.807 | 0.420 |
| Slope (°) | 0.0499*** | 0.00851 | 5.868 | 0.000 |
| Sine aspect | ns | ns | 1.682 | 0.092 |
| Cosine aspect | -0.303** | 0.0939 | -3.221 | 0.001 |
| Soil type | ns | ns | 0.432 | 0.666 |
| Quickflow (mm) | 0.000360** | 0.000111 | 3.243 | 0.001 |
| Distance to stream (m) | ns | ns | 0.950 | 0.342 |
| Distance to town center (m) | 0.000198* | 0.0000836 | 2.366 | 0.018 |
| Distance to road (m) | -0.000281* | 0.000129 | -2.179 | 0.029 |
| Distance to tourist hotspot (m) | ns | ns | -0.532 | 0.594 |
| World heritage site status | -0.841* | 0.404 | -2.080 | 0.038 |
| Forest density | 1.210* | 0.587 | 2.057 | 0.040 |
| Low vegetation density | 2.010** | 0.617 | 3.256 | 0.001 |
| Built-up density | ns | ns | -1.456 | 0.145 |
| Paddy field density | -2.540*** | 0.544 | -4.673 | 0.000 |
| | | | | |
| Accuracy: Pseudo R-squared | 0.225 | | | |
| Accuracy: AUC ROC | 0.804 | | | |

ns: $P > 0.05$ (insignificant)

*: $0.01 \leq P < 0.05$

**: $0.001 \leq P < 0.01$

***: $P < 0.001$

Table 4.5 Optimal probability thresholds for maximizing fuzzy Kappa statistics between simulated and actual maps of agricultural abandonment

| Period | Optimal probability threshold | Maximum fuzzy kappa |
|---|---|---|
| 1990–1995 | 0.82 | 0.3718 |
| 1995–2000 | 0.86 | 0.5062 |
| 2000–2005 | 0.87 | 0.3978 |
| 2005–2010 | 0.87 | 0.4440 |
| 2010-2015 | 0.73 | 0.4327 |

*4.4.2. Linear regression of optimal probability threshold with non-spatial explanatory variables*

Optimal probability thresholds for maximizing the similarity between simulated maps and actual maps were derived using a GA (Table 4.5). The minimum attained Fuzzy Kappa statistic for all simulated maps was 0.3718 while the maximum statistic is 0.5062. On the other hand, the optimal probability threshold ranges only from 0.73 to 0.86, revealing that the optimal probability threshold only underwent small variations between periods. This however does not imply that the subsequent quantitative change in LUCC will have the same variation as quantitative change also depends in the values in the probability maps.

Using the optimal probability thresholds as the response variable, linear regression based on using forest total area, precipitation (5-year smooth), and maximum temperature (annual mean) as non-spatial explanatory variables produced a linear model with adjusted R-squared of 0.9999996 and significance F of 0.0003817, indicating that the linear model was of excellent fit (Table 4.6). All explanatory variables attained significant P values ($P < 0.01$), with forest total area and max temperature having P values less than 0.001.

Table 4.6 Summary statistics of the linear model of global probability threshold of agricultural abandonment

| Temporal non-spatial variables (unit) | Coefficients | Standard error | t-stat | P-value |
|---|---|---|---|---|
| (Intercept) | 7.3859*** | 0.00342 | 2158.31 | 0.00029 |
| Forest total area ($m^2$) | -0.00039391*** | 0.000000208 | -1895.66 | 0.00034 |
| Precipitation – 5-year smooth (mm) | -0.0000354805** | 0.0000000940 | -377.446 | 0.0017 |
| Max Temperature – annual mean (°C) | -0.16666*** | 0.000117 | -1422.39 | 0.00045 |
| | | | | |
| Accuracy: Adjusted R-squared | 0.9999996 | | | |
| Accuracy: Standard error | 0.0000357 | | | |
| Accuracy: Significance F | 0.0003817 | | | |

*4.4.3. Statistical model for mapping agricultural abandonment*

By integrating the logistic model based on spatial explanatory variable and the linear model based on non-spatial explanatory variables, a statistical model was derived for mapping agricultural abandonment, in the form:

$$
Z = \begin{cases}
1, \dfrac{1}{1+e^{-1\left(\begin{smallmatrix} 0.050S-0.303C \\ +3.60(10^{-4})Q \\ +1.98(10^{-4})T \\ -2.81(10^{-4})R \\ -0.841H+1.21D_L \\ +2.01D_F-2.54D_P \end{smallmatrix}\right)}} > 7.39 - 3.94(10^{-4})A_F - 3.55(10^{-5})P_A - 0.170T_{max} \\[4em]
0, \dfrac{1}{1+e^{-1\left(\begin{smallmatrix} 0.050S-0.303C \\ +3.60(10^{-4})Q \\ +1.98(10^{-4})T \\ -2.81(10^{-4})R \\ -0.841H+1.21D_L \\ +2.01D_F-2.54D_P \end{smallmatrix}\right)}} \le 7.39 - 3.94(10^{-4})A_F - 3.55(10^{-5})P_A - 0.170T_{max}
\end{cases}
\quad \text{(Eq. 4.5)}
$$

where $Z$ is the occurrence of agricultural abandonment in a pixel in a particular period where a value of 1 denotes occurrence while 0 denotes no occurrence, S is the slope, C is the cosine aspect, Q is the Quickflow, T is the distance to town center, R is the distance to road, H is the status as world heritage site, $D_L$ is the low vegetation density, $D_F$ is the forest density, $D_P$ is the paddy field density, $A_F$ is the forest total area, $P_A$ is the average precipitation within 5 years, and $T_{max}$ is the annual mean of the daily maximum temperature. The statistical model includes nine spatial explanatory variables and three non-spatial explanatory variables. All variables vary through time, hence given a pixel of indices $(u, v)$, the occurrence of agricultural abandonment at different periods may vary depending on the temporal variation of the explanatory variables (such as quickflow, forest density, or precipitation).
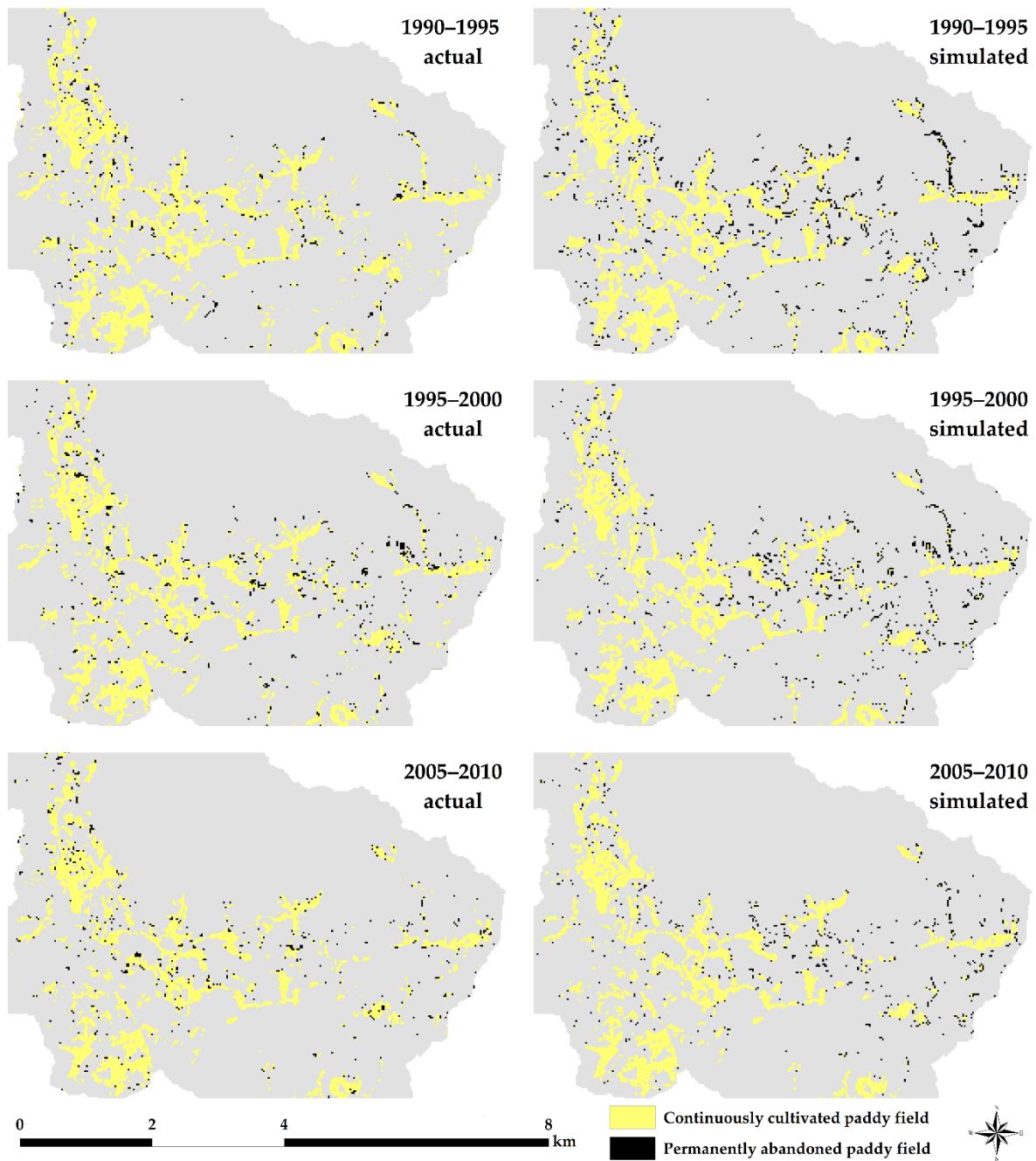
Fig. 4.5 Side-by-side comparison of actual and simulated agricultural abandonment maps for the periods 1990–1995 (the period with the worst Fuzzy Kappa and ADP), 1995–2000 (the period with the best Fuzzy Kappa), 2010–2015 (the period with the best ADP).

*4.4.4. Accuracy assessment of modeled maps*

Through the statistical model, maps of agricultural abandonment for every period were simulated using the spatial and non-spatial explanatory variables in every respective period

(Fig. 4.5). The accuracies of these simulated maps were assessed by comparing them to the actual maps of agricultural abandonment for the respective period (Table 4.7). As the fit of the linear model is almost equal to 1.0 (Table 4.6), the derived Fuzzy Kappa statistics for the simulated maps are almost equal as those derived from the optimal probability thresholds (Table 4.5). The maximum ADP for all modeled maps was 1.053%, indicating that the differences in derived quantitative values of agricultural abandonment is minimal, even when optimization of probability threshold is aimed on maximizing Fuzzy Kappa which focuses on neighborhood similarities.

Analyzing each simulated map, the simulated map for the period 1990–1995 attained both the highest ADP and lowest fuzzy kappa, indicating that this map had the lowest neighborhood similarity and highest difference in quantitative value with an actual map. However, this does not indicate that Fuzzy Kappa is inversely proportional to ADP. The simulated map for the period 1995–2000 attained the highest fuzzy Kappa but did not attain the lowest ADP. Similarly, the simulated map for the period 2005–2010 attained the lowest ADP but did not attain the highest fuzzy kappa. This implies that high neighborhood similarities in a map do not equate to high global similarities.

Table 4.7 Accuracy statistics for the simulated agricultural abandonment maps of every period

| Period | Fuzzy Kappa | ADP |
|---|---|---|
| 1990–1995 | 0.3718 | 1.053% |
| 1995–2000 | 0.5062 | 0.277% |
| 2000–2005 | 0.3978 | 0.576% |
| 2005–2010 | 0.4440 | 0.113% |
| 2010–2015 | 0.4327 | 0.863% |

## 4.5. Discussion

### *4.5.1. Implications of the developed LUCC statistical model*

The structure of the developed statistical model of LUCC that is composed of a logistic model and a linear model implies a different mechanism of simulating LUCC than the demand-allocation models that also incorporate a logistic model. Demand-allocation models incorporate two modules, allocation and demand (T. Liu & Yang, 2015; Ren et al., 2019). The demand module generates the quantitative value of LUCC by adopting models such as System dynamics or Markov Chain (Boavida-Portugal et al., 2016; Dang & Kawasaki, 2017; Xu et al., 2016). The derived quantitative value of land cover change from the demand module are then allocated into an LUCC map through the allocation module. Thus, the allocation module dictates the spatial pattern of LUCC by deriving probability maps using a logistic model derived from historical patterns of spatial explanatory variables. Through a probability map, LUCC is allocated to pixels starting from the pixel with the highest probability of change going to the next highest one, until the quantitative value of LUCC is met. Previous studies have also incorporated rules in allocation such as cellular automata that takes into account neighborhood effects and limitations on transitions (Mao et al., 2014; Mustafa et al., 2017).

In the proposed statistical model, instead of a demand module, the model utilizes a linear model of global probability threshold which dictates which pixels undergo LUCC based on comparing the local probability and the global probability threshold. This structure implies that the probability map also dictates the quantitative value of the LUCC, as compared to demand-allocation models where probability maps only dictate the spatial pattern. For example, in a demand-allocation model, adding a constant probability value in a particular area in the probability map will not affect the total quantitative value of the LUCC but will only affect the spatial pattern. However, in the developed statistical model, subtracting a constant probability value in a particular area will not only affect the spatial pattern but also the quantitative value. In relation to this, global probability thresholds hold a role of dictating on which probability value pixels start to change, where lower thresholds lead to more changes, and vice versa. Global probability thresholds can hence be treated as an inverse global probability of the LUCC occurring in the whole mapping area.

In essence, spatial explanatory variables, which dictate the probability maps, control

the local probabilities of LUCC and hold an effect not only to the spatial pattern but also to the quantitative value of LUCC. For example, in the case study, adding more conservation areas in a political restriction variable will affect the simulated quantitative value of agricultural abandonment. Another example is improving the values in a productivity variable which will lead to less quantities of agricultural abandonment. In a demand-allocation model which uses system dynamics, modifying the stocks or flows in the SD module should be implemented if quantitative value of LUCC based on changes in spatial variables need to be simulated. However, in the developed model, this is not needed as changes in the spatial explanatory variable directly affect the quantitative value of LUCC.

On the other hand, non-spatial explanatory variables, which dictate the global probability threshold, control the global probability of LUCC which affects the quantitative value of LUCC. For example, the results show that precipitation has a significant inverse linear relationship with the global probability threshold. As the global probability threshold has a negative relationship with quantitative value of LUCC, precipitation can be treated as a determinant that has a positive relationship on the probability of agricultural abandonment, where an increase in precipitation leads to an increase in the overall probability of agricultural abandonment in the study area.

Lastly, the developed statistical model simulates LUCC by utilizing the generated significant statistical relationships with spatial and non-spatial explanatory variables. In modeling terms, the statistical model acts like a black box that accepts inputs and generates an output without an understanding of the socio-ecological processes that produce the statistical relationships between entities. This differentiates itself from process-based models where a thorough manifestation of system processes is used to generate outputs based on inputs. Thus, in the spectrum of LUCC models, the developed statistical model can be put under the classification of pattern-based models (Ren et al., 2019). Regardless of the model type, the developed statistical model also follows the capabilities of other models in simulating future scenarios where inputs or parameters are modified to match the circumstances of a scenario. For example, as the statistical model has shown that "distance to road" is a significant spatial driver of agricultural abandonment, modifying the map of this variable to show a scenario where new roads are established can be implemented to simulate the effects of building roads to agricultural abandonment.

*4.5.2. Application of the model: spatial and non-spatial drivers of agricultural abandonment*

The produced logistic model for the period from 1990 to 2015 attained a Pseudo R-squared a value greater than 0.2, indicating that models is of good fit and can be used to explain the explain the significance of each spatial driver to the occurrence of permanent abandonment in each period (Hu & Lo, 2007). Based on the logistic model, slope and paddy field density were the most significant spatial drivers of agricultural abandonment in the rice terraces. This indicates that fields of steep slopes and low neighborhood percentages of paddy field experienced the highest probability of agricultural abandonment. This result aligns with the study of Corbelle-Rico et al. (2012) which found that agricultural parcels with steeper slopes and higher distances to farm (hence, less neighborhood of agricultural parcels) lead to more abandonment. The next set of significant variables were cosine aspect, quickflow, and low vegetation density. Results show that fields that face south, experience heavy quickflow during rainy periods, and have high neighborhood percentages of low vegetation are also most likely to experience permanent abandonment. Results for the low vegetation density aligned with the study of Pazúr et al. (2014) which showed that fields that are nearer to shrubs have higher chances of being abandoned. The last set of significant spatial drivers are distance to town center, distance to roads, status as world heritage site, and forest. Fields that are far from the town center, are near to roads, are not part of the world heritage site, and have high neighborhood percentages of forest also have high chances of being abandoned. Pazúr et al. (2020) also showed that forest density increases the likelihood of abandonment. Results for the distance to town center aligned with the results of previous studies, such as of Pazúr et al. (2014) which showed that increasing the distance to a county center increased the likelihood of agricultural abandonment and of Perpiña Castillo et al. (2021) which showed that remoteness, represented by the travelling time to the nearest town, also increased the likelihood of agricultural abandonment. For the results of the world heritage site, it is worth noting that status as world heritage site was highly significant (P < 0.01) for the particular period of 2000–2005, which may be attributed to the inclusion of the Ifugao rice terraces heritage cluster into UNESCO's list of World Heritage in Danger in 2001 (UNESCO, n.d.), influencing the farmers to exclude the fields in the heritage cluster for abandonment. Increase in probability of abandonment in areas neared to roads may be attributed to the conversion of paddy fields near roads to built-up cover, which is related to the findings of Nainggolan et al. (2012) which

showed that likelihood of abandonment was higher in areas close to the village due to the demand for settlement expansion.

For the linear model, the linear regression attained a significance F of 0.0003817, indicating that the non-spatial explanatory variables were of good fit to the global probability threshold. The linear model revealed that total forest area, precipitation, and average daily maximum temperature were significant determinants of the probability of agricultural abandonment. Higher areas of forest cover led to higher probability of agricultural abandonment in the study area. This is in line with previous studies in the Ifugao rice terraces where increases in forest cover decreased the total water yield, thereby promoting further agricultural abandonment (Estacio et al., 2022; Soriano & Herath, 2018). This implies that even though water scarcity is an existing problem in the Ifugao rice terraces, high precipitation promotes agricultural abandonment because of the resulting increase in erosion. Combining the implications of the total forest area and precipitation, results indicate that it is the water yield during the dry season, not the amount of precipitation during the wet season, that is important in the rice terraces as cultivation of rice occurs during the dry season. Lastly, increasing daily maximum temperature was found to increase chances of abandonment. This can also be related to the water yield as the rice terraces suffer insufficient supply of water in the dry season, hence the paddy fields are sensitive to increases in evaporation brought by increasing temperature, leading to more abandonment.

### 4.5.3. Future direction in LUCC modeling

Simulated maps of agricultural abandonment using the statistical model attained Fuzzy Kappa statistics ranging from 0.3718 and 0.5062 and ADP ranging from 1.053% to 0.277%, which are satisfactory accuracy values for LUCC simulations. For example, the hybrid ABM developed by Mustafa et al. (2017) simulated maps in three experiments and achieved Fuzzy Kappa ranging from 0.3942 to 0.4792 and ADP ranging from 43.22% to 22.11%. The simulated maps from the developed statistical model achieved fuzzy kappa values in the same range while the ADP values are much more accurate. Ahmed et al. (2013) compared maps simulated from three types of Markov models (Stochastic, Cellular Automata, and Multi-layer Perceptron) and calculated Fuzzy Kappa accuracies of 0.304, 0.862, and 0.953, respectively. Based on this, the performance of the statistical model can be assessed to be in between a Stochastic Markov

model and a Cellular Automata Markov model. Based on this assessment, the statistical model can then be deemed suitable for simulating future LUCC maps.

The statistical model differentiates itself from other LUCC models through its capability of identifying the significant non-spatial drivers of an LUCC. In using established LUCC simulation models, input variables are already set thus users are limited with their ability to incorporate variables that may be significant for the LUCC. A user can opt to develop a hybrid LUCC model coupled with system dynamics or agent-based model to be able to incorporate all significant non-spatial drivers. However, building such a complicated model needs detailed capturing of the system processes hence can take a lot of time. Thorough calibration of the model to ensure that generated LUCC maps are of acceptable accuracy also takes plenty of trial-and-error. With the proposed statistical model, the significant non-spatial drivers can be identified and, at the same time, be incorporated in the model right away for simulation.

To simulate future LUCC through the statistical model, generating the future values of the explanatory variables is essential, thus coupling with another established models to derive these future values may be essential if the situation calls for it. For example, in the case study where future agricultural abandonment is to be simulated, predictions of some explanatory variables are needed such as future land cover maps, quickflow maps, precipitation, and temperature. For this purpose, existing models can be utilized such as Markov Chain for predicting future land cover values, the InVEST seasonal water yield model for mapping quickflow, and climate models for projecting future trends of precipitation and temperature.

Aside from being used for simulation of scenarios, the statistical model can also be used as a step before using process-based models to identify first the significant drivers of LUCC. After the identification of the significant drivers of LUCC using the statistical model, a user will then be informed on which current process-based LUCC model is most suitable to use for scenario simulation. At the same time, a modeler can also use the model to gain insight on the drivers of a LUCC before proceeding to model the socio-ecological processes of an LUCC in hand.

A main limitation of the statistical model that users should remember is its capability of simulating only one type of LUCC, as in the case study, agricultural abandonment. In reality, LUCC occurs in various land cover types which also transition into more than one LUCC type. Hence, the statistical model is limited in its ability to project the full end-state land cover of a

study area. The statistical model can however be useful when only one type of LUCC is of concern, such as urban expansion, deforestation, or reclamation. The proposed statistical model is especially useful to inform relevant land use stakeholders of the significant drivers of an LUCC they are concerned about and to show the future circumstance of the LUCC based on future values of these drivers.

In the future, studies can explore the calibration of global probability thresholds based on a different objective function. In the developed statistical model, global probability threshold values were derived using an optimization routine based on a GA that maximizes fuzzy kappa, a map comparison statistic which is on similarities in local neighborhood similarities. However, maximizing fuzzy kappa does not guarantee similarities in global value of the LUCC. In the future, LUCC studies can explore minimizing the ADP, which focuses on differences in global quantitative value, to find the optimal probability threshold. Examples of such studies may focus on simulation of future reclamation, mangrove extent change, or urbanization which focuses more on quantity prediction.

## 4.6. Conclusions

This paper developed a statistical model for simulating LUCC by integrating a logistic model based on spatial explanatory variables that generates a probability map and a linear model based on non-spatial explanatory variables that generates a global probability threshold. Previous LUCC models integrated an allocation module based on a logistic model with a demand module such as systems dynamics to compute a quantitative value of LUCC based on non-spatial explanatory variables. These allocation-demand models can produce accurate maps but are too complex to develop if a list of significant non-spatial explanatory variables should be included in a model. The developed statistical model adopts a simple pattern-based approach where non-spatial explanatory variables are incorporated in simulating LUCC by relating these non-spatial variables to a global probability threshold through a linear model. By comparing the pixel values in the probability map with the global probability threshold, maps of LUCC occurrence can be simulated. To derive optimal probability thresholds for linear regression, optimization through a GA was implemented that will maximize the Fuzzy Kappa or neighborhood similarities between simulated and actual maps.

The statistical model was applied in a watershed in the Ifugao rice terraces, Philippines

to simulate the occurrence of agricultural abandonment. Results showed that slope, cosine aspect, quickflow, distance to town center, distance to road, world heritage site status, forest density, low vegetation density, and paddy field density were significant determinants of the local probabilities of agricultural abandonment while total forest area, five-year average precipitation, and average daily maximum temperature were significant determinants of the global probabilities of agricultural abandonment. Accuracy assessment of the simulated maps showed satisfactory accuracies for LUCC simulation applications. This confirms that the developed statistical model that uses time-series trends of spatial and non-spatial explanatory variables can be utilized to simulate future LUCC.

The developed statistical model brings forward the field of LUCC modeling by providing land use scientists and planners with another option in modeling and simulation with its capability to identify the significant spatial and non-spatial driving factors of LUCC and use these factors for future simulation. In future research, derivation of global probability thresholds based on optimization can be geared towards minimizing ADP to align simulated quantitative value of LUCC to actual quantitative values. Coupling the statistical model with simulation models to simulate LUCC based on future values of explanatory variables can also be explored.

# Chapter 5:

## Simulating the future status of the cultural landscape

**The contents of this chapter have been considered for major revision under the *Ecological Informatics* journal:**

Estacio, I., Sianipar, C. P. M., Onitsuka, K., & Hoshino, S. (in revision). Impacts of socio-environmental policy mix on mitigating agricultural abandonment: An empirical agent-based modeling. Ecological Informatics.

## 5.1. Introduction

To formulate science-based policies for agricultural landscapes, the complexity of agricultural landscapes, which is composed of social and ecological components, should be considered. A way to analyze such systems is through Agent-Based modeling, a bottom-up modeling paradigm where interaction of system actors are modeled to see the emergent phenomenon (Bonabeau, 2002; Groeneveld et al., 2017) An advantage of agent-based modeling over other modeling paradigms such as Statistical Modeling or System Dynamics is it can simulate the effects of decisions, processes, and interactions of actors. Thus, a modeler can create simulations of different scenarios by modifying the characteristics of actors in the system. Because of this, agent-based modeling is especially useful in simulating planning scenarios involving human behavior (Le Page et al., 2017).

Several Agent-Based Models (ABMs) have already been developed for modeling agricultural systems and simulating policy scenarios. Kremmydas et al. (2018) have reviewed ABMs developed for evaluating the impacts of agricultural policies. However, to the best of the authors' knowledge, there has not yet been any agent-based model developed that incorporated the passing down of farmlands of farm owners to their children. This is a vital component that needs to be considered as lack of farmland successors is one of the main global drivers of agricultural abandonment (Piras & Botnarenco, 2019; Qiu et al., 2014). Incorporating the process of farm succession within a farm household will lead to a better understanding of the dynamics of agricultural abandonment in mountainous landscapes where selling of

farmlands rarely occurs.

In addition to the research gap above, efforts in creating accurate maps based on agent-based models are lacking. Despite the fact that spatial agent-based models have been developed in the past, most of the modeling process did not incorporate a validation process for checking the accuracy of the produced maps. There have been efforts to check the accuracies of simulated maps in the past (Drogoul et al., 2016; Truong et al., 2016), but the maps only achieved moderate accuracies. In addition, there has not been a methodology established for developing models that simulate land cover maps based on non-spatial agents. This is a research gap that needs to be addressed because most human agents are difficult to spatialize like farmers.

This study aims to develop an ABM to simulate the impacts of various socio-environmental policy mixes on the spatial patterns of agricultural lands in a farm succession-based agricultural landscape. The ABM considers the interactions between the environment, government, and farm households composed of farm owners, farmlands, and children. The model generates the spatial patterns of paddy fields by simulating first the emergent total area of agricultural abandonment based on small-scale processes and allocates the abandonment area into land grids. To model the spatial aspect of the system, the ABM utilizes GIS raster files and a logistic model. To calibrate the model, Pattern-oriented modeling (POM) was adopted where a Genetic Algorithm was utilized to find the set of parameters that simulates system patterns closest to actual data (Grimm et al., 2005). This study is expected to advance the understanding of farm succession in agricultural landscapes. The developed ABM framework is also expected to advance the field of agent-based modeling in terms of simulating accurate maps without the need for spatial agents.

## 5.2. Methods

### 5.2.1. Empirical characterization and parametrization of the ABM

To empirically model the socio-ecological system of the Banaue rice terraces using an agent-based model, it is important to properly parametrize the attributes and behavior of actors in the system. For this purpose, the CAP (Characterization and Parametrization framework) was followed (Smajgl & Barreteau, 2017). A contextual circumstances case was adopted where

a large population exists, census data is not available, and only small-scale fieldwork can be implemented. In this case, expert knowledge and participant observation were utilized to characterize the model and elicit behavioral and attribute data of farm households in Banaue (Smajgl et al., 2014).



Fig. 5.1 One of the Ifugao farmers interviewed during the fieldwork. Permission was asked to take the photo.
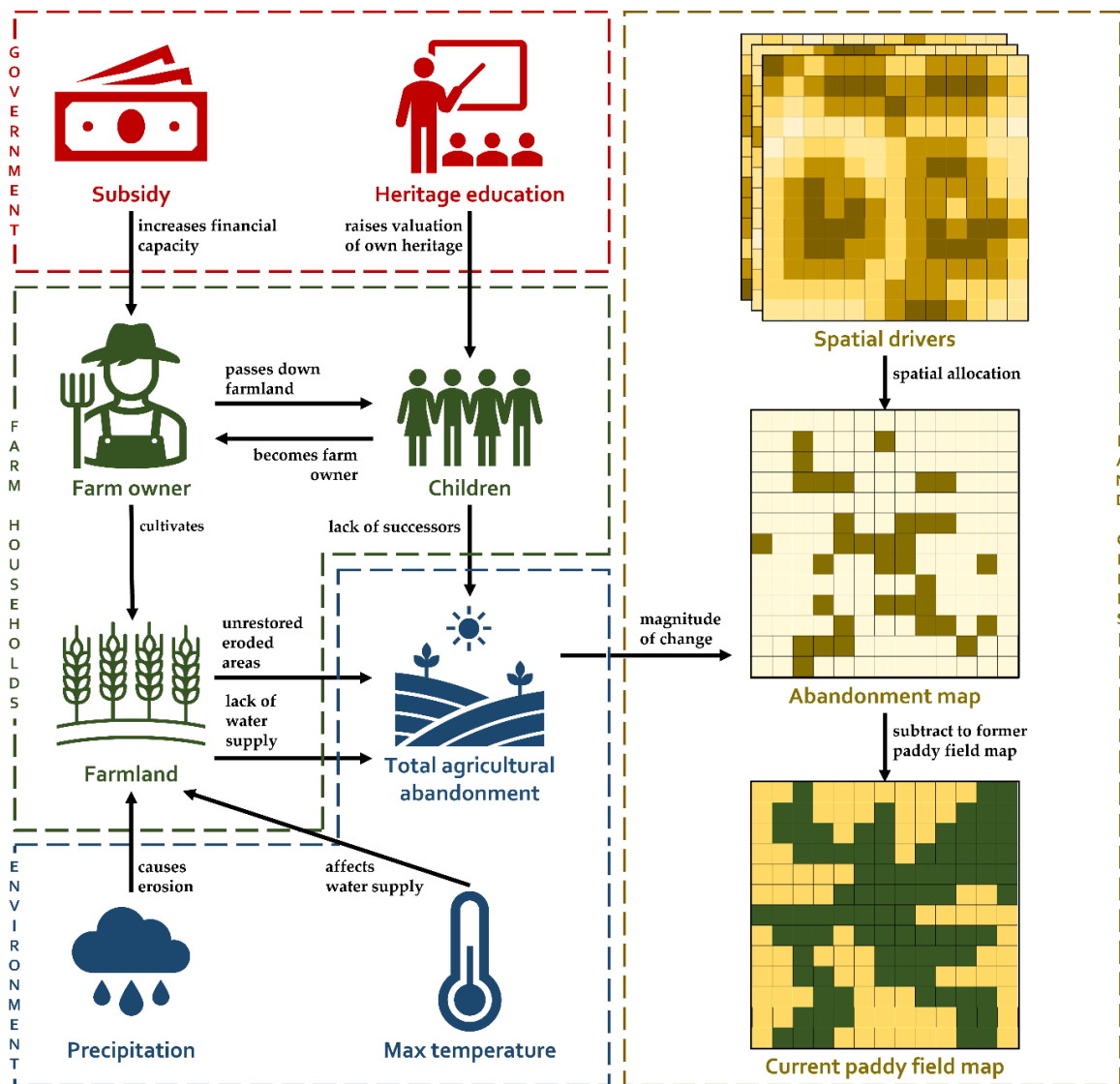
Fig. 5.2 The conceptual framework showing the interaction between the entities in the ABM

A small-scale fieldwork was conducted in August 2022 in the province of Ifugao, Philippines with the goal of interviewing academic experts, government officials, and farmers to elicit different points of views with regards to the abandonment of the rice terraces (Fig. 5.1). For these interviews, a semi-structured questionnaire was used to gather behavioral data in relation to attribute data. The questionnaires tackled the following: decision-making of farmers in abandoning their farmlands, drivers of abandonment, and possible mitigating policies. For the academic expert, an interview was conducted with the director of *Center for Ifugao Rice Terraces as Globally Important Agricultural Heritage Systems*, *Ifugao State University*, a research center established specifically to conduct focused research on the conservation of the

Ifugao Rice Terraces. For the point of view from the government, an interview with the agriculture division of the municipal government of Banaue was conducted. For the farmers, focus group discussion with five farmers ranging from 21 to 60 years old was conducted. Based on these interviews, agent classes, agent attributes, agent behaviors, and agent interactions were formulated (Fig. 5.2).

Aside from expert knowledge elicited from interviews, publicly available data were also used to parametrize the model. Data from the *Philippine Statistics Authority* were used to represent time-varying social data such as number of farm owners, family size, and life expectancy. Data from the public archive *Climate Change Knowledge Portal Time* were used to represent time-varying climate data such as precipitation and maximum temperature. Data from literature were also referred to parametrize the model.

Table 5.1 Global parameters in the model, its sources, and values

| Group | Parameter | Source | Unit | Default value |
|---|---|---|---|---|
| Environment | Coefficient of precipitation | Calibrated | $mm^{-2}$ | 10 |
| | Coefficient of max temperature | Calibrated | $°C^{-2}$ | 69 |
| Government | Government restores eroded terraces | Field survey | binary | False |
| | Ratio of heritage-valuing youth | Dizon et al., 2012 | - | 0.25 |
| | Subsidy per farm owner | Field survey | ₱ | 0.0 |
| Farm household | Initial number of farm owners | Philippine Statistics Authority | - | 1746 |
| | Initial lowest farm owner age | Calibrated | - | 29 |
| | Initial highest farm owner age | Calibrated | - | 60 |
| | Initial total paddy field area | Estacio et al., 2022 | Ha | 493.47 |
| | Monthly average family income | Philippine Statistics Authority | ₱ | 18166.67 |
| | Income threshold to consider migration | Calibrated | ₱ | 19,000.00 |
| Land cells | Coefficient of slope | Logistic regression | $°^{-1}$ | 0.0499 |
| | Coefficient of cosine aspect | Logistic regression | - | -0.303 |
| | Coefficient of quickflow | Logistic regression | $mm^{-1}$ | 0.000360 |
| | Coefficient of distance to town center | Logistic regression | $m^{-1}$ | 0.000198 |
| | Coefficient of distance to road | Logistic regression | $m^{-1}$ | -0.000281 |
| | Coefficient of heritage | Logistic regression | - | -0.841 |
| | Coefficient of density of forest | Logistic regression | - | 1.21 |
| | Coefficient of density of low vegetation | Logistic regression | - | 2.01 |
| | Coefficient of density of paddy field | Logistic regression | - | -2.54 |

*5.2.2. Development of the ABM*


The aim of the ABM is to simulate maps of paddy fields in Banaue as a result of farm cultivation, farm succession, and environmental conditions. By modifying selected parameters in the model, the model can also simulate the effects of policies in mitigating agricultural abandonment. The model utilizes combinations of spatial and non-spatial data that can be static or temporally-varying. Unknown global parameters were calibrated such that simulated temporal patterns of number of farm owners and area of paddy fields match actual data (Table 5.1). The ABM was developed through the open-source agent-based modeling software GAMA (GIS & Agent-based Modelling Architecture 1.8).
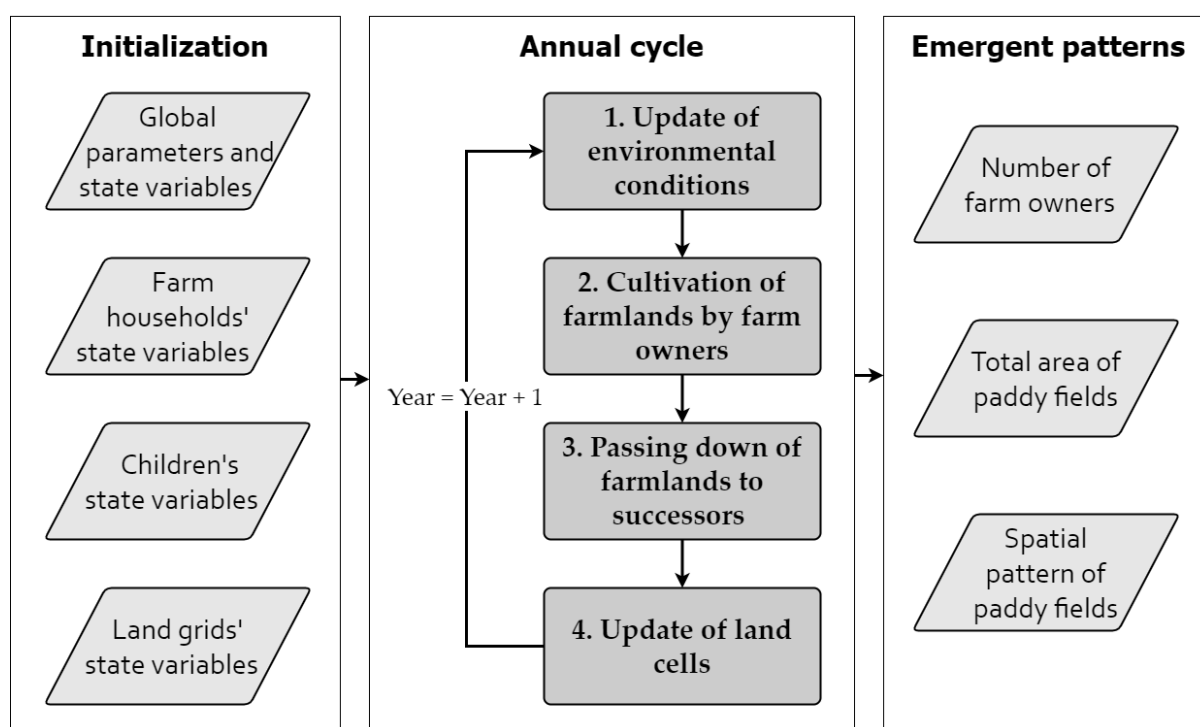


Fig. 5.3 The general flowchart of the ABM, showing the initialization of agents, the steps in the annual cycle, and the emergent patterns.

The mechanism of the ABM is based on the interaction between the environment, government, land grids, and farm households that consist of farmland, a farm owner, and their children. To implement this concept, three types of agents were used. The first type is a farm household agent where one agent represents both a farm owner and the respective farmland. The second type is a child agent which is an agent under a farm household. For each farm household, child agents exist which can potentially succeed the farmland and be future farm owners. The third type is a land grid agent which represents the characteristics of land for a grid of 30-m length. Input raster files were utilized to instantiate the state variables of these land grid agents such as land cover classification and spatial explanatory variables. The farm household agents, child agents, and land grid agents are all enclosed under a global agent which represents both the environment and government.

The time step of the model is set at 1 year, where in each time step the environment and government affect farm households, farm owners till their lands, farm owners can pass their lands to their children, and land grid cells change (Fig. 5.3). By the final simulation year, the number of farm owners, the total paddy field area, and a paddy field map are generated as emergent patterns of the system. The Overview, Design concepts, and Details (ODD) of the Banaue ABM was also laid out (Table 5.2) (Grimm et al., 2020). ODD is a generic format and a standard structure for documenting ABMs so that they can be replicated (Grimm et al., 2010).

Table 5.2 ODD (Overview, Design concepts, Details) protocol for the model (Grimm et al., 2020)

| Elements of ODD protocol | | Description |
|---|---|---|
| Overview | 1. Purpose and Patterns | **Purpose** |
| | |     The purpose of the model is to simulate maps of agricultural lands as a result of farm cultivation, farm succession, and changing environmental conditions. In parallel to this, the model also aims to simulate the resulting agricultural map based on a policy mix. |
| | | **Patterns** |
| | |     The model reproduces three patterns as a result of bottom-up processes: number of farm owners, area of paddy fields, and spatial pattern of paddy fields. |

2. Entities, state variables, and scales

**Entities**

The model includes four types of agents: a farm household agent which represents a farm owner and the respective farmland, a child agent which represents a child under a farm household, a land grid agent which represents grids that vary through space in the model, and a global agent which represents the both the environment and the government that encloses all the other agents. Thus, a hierarchical representation would be child agents populate a single farm household, and farm household agents and land grid agents populate a global agent.

**State variables**

Global agent:

*Environment*
- Precipitation
- Maximum temperature
- Average family size
- Life expectancy
- Erosion rate
- Water availability rate
- Total area of agricultural lands
- Total agricultural abandonment
- Farm household agents
- Land grid agents

*Government*
- Ratio of heritage-valuing youth
- Provision of aid in restoring eroded terraces exists?
- Amount of subsidy per farm household

Farm household agent:

*Farm owner*
- Age
- Child agents

*Farmland*
- Area of farmland
- Area of cultivated paddy fields
- Area of fallowed paddy fields (three-item list representing the area of fallowed land for the last three years)

Child agents:
- Age

- Income
- Stayed or migrated?
- Values the heritage of the terraces?
- Can inherit?

Land grid agents:
- Is a paddy field?
- Slope
- Cosine aspect
- Distance from town center
- Distance from road
- Is a world heritage site?
- Quickflow
- Density of forests
- Density of paddy fields
- Density of low vegetation

**Scales**

Spatial:

    The extent of the Bangaan watershed, which is around 8 km x 15 km long, is covered by spatially-varying 30 m x 30 m grids.

Temporal:

    The model runs at a 1-year time step. For calibration and validation, the model ran from the year 1990 to 2020 while for the simulation of policies, the model ran from 1990 to 2050.

3. Process overview and scheduling

1. Initialize the simulation. Load the raster files and store them as state variables of the land grid agents. Create farm household agents along with its child agents. Start the simulation.

2. At the start of every year, the global agent runs its "Update the environment" sub-model which updates its state variables *precipitation*, *max temperature*, *average family size*, *life expectancy, erosion rate*, and *water supply rate*.

3. Each farm household agent executes its "Cultivation" sub-model which updates its farmland area, cultivated area, and fallowed area.

4. Each farm household agent executes its "Succession" sub-model which updates its age and asks each of its child agents if they are willing to succeed the farmland. A child agent

updates its age and decides if it will choose to inherit the farmland. A farm household agent is removed from the model (the farm owner dies and the farmland becomes abandoned) if the farm owner's age exceeds the life expectancy.

5. The global agent runs its "Update land grids" sub-model which updates the total area of agricultural lands and the land grid agents' Boolean variable *Is a paddy field?*

6. Repeat steps 2 to 5 for each year until the final year. By the final year, export the land grids as a map along with other information such as number of farm owners and area of paddy fields.

| Design concepts | 4. Design concepts | **Basic principles** |
|---|---|---|

**Basic principles**

At the system level, the model addresses the question of how farm succession affect the area and spatial pattern of agricultural lands. The model also addresses a question in rural planning of how policies addressing farm owners will affect the farmlands.

**Emergence**

The primary result of the model is a map of the agricultural lands which emerges from cultivation based on environmental conditions and farm succession based on children's incomes and heritage values.

**Adaptation**

Farmers adapt to water unavailability by fallowing paddy fields that cannot be supplied by water. Child agents adapt to financial incapability by choosing to not inherit farmlands and migrate.

**Objectives**

Child agents who do not value the terraces decide whether to migrate by comparing their future total income to a threshold income.

**Prediction**

The decision-making of child agents in choosing to succeed the farmland is based on the implicit prediction that succeeding the farmland when the future total income is below a threshold will result to a poor quality of life.

**Interaction**

There are two kinds of interaction in the model: a direct interaction between farm household agents and their child agents and a mediated interaction between farm household agents and land grid agents. Farm household agents interact directly with their child agents by asking each of their child agents if they are willing to succeed the farmland. Child agents who are willing to succeed become new farm household agents while the previous farm household agent is removed. Meanwhile, farm household agents interact with land grid agents by altering the total area of cultivated paddy field, thereby altering the total abandonment area that will be allocated to land grid agents.

**Stochasticity**

During initialization, the initial farmland area, farm owner age, and number of children are randomized for each farm household agent. For each created child agent, its age, future income, and heritage valuation are also randomized.

**Observation**

By the end of the simulation, the model produces a map of the paddy fields as a result of a policy mix.

Details    5. Initialization

The simulation space of the model is first created by importing all raster files that will be used in the simulation (e.g., raster files of paddy field cover and spatial explanatory variables of agricultural abandonment). The extent of the raster files (all of which have the same extent) is set as the simulation space of the model. CSV files enumerating the values of precipitation, maximum temperature, average family size, and life expectancy for every year from 1990 to 2020 are imported. For calibration and validation, CSV files of the number of farm owners and area of paddy fields for years with available data are also imported.

Global parameters such as coefficients from the logistic model and calibrated parameters are set. Depending on the scenario, the values of heritage-valuing youth ratio, existence of erosion aid, and subsidy are assigned.

Land grid agents are instantiated throughout the simulation space based on the cells of the 1990 paddy field raster file. The initial paddy field classification is based on the classification in the same 1990 paddy field raster file. The spatial explanatory variables of the land grid agents are

adopted from the respective raster files for the year 1990.

Farm household agents are instantiated based on the number of farm owners in 1990 (1746 farm owners). Farm area for each farm household agent is assigned such that the total farm area of all agents equals the total paddy field area in 1990, *Totalpaddyfieldarea*. To do this, a variable *areafactor* ranging from 1 to 3 is assigned to each farm household agent. The sum of all farm household agents' *areafactor* is computed as *areafactorsum*. The area of *Farmland* for each farmer is then computed as follows:

$$Farmland = \frac{Totalpaddyfieldarea * areafactor}{areafactorsum}$$

Meanwhile, a farm owner's age is randomized from an equal distribution ranging from 26 to 50. The number of child agents in a farm household agent, *NC*, is also randomized based on the average family size, *FS*, as shown below:

$$NC = rnd\big((FS - 2) - 0.5, (FS - 2) + 0.5\big)$$

Child agents are instantiated as belonging under a farm household agent. The age of a child is determined from an equal distribution based on the farm owner's age using the equation below:

$$Childage = Farmownerage - rnd(26,35)$$

The income of the child is randomized based on an equal distribution centered on the average income in the Banaue municipality, represented by the following equation below:

$$Income = rnd(8167.0, 28167.0)$$

Even though the child has just been created (hence is a baby), the income was already assigned assuming that it will be the future income of the child.

6. Input data

For the years 1990 to 2020, CSV files enumerating the annual values of precipitation, maximum temperature, average family size, and life expectancy are used to update the annual values of respective variables. Every five years (e.g., 1995, 2000, 2005), raster files of spatial explanatory variables are used to update the respective variables in the land grid agents.

| 7. Sub-models | **Update the environment sub-model** |
|---|---|
| | Details of this sub-model can be found in subsection *5.2.2.1. Update of the global environment* |
| | **Cultivation sub-model** |
| | Details of this sub-model can be found in subsection *5.2.2.2. Cultivation of farmlands by farm owners* |
| | **Succession sub-model** |
| | Details of this sub-model can be found in subsection *5.2.2.3. Passing down of farmlands to children* |
| | **Update land grids sub-model** |
| | Details of this sub-model can be found in subsection *5.2.2.3. Update of land grids* |

*5.2.2.1. Update of the global environment*

Based on the fieldwork interview and related literature, erosion occurs in the Banaue rice terraces when heavy rains occur. Meanwhile, lack of available water occurs due to drying of creeks and streams in the dry season (Calderon et al., 2009; Soriano & Herath, 2018). In the model, erosion and water availability are represented by erosion rate and water availability rate, respectively, which indicate the rates that the two environmental factors affect farmlands. Erosion rate, $ER$, which indicates the percentage of a farmland affected by erosion, is represented by the following equation:

$$ER = 10^{-10} * c_{ER} * Precip^2 \qquad \text{(Eq. 5.1)}$$

where $Precip$ is the mean annual value of precipitation for the current simulation year while $c_{ER}$ is a coefficient for calibrating the effect of precipitation to erosion rate. Meanwhile, water availability rate, $WR$, which indicates the percentage of paddy fields that can be supplied by water, is represented by the following equation:

$$WR = 10^2 * c_{WR} * Temp_{max}^2 \qquad \text{(Eq. 5.2)}$$

where $Temp_{max}$ is the mean annual value of the maximum temperature for the current simulation year while $c_{WR}$ is a coefficient for calibrating the effect of max temperature to water availability rate. Both precipitation and maximum temperature vary through time using trends based on historical values. Aside from these environmental factors, the model also updates the annual values of demographic variables such as average family size and average life expectancy.

*5.2.2.2. Cultivation of farmlands by farm owners*

The farmers in the study area practice fallowing and recultivation depending on the available water supply (Estacio et al., 2022). For each farm household agent, a flowchart is followed to compute the area of paddy field that will be cultivated in a year (Fig. 5.4). This decision flowchart considers current values of erosion rate, water availability rate, area of the farmland, area of active paddy fields, area of fallowed fields, and age of the farm owner to calculate the area of recultivated fields, area of fallowed fields, and the consequent area of the farmland.

The flowchart starts with the computation of the area of eroded paddy fields, $Field_{eroded}$, based on the current year's erosion rate $ER$:

$$Field_{eroded} = ER * Field_{active} \qquad \text{(Eq. 5.3)}$$

where $Field_{active}$ is the area of the active paddy fields. If the government does not provide aid in restoring eroded terraces, the eroded paddy fields are immediately treated as abandoned. Next, the maximum area that can be supplied by water, $Maxwatered$, is computed based on the current water availability rate $WR$:

$$Maxwatered = WR * Farmland \qquad \text{(Eq. 5.4)}$$

Old farmers will also opt to cultivate only a portion of their land based on their capability. This is represented by the following equation:

$$Maxcapable = \frac{80 - age}{20} * Farmland \qquad \text{(Eq. 5.5)}$$

Equation 5.5 is only applied when a farm owner's age is greater than 60 and less than 80. The equation indicates that after the age of 60, a farm owner slowly loses the capability to farm and by the age of 80, is already incapable of tilling the farmlands. The harvestable land for the current year, $Land_{harvestable}$, is based on the lowest area between the maximum watered land, the maximum land that the farm owner is capable of cultivating, and farmland still not eroded, which is represented by the following equation:

$$Land_{harvestable} = \min(Maxwatered, Maxcapable, Farmland - Field_{eroded}) \quad \text{(Eq. 5.6)}$$
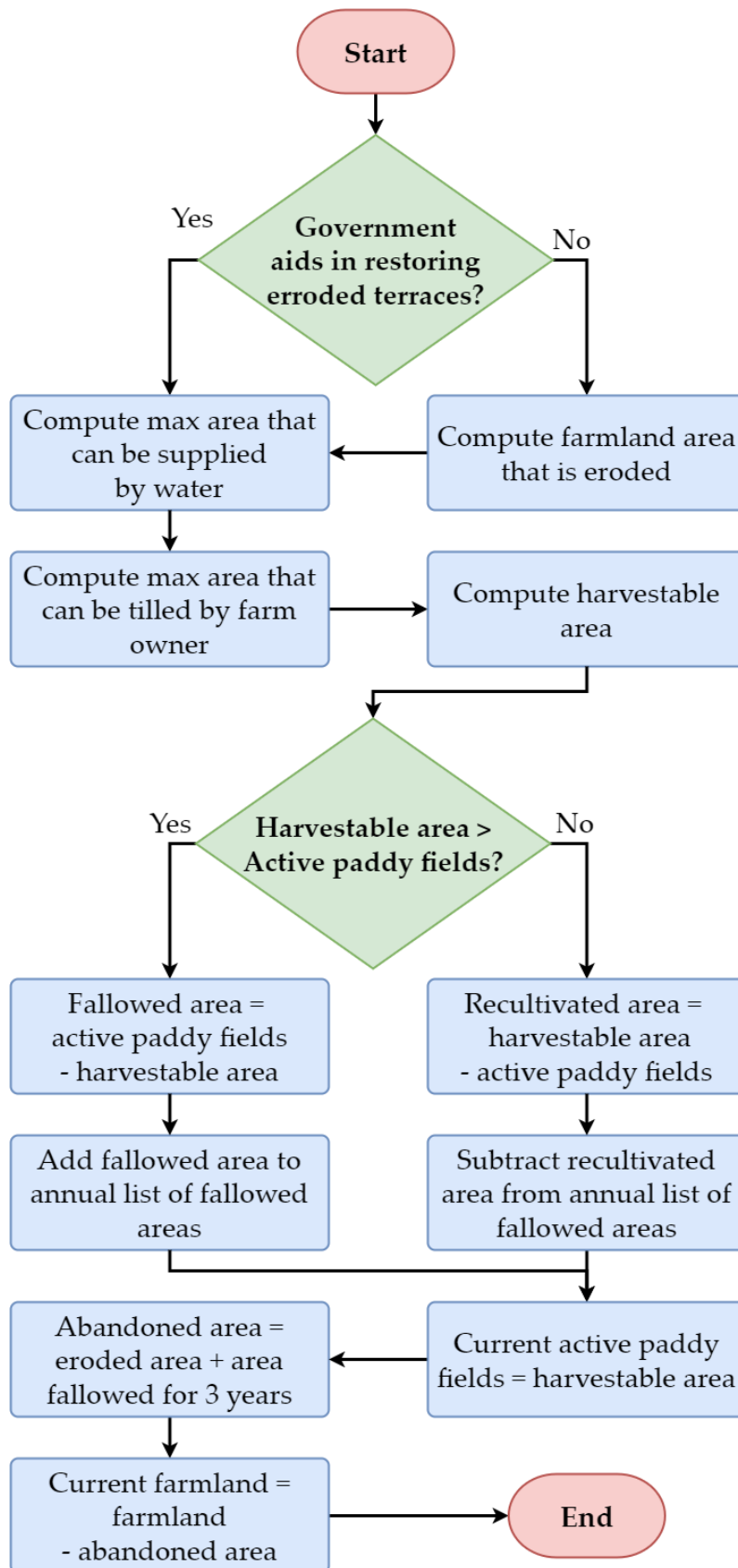
Fig. 5.4 Flowchart of processes in the cultivation sub-model of each farm household

If harvestable land is less than the active paddy fields, fallowing occurs where the

fallowed land is saved for 3 years. If it exceeds by 3 years, it will be considered permanently abandoned. If harvestable land is more than the active paddy fields, recultivation occurs. In this case, the area of fallowed land decreases by the area of the recultivated land. Whether recultivation or fallowing occurs, the area of the current active paddy fields for the current year is always equal to the area of the harvestable land.

The area of abandoned land for the current year is computed as the sum of the areas of eroded fields, $Field_{eroded}$, and fallowed fields for 3 years, $Field_{fallowed3years}$, which is as follows:

$$Field_{abandoned} = Field_{eroded} + Field_{fallowed3years} \qquad \text{(Eq. 5.7)}$$

Lastly, the area of the $Farmland$ decreases by the area of the abandoned field, as represented by the following equation:

$$Farmland_{current} = Farmland - Field_{abandoned} \qquad \text{(Eq. 5.8)}$$

*5.2.2.3. Passing down of farmlands to children*

Another main driver of agricultural abandonment is a lack of farmland successors. Based on the fieldwork interviews, almost all farm owners in Banaue work other jobs and treat farming as their part-time job. Farming on the rice terraces is almost unprofitable, hence selling of farmlands seldom occurs. In the rare occasion that a farmland is sold, the whole farmland is said to be retained hence no land is abandoned. Land abandonment mainly occurs when farmland is not inherited by any of the farm owner's children and the farm owner loses the capability to cultivate the farmland. From the perspective of a farm owner's child, the decision of inheriting the parents' farmland is based on the future income and valuation of the terraces as a heritage.

Based on this, a decision flowchart was formulated based on the dynamics of farm succession (Fig. 5.5). First, for a specific farm household agent, the ages of the farm owner and all children increase. For each child agent whose age is greater than 18 years old, the valuation of the rice terraces will be inspected. If the child agent values the rice terraces, it will still stay. If not, its income plus the government subsidy is computed to predict the total income once the child agent becomes a farm owner. If the total income is more than the global income threshold, the child will choose to stay. If not, it will migrate.
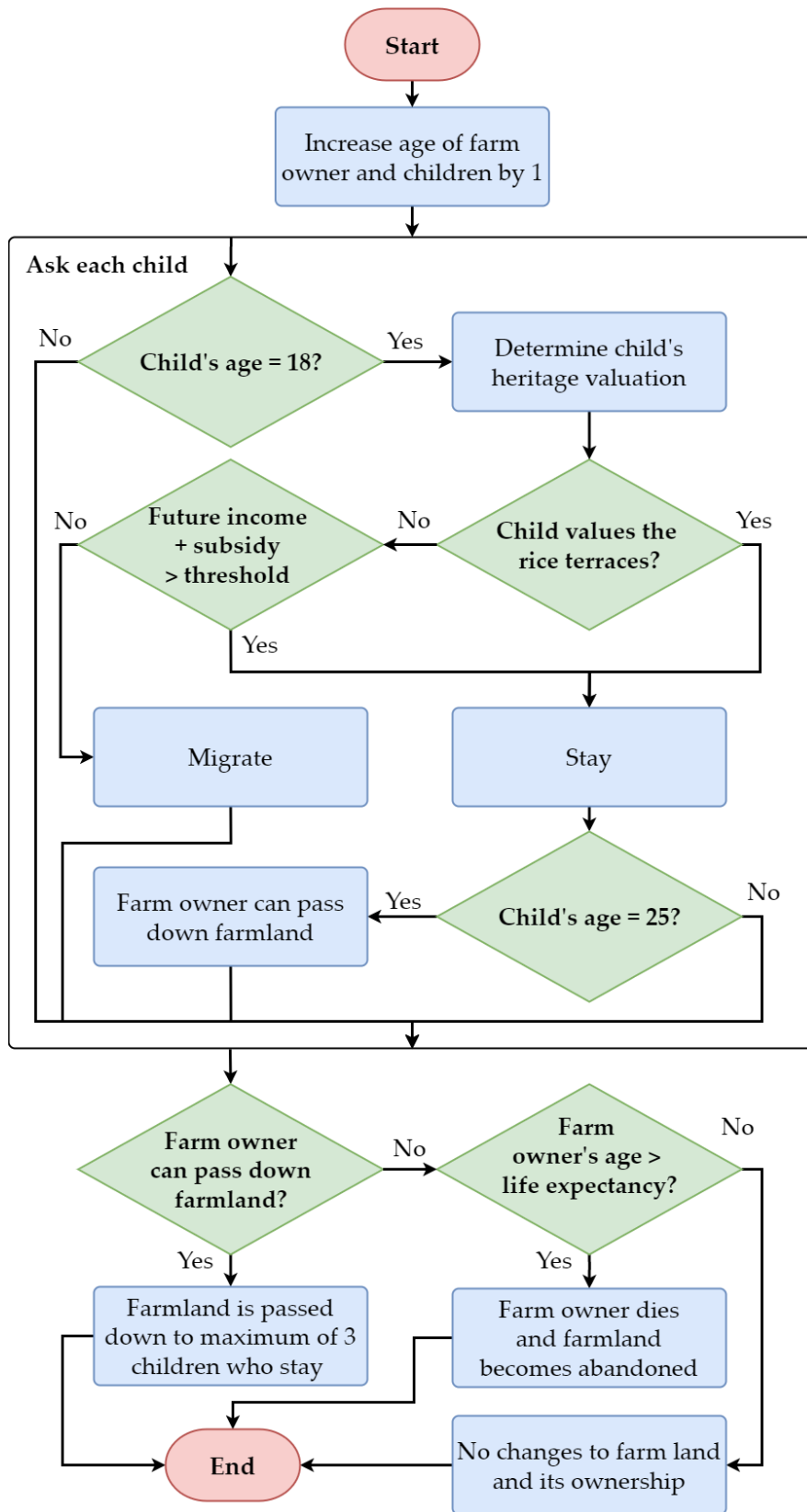
Fig. 5.5 Flowchart of processes in the succession sub-model of each farm household

The farmland is usually passed down by a farm owner once a succeeding child becomes married, per say as a way to increase the source of income of the newly married child. Thus, in the flowchart, the farmland is passed down once the oldest child turns 25. Most lands are passed down and distributed to the three eldest children who do not migrate, hence in the model, the farmland area is divided and distributed to a maximum of three child agents who stay. Abandonment of the farmland mainly occurs if there are no inheritors among the children in a farm household. This is represented in the flowchart as when a farmer exceeds the average life expectancy, the farm owner dies and the farmland becomes abandoned.

*5.2.2.4. Update of land grids*

After implementing the processes in the farm household agents, the emergent total paddy field area is computed by taking the sum of the farmland area of all farm household agents. Subtracting the total paddy field area to the former total paddy area results in the total agricultural abandonment for the current year.

To spatially allocate the value of agricultural abandonment, the probability of agricultural abandonment for each land grid agent is first computed using the produced logistic model, where state variables in the land grid agents are used as explanatory variables. The area of agricultural abandonment is then allocated to land grid agents one by one, where the land grid with the highest probability is assigned first as abandoned, then into the next land grid with the highest probability, until the total area of agricultural abandonment has been allocated. It is also possible that the total paddy field area for the current year is greater than last year's area. In this case, total recultivation occurred and the allocation procedure is skipped for the current year. The allocation procedure is resumed once the total paddy field area becomes less than the total paddy field area during the time the last allocation procedure was implemented.

*5.2.3. Model calibration and validation*

To ensure that the developed ABM closely imitates reality, the concept of Pattern-oriented modeling was adopted where model calibration is implemented until simulated system patterns match observed patterns in the agricultural landscape (Grimm et al., 2005). The temporal values of number of farm owners and area of paddy fields were used to calibrate

selected model parameters while spatial patterns of paddy fields were used to validate the model.

The calibration procedure employs a Genetic Algorithm to find the set of parameters in the model that minimizes the difference between simulated and actual patterns. To do this, an optimization measure, $OM$, was formulated as follows:

$$OM = SD_{farmownersnumber} * SD_{paddyfieldarea} \qquad \text{(Eq. 5.9)}$$

where $SD_{farmownersnumber}$ is the standard deviation between the actual and simulated numbers of farm owners while $SD_{paddyfieldarea}$ is the standard deviation between actual and simulated total areas of paddy fields. This optimization measure ensures that both the standard deviations in number of farm owners and area of paddy field were minimized. The parameters chosen for calibration were coefficient of erosion (from 1 to 100), coefficient of water availability (from 1 to 100), income threshold to consider migration (from ₱10,000 to ₱20,000), initial lowest farm owner age (varied from 26 to 35), and initial highest farm owner age (varied from 50 to 60). A simulation for each set of parameters was run with 30 repetitions to consider randomness.

After incorporating the optimized set of parameters, a validation procedure was implemented to check the robustness of the model in simulating system patterns close to reality. In addition to the number of farm owners and area of paddy fields, the simulated maps were also assessed for their accuracies. For the number of farm owners, except for the initial year, data were available only for the years 2002 and 2012. For the land cover, maps were available from 1990 to 2020 in five-year intervals. However, only data for the years 1995, 2000, 2015, and 2020 were used for validating the area and spatial patterns of paddy fields. The years 2005 and 2010 were excluded as expansion of paddy fields occurred after the declaration of the world heritage sites in the Ifugao rice terraces as "in danger" in 2002 (Estacio et al., 2022). The expansion of paddy fields during this period was treated as the effect of an external driver and not of a naturally occurring process in the Ifugao rice terraces, hence the maps for 2005 and 2010 were not included for validation. The fuzzy Kappa statistic, which represents the similarities between two maps based on local neighborhoods, was used as the accuracy measure for comparing simulated and actual maps (Drogoul et al., 2016; Visser & De Nijs, 2006).

Table 5.3 Policies considered for mitigating agricultural abandonment

| Policies | Description | Parameter to be varied | Experimental values |
|---|---|---|---|
| Provision of aid in restoring eroded terraces | A program where the local government provides aid to farmers whenever a portion of their farmlands is eroded. In this policy, all eroded terraces are restored hence farmers do not have to abandon this portion of their land. | Government restores eroded terraces | True |
| Promoting heritage valuation through education | A program where the education curriculum in the Ifugao has an intensive focus on establishing the valuation of the Ifugao rice terraces to the youth | Ratio of heritage-valuing youth | 0.30 – 0.50 (increments of 0.05) |
| Provision of subsidy per farm household | A program where the local government provides a monthly subsidy to each farm household for choosing to participate in preserving the Ifugao rice terraces | Subsidy per farm owner | ₱0 – ₱3000 (increments of ₱500) |

*5.2.4. Simulation of policies through batch experiments*

Three policies were considered for the mitigation of the agricultural abandonment in the rice terraces: (i) Provision of aid in restoring eroded terraces, (ii) Promoting heritage valuation through education, and (iii) Provision of subsidy per farm household. To determine if a synergistic effect exists between these policies, a batch simulation was implemented where policy-related parameters were varied one-by-one until every mix of parameters was used (Table 5.3). A simulation for each set of parameters was run in 30 repetitions. Temporally-varying parameters used trends from past values to forecast their future values. Thus, the simulations consider climate-change and changing demographic profile.

Table 5.4 Actual and simulated values of number of farms and area of paddy fields through different years

| Patterns | Year | Actual | Simulated | Residual | Percent deviation |
|---|---|---|---|---|---|
| Number of farm owners | 2002 | 1946 | 2186 | 240 | 12.32% |
| | 2012 | 2615 | 2449 | -166 | -6.35% |
| Area of paddy field (ha) | 1995 | 600.03 | 603.22 | 3.19 | 0.53% |
| | 2000 | 528.21 | 580.64 | 52.43 | 9.93% |
| | 2015 | 503.28 | 502.27 | -1.01 | -0.21% |
| | 2020 | 493.47 | 479.32 | -14.15 | -2.87% |
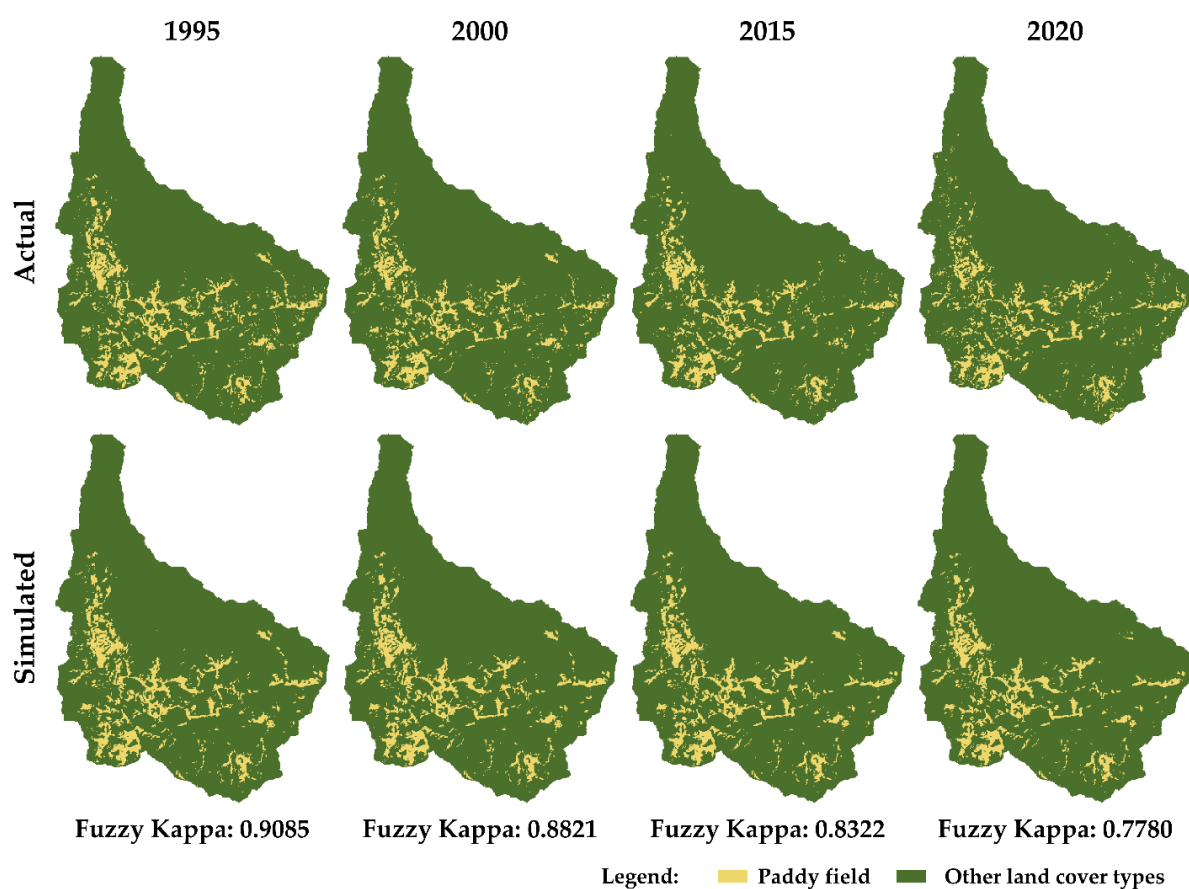


Fig. 5.6 Comparison between actual and simulated maps of paddy fields in the study area

## 5.3. Results

### 5.3.1. Calibration and Validation

Validation of the ABM based on comparing the simulated system patterns with actual data produced accuracy measures for every year (Table 5.4 and Fig. 5.6). For the simulated

area of paddy fields, the maximum magnitude of the residual was 52.43 ha (for the year 2000) and the maximum magnitude of the percent deviation was 9.93% (also for the same year). Given that the maximum absolute percent deviation was less than 10%, the model was deemed able to simulate the area of paddy fields with an acceptable accuracy.

For the simulated number of farm owners, the maximum magnitude of the residual was 240 (for the year 2002) and the maximum magnitude of the percent deviation was 12.32% (also for the same year). Even though the maximum absolute deviation was above 10%, given the difficulty of modeling the complexity of population dynamics and how close the deviation is to the 10% value, the maximum absolute percent deviation of 12.32% was accepted. Thus, the model was deemed to simulate the number of farm owners at an acceptable but low accuracy.

For the simulated spatial patterns of paddy fields, it can be observed that the Fuzzy Kappa statistic, which represents the local neighborhood similarities between two maps, decreases through time from the initial year. This was expected as the initial paddy field map in the model was initialized using an actual map. In the real world, a current land cover will be more similar to land cover five years from now than land cover twenty years from now. Given that there will be more variation in land cover change as the year passes, the difference between actual and simulated maps will also be higher. Given this circumstance, the lowest fuzzy Kappa statistic produced was 0.7780 for the latest year of 2020, 30 years from the starting year. Given that the fuzzy kappa statistic is still of high value even  after a 30-year period from the initial year, the model was deemed able to simulate the spatial patterns of paddy fields at an acceptable accuracy.

*5.3.2. The future of the terraces given a business-as-usual scenario*

Based on the BAU scenario where climate change and demographic changes were considered by assuming that past trends will continue, simulation results showed that the area of paddy fields will continue to decrease from 479 ha in the year 2020 to 336 ha by the year 2050 (Fig. 5.7). This is a 143-ha decrease in a span of 30 years. Interestingly, in the 30-year period between 2020 and 1990, the rice terraces decreased in area by 178 ha. Thus, even with the consideration of future climate changes, the amount of abandonment for the next 30 years is less than the abandonment in the previous 30 years.
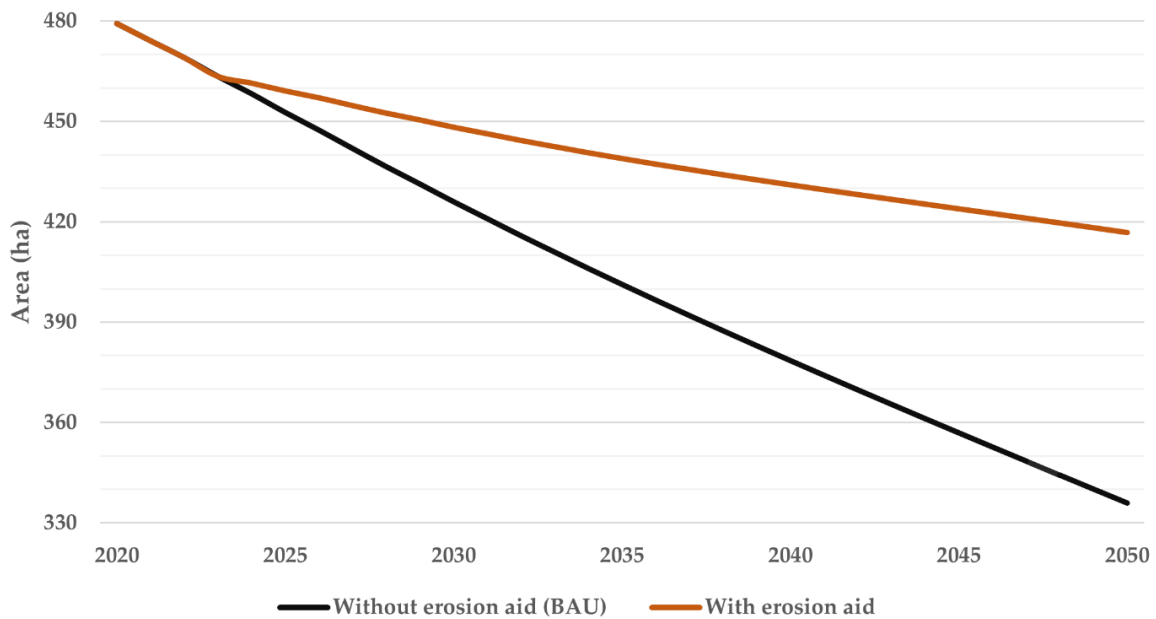
Fig. 5.7 Trend in total area of paddy fields from 2020 to 2050 with and without the provision of aid in restoring eroded terraces

*5.3.3. Effect of each proposed policy*

Simulations showed that providing aid to farmers in restoring eroded terraces will make the total area of the rice terraces to 417 ha by 2050, preventing 81 ha of abandonment if compared to the BAU scenario (Fig. 5.7). This is a 56% decrease in abandoned areas through the 30-year period from 2020 to 2050, hence restoration of eroded areas can be deemed an effective policy for mitigating agricultural abandonment.

For promoting heritage valuation through education, the simulations showed that increasing the ratio of heritage-valuing youth leads to an increase in the the future area of the paddy fields (Fig. 5.8). This was expected as a higher percentage of children valuing the terraces lead to less migration which also leads to an increase of successors. However, contrary to expectations, strengthening the heritage valuation of the youth only showed negligible effects in mitigating land abandonment. By the year 2050, a 0.5 ratio of youth valuing the terraces will lead to a total paddy field area of 341 ha, only a 5-ha increase from the BAU value of 336 ha. This is only 4% of the 143-ha of abandoned land from 2020 to 2050. Hence, even though the interviewed experts suggested the promotion of the rice terrace's heritage value as a mitigating solution, it may not be deemed as an effective solution based on the simulation

results.
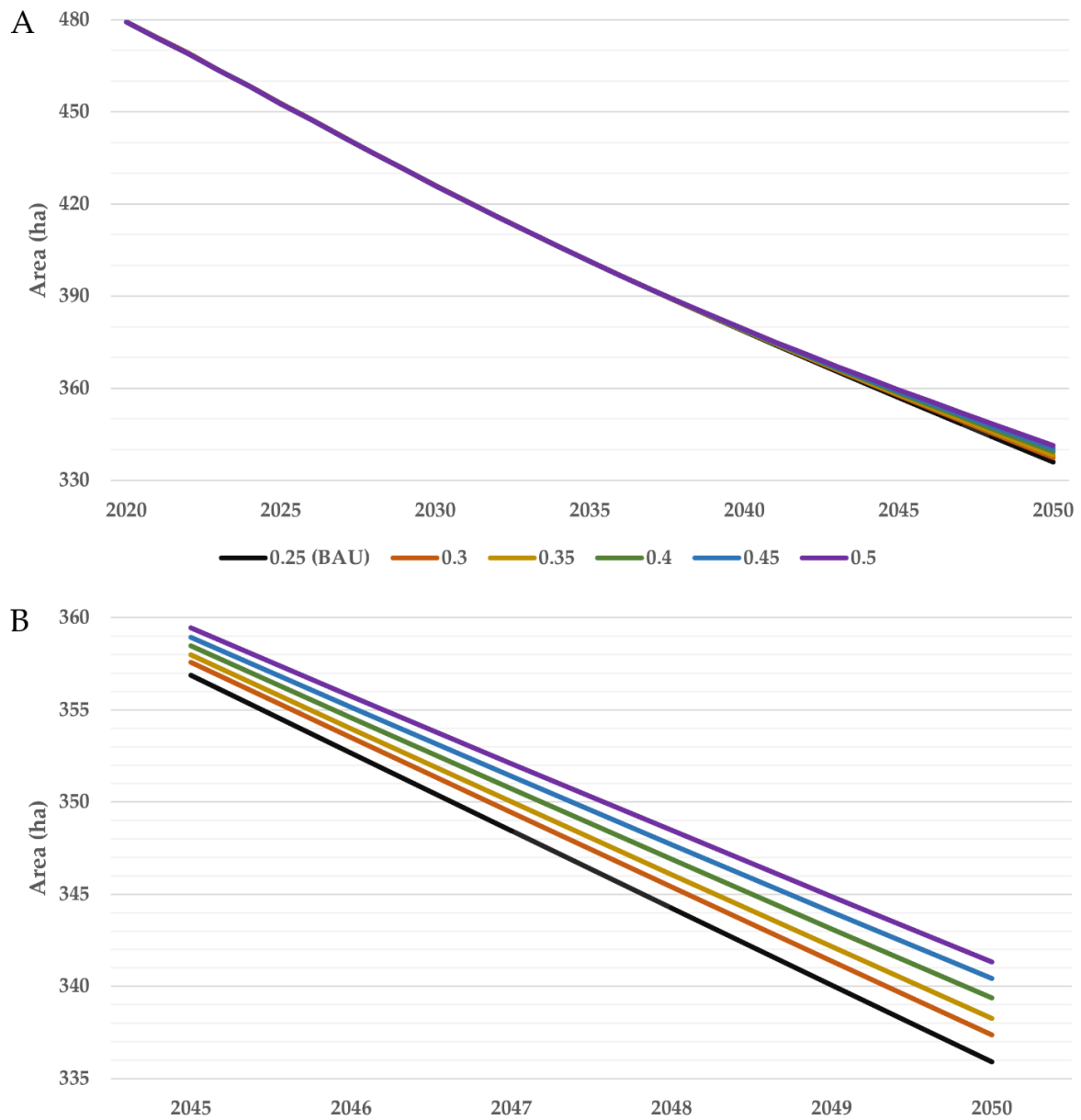


Fig. 5.8 Trend in total area of paddy fields through scenarios of varying average ratios of youth valuing the rice terraces: (A) Trend from 2020 to 2050; (B) Trend from 2045 to 2050 to emphasize the differences in total area
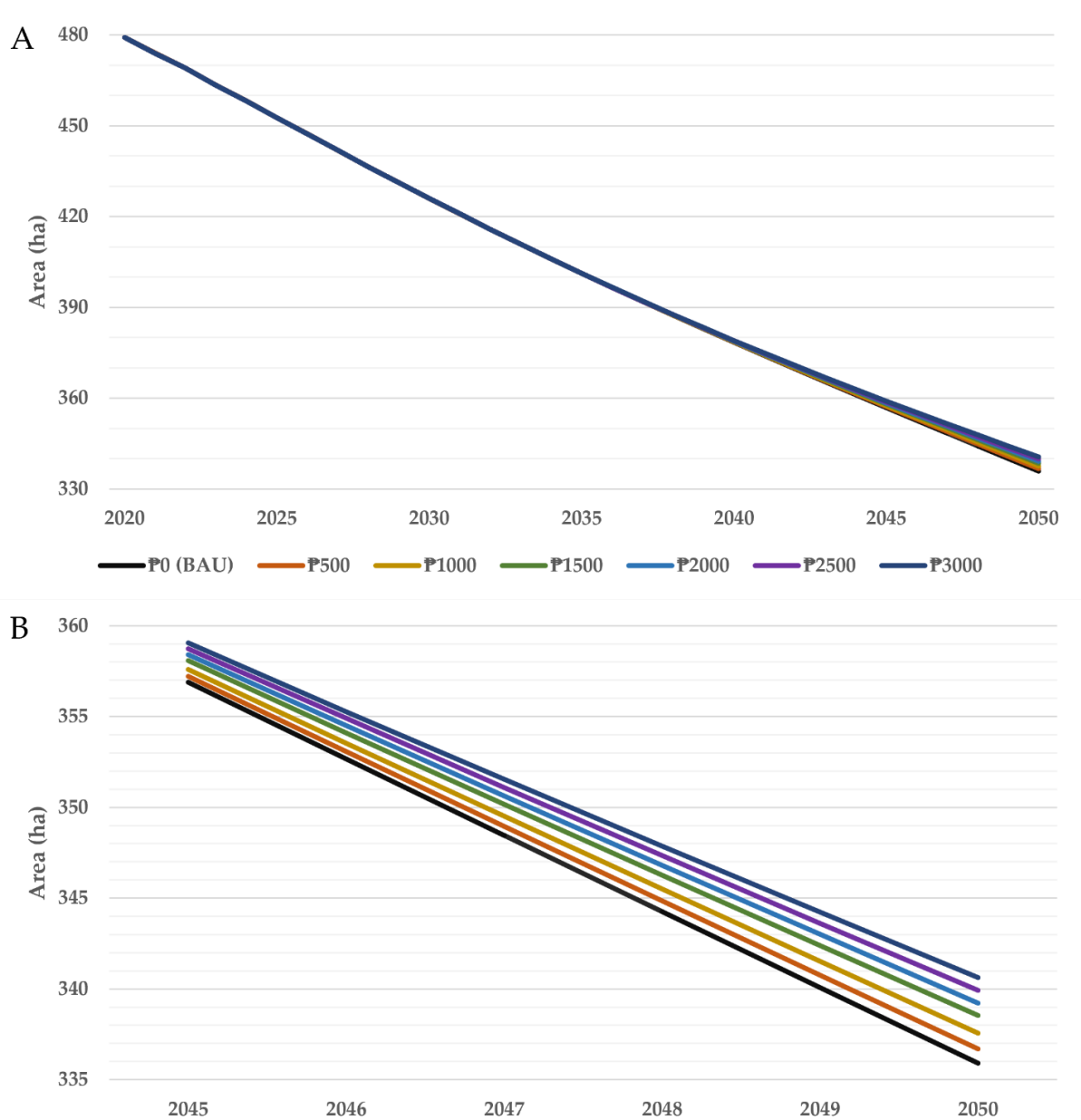
Fig. 5.9 Trend in total area of paddy fields through scenarios of varying amounts of monthly subsidy given to each farm owner: (A) Trend from 2020 to 2050; (B) Trend from 2045 to 2050 to emphasize the differences in total area

Lastly, simulations showed that provision of subsidies to farm owners results in the mitigation of agricultural abandonment (Fig. 5.9). This was an expected effect as providing subsidies motivates children in inheriting the farmlands because of a predicted increase in financial capability. Similar to the previous policy, the simulations showed that provision of subsidy only had negligible effects in mitigating agricultural abandonment, with only 3% of the abandonment starting from the year 2020 mitigated. Overall, the simulation results indicate

that providing subsidies to farm households is ineffective for mitigating agricultural abandonment.

*5.3.4. Policy mix*

Implementing a policy mix has a higher mitigating effect on agricultural abandonment than implementing just a single policy (Fig. 5.10). However, the provision of subsidy and promoting heritage valuation showed an antagonistic relationship, where increasing the input of one of the policies lessens the effect of the other policy. For example, at a subsidy of ₱0 without aid in restoring eroded areas, increasing the heritage-valuing youth ratio by 0.05 led to a paddy field area increase of around 1 ha. However, at a subsidy of ₱3,000 (still without aid in restoring eroded areas), increasing the youth ratio by 0.05 only led to paddy field area increase of around 0.5 ha. The other way around can also be the case, where increasing the subsidy at lower heritage values has higher impact to the paddy field area than increasing the subsidy at higher heritage values. This circumstance can be explained by both policies affecting the migration rate which may lead to redundancy. An increase in heritage-valuing youth leads to less people needing subsidies to be persuaded not to migrate, and vice-versa. In that sense, applying these policies in parallel as a policy mix is inefficient.

On the other hand, providing aid in restoring eroded areas displayed a synergistic effect, where implementing it also increased the effect of the other policies. For example, increasing the heritage-valuing youth ratio at ₱0 subsidy when restoration aid was provided showed an average increase of around 1 ha while the increase was only around 0.8 ha for the same case without the restoration aid. The same can also be said for increasing the subsidy, where providing subsidies with erosion aid has more impact on mitigating abandonment than providing subsidies without erosion aid. Thus, mixing the provision of aid in restoring eroded terraces with one of the other policies (selective policy mix) is deemed efficient.
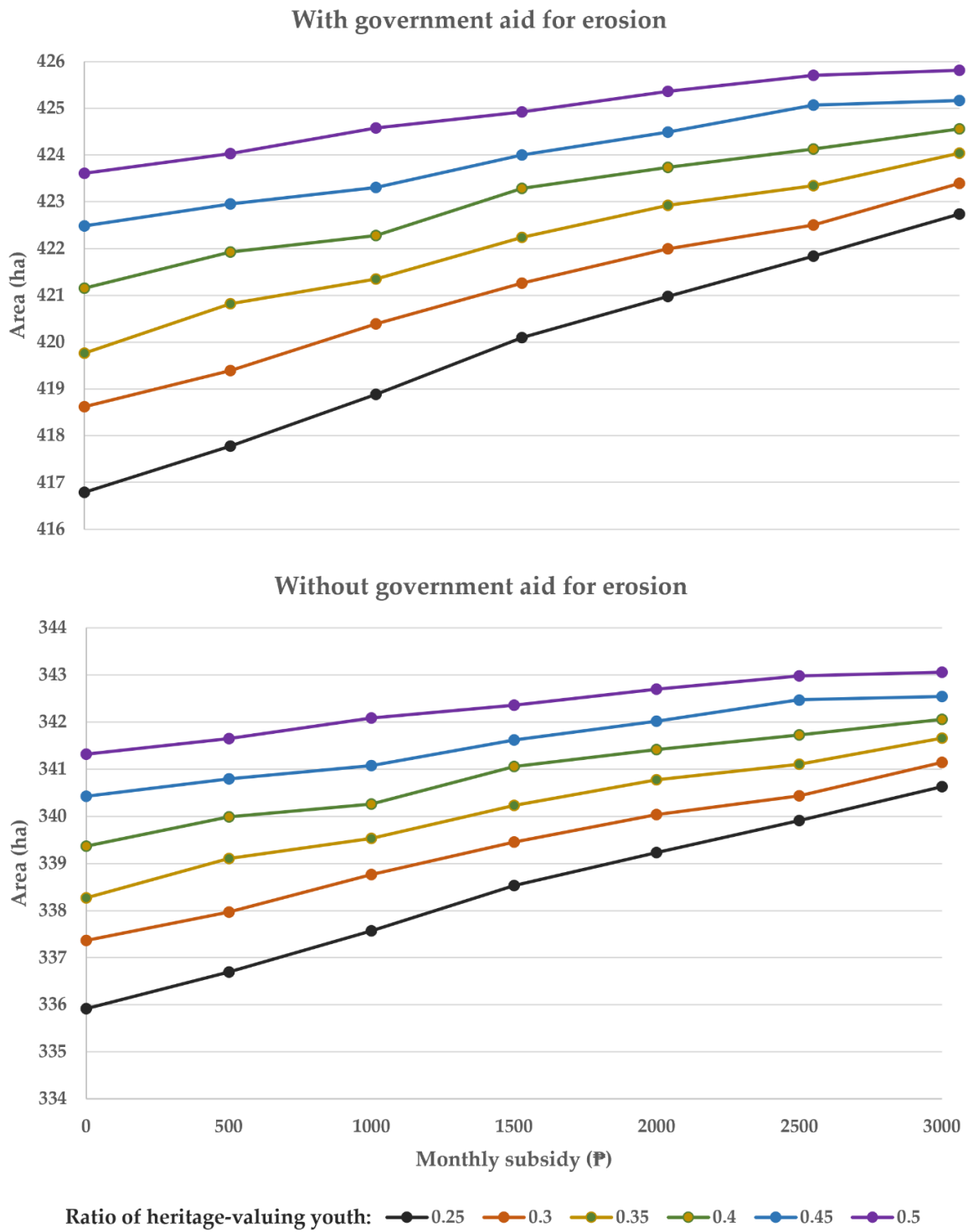
Fig. 5.10 Effect of different policy mix on the total area of paddy fields by the year 2050.

## 5.4. Discussion

### 5.4.1. Robustness of the ABM in simulating spatial and non-spatial patterns

To calibrate the model, an optimization procedure was implemented where a Genetic Algorithm was utilized for adopting pattern-based modeling. A key component of this procedure is the formulation of an optimization measure where the standard deviation of every pattern is treated as a controlling factor. By minimizing this optimization measure through a Genetic Algorithm, the set of global parameters that minimizes the differences between simulated and actual patterns can be found. This can be useful in ABM studies where calibration for pattern-oriented modeling is needed.

Validation of the calibrated model showed that the simulated patterns of number of farm owners and areas of paddy fields reached acceptable accuracies. Thus, the developed ABM can be considered generating non-spatial system patterns similar to observed patterns. For the spatial patterns of paddy fields, the accuracies of generated land cover maps were shown to decrease as the years from the initial simulation year increase. However, as the ABM utilizes a spatial allocation based on a logistic model, the model will create a map based on the dominant spatial pattern of paddy fields which is the main clusters of terraces. Thus, despite the nature of the simulations where accuracies of generated map decrease through time, it can still be deemed that the generated maps still capture the dominant patterns of the paddy fields. Moreover, despite a 30-year difference from the initial year, the generated paddy field map can still be considered of high accuracy (Drogoul et al., 2016; Truong et al., 2016). Thus, the developed ABM can also be considered generating accurate spatial patterns of land cover despite the usage of non-spatial agents.

### 5.4.2. Policy implications for conserving the Ifugao rice terraces

Based on the fieldwork interviews and proposals from literature (Calderon et al., 2009; Castonguay et al., 2016), three policies were considered for mitigating the agricultural abandonment in the Ifugao rice terraces: aid in restoring eroded terraces, increasing heritage valuation through education, provision of subsidy per farm household. Based on the simulations, providing aid to farmers in restoring terraces in their farmlands is highly effective

in mitigating agricultural abandonment. The simulation results imply that erosion contributes to almost half of the total abandonment in the rice terraces, and that restoring these eroded areas has the highest impact in mitigating agricultural abandonment. Meanwhile, increasing the heritage valuation of the rice terraces among the youth through education was found to be ineffective in mitigating agricultural abandonment, mitigating only 4% of the total agricultural abandonment from a BAU scenario. Provision of subsidy to farm owners was also found ineffective, mitigating only 3% of the total abandonment. Overall, given the restricted budget of the municipal government of Banaue for conserving the rice terraces, it is recommended that government officials should just focus on providing continuous aid in restoring eroded areas to mitigate as much agricultural abandonment as possible (Fig. 5.11).
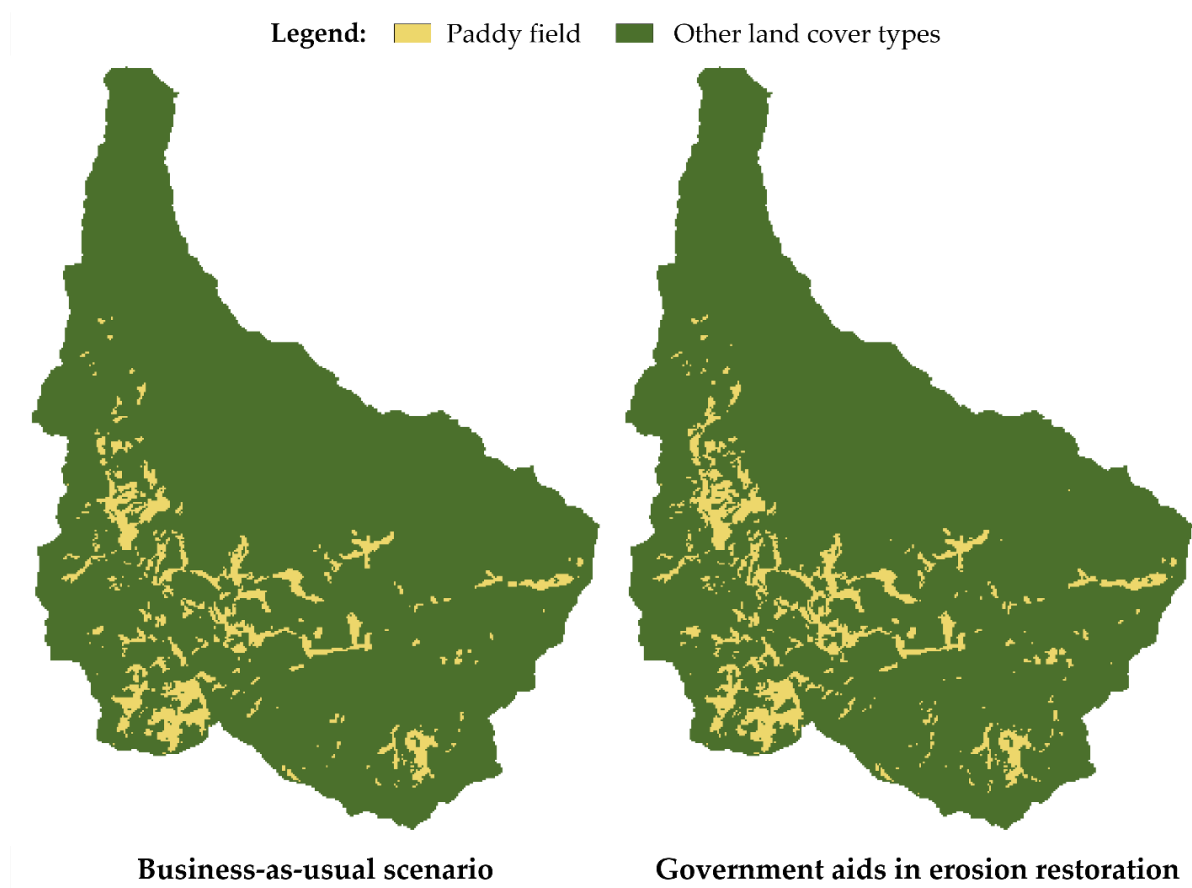


Fig. 5.11 Maps of paddy fields by the year 2050 through a business-as-usual scenario and a scenario where the government aids in restoring eroded terraces.

The effectiveness of restoring eroded areas can be attributed to two factors. First, the results imply that the environmental driver erosion has a larger contribution to the agricultural abandonment than the social driver lack of successors brought by financial incapability and low heritage valuation. Contrary to former hypothesis that social policies may have a huge environmental effect, simulations showed that the emergent effect is small relative to environmental policies. Thus, addressing erosion brought a much higher mitigating effect than addressing financial incapability and low heritage valuation. Second, the effectiveness of restoring eroded areas can also be attributed to its instant effect to the paddy fields. Restoring eroded areas directly affects the paddy fields, hence its effect in increasing paddy field area manifests instantly. On the other hand, the effect of subsidy and education takes time to manifest as a lack of successor only takes of effect on the rice paddy fields once the farm owner without a successor starts to age and then dies, leaving the farmlands abandoned. Hence, the effect of social policies may take at least one generation for its effect to manifest.

It is also expected that agricultural abandonment due to a lack of successor will ease in the future if the trend of increasing family size continues. During the field work, the authors suggested in interviews if birth control may have an impact in mitigating the agricultural abandonment, to which all correspondents answered that it may not have a significant effect. Based on the simulation results, the answer of the respondents may prove to be correct as more children ensure the likeliness that a successor will be present in one of the children. However, even with the existence of an inheritor, large decreases in the paddy fields will still occur brought by the environmental driver. With the advent of climatic change which drives increases in precipitation brought by more intense typhoons, it is also expected that agricultural abandonment will intensify. Overall, given the larger effect of environmental drivers over social drivers, agricultural abandonment for the next 30 years may have a larger magnitude than for the last 30 years. In the end, policies that directly affect agricultural lands have much higher mitigating impacts than policies that affect the social aspects of farm households.

### 5.4.3. Limitations and future direction

An inevitable part in modeling is the simplification of processes as some processes are too complex to be incorporated. Hence, the developed ABM has several limitations and may need improvements in the future.

First, the process of computing the values of erosion and water supply were simplified to only be caused by precipitation and maximum temperature, respectively. In reality, several factors affect the magnitude of these environmental drivers. For example, erosion is affected not only by precipitation but also by the slopes of the land and the types of soil. In the model, it was assumed that the mountain slopes and soil types do not change through time, hence only the precipitation rates will have an effect in the temporal variation of erosion values. Same with erosion, water supply is affected not only by temperature but also by the quality of the land. Again, the quality of the land was also assumed to be constant through time and only temperature affects the temporal variation of water supply. In the future, determination of erosion and water supply based on additional factors can be incorporated in the ABM to make the simulation results more accurate.

The model also does not consider the feedback caused by the changing land cover. Several studies have shown that the transitions between paddy fields and vegetation cover changes the water yield and further aggravates agricultural abandonment, creating a feedback loop between land cover and farmers' cultivation processes (Estacio et al., 2022; Soriano & Herath, 2018). Aside from this, the density of a land cover type in the surrounding of a parcel also determines the likelihood of abandonment, thus the feedback loop is also spatial in nature. The complexity of this feedback loop needs thorough calibration and validation, hence should be meticulously incorporated in the model.

Lastly, the model does not consider social changes in the real world. For example, the marrying age in almost all parts of the world is increasing over time. The income of people and the prices of commodities also change according to the economy. To make a more accurate (but more complicated) model, these demographic and economic changes need to be incorporated.

The socio-ecological system of Ifugao is a complex system composed of interacting social, economic, and environmental entities that change through time. Therefore, future studies are still needed to fully capture the processes in the system. It should be worth mentioning that not every process in the model needs to be captured to develop a decision-making model. A more complicated model does not necessarily translate into a more effective model (Sun et al., 2016).

## 5.5. Conclusion

This study presents an ABM that simulates the impacts of socio-environmental policy

mix to the spatial patterns of paddy fields in the mountainous agricultural landscape of Ifugao rice terraces. The ABM models the interactions between the environment, government, and farm households composed of farm owners, farmlands, and children. The model employed a procedure to generate accurate land cover maps even with the use of non-spatial agents by simulating first the emergent change in area of a land cover then allocating it into map through a logistic model. To calibrate the model, pattern-oriented modeling was adopted so that simulated system patterns match actual data. To simulate the impact of a policy mix, selected parameters were varied to represent policy scenarios.

The validation of the model showed that simulated system patterns such as number of farm owners, area of paddy fields, and spatial patterns of paddy fields were of acceptable accuracy. The simulation results showed that providing aid in restoring eroded terraces mitigates almost half of the agricultural abandonment. Meanwhile, increasing the ratio of youth valuing the terraces and providing subsidies to farm households showed only negligible impacts on mitigating agricultural abandonment. Thus, it is recommended that the local government of Banaue should just focus on providing aid in restoring eroded terraces for effectively mitigating agricultural abandonment. The results of the simulations also imply that the environmental driver erosion has a higher contribution to the agricultural abandonment problem than the social driver lack of successors.

The employed methodology of utilizing non-spatial agents to create accurate land cover maps can be adopted in other agent-based modeling studies where agents do not have locations but emergent spatial patterns of environmental changes need to be simulated. The employed calibration routine of using GA to implement pattern-oriented modeling can also be used in other studies. In the future, the developed ABM can be recalibrated and applied to other mountainous agricultural landscapes where farm succession occurs. Future improvements to the model can be used such as incorporating the feedback of changing land cover to the farmers' cultivation process.

# Chapter 6:

# Summary and Conclusion

## 6.1. Introduction

Due to the ever-changing demands of human society, land cover changes occur globally. Among the landscapes present, mountainous agricultural landscapes are one of the most vulnerable to changes because of the tight interaction between the local people and its environment (Aguilar et al., 2021; Y. Cao et al., 2013; Pôças et al., 2011; Tarolli & Straffelini, 2020). Not only do actors in these socio-ecological systems regularly alter the environment, modernization in the 20th century also brought unprecedented changes to these systems (Gellrich, Baur, Koch, et al., 2007; Gellrich & Zimmermann, 2007; MacDonald et al., 2000; Xystrakis et al., 2017). For example, the mountainous agricultural landscape of Ifugao rice terraces has been experiencing intensive agricultural abandonment for several decades already (Bantayan et al., 2012; Calderon et al., 2015; FAO, 2018). If left unmanaged, changes in mountainous agricultural landscapes may lead to changes in the ecosystem services that can lead to harsh consequences to the people and the environment (B. Li et al., 2016; Y. Liu et al., 2020; Wang et al., 2018; Zhang et al., 2019). Thus, it is of importance that these landscapes are managed based on information of past changes, driving factors, and future status. This thesis aims to aid in formulating science-based policies for managing a mountainous agricultural landscape by characterizing the dynamics of the agricultural abandonment. Based on this objective, the current research was structured to include proposing of a Geomatics framework for informing environmental management, observing the past land cover changes, identifying the spatial and non-spatial drivers of agricultural abandonment, and simulating the impact of policies on the mitigation of agricultural abandonment. This chapter summarizes the discussions of each chapter and synthesizes the implications for managing the Ifugao rice terraces, contributions to research of mountainous agricultural landscapes, and novelties in the applied methods. To conclude the thesis, the future direction of the current research is discussed.

## 6.2. Summary of the discussions

*6.2.1. A Geomatics framework for aiding environmental management*

The goal of Chapter 2 was to present a general methodological framework that mainly utilizes spatial data for "simulating the future through observations of the past". This Geomatics framework is composed mainly of the following steps: data acquisition, spatial analysis, and Geosimulation to provide key information spanning from the past to the future conditions of an environment. Adopting this framework will then provide holistic information for decision-making in environmental management. To provide examples on how to adopt the Geomatics framework, two case studies were presented which were completed research that utilized the three main steps of the framework to address ongoing environmental problems and provide solutions to them. This is also the same general methodological framework adopted in this thesis to understand the dynamics of agricultural abandonment in the Ifugao rice terraces

By presenting the Geomatics framework, this chapter thus provided a proposal of concretizing the role of Geosimulation in Geomatics. Without a doubt, simulations of impacts of policies on addressing an environmental problem have added value for policy-making. On top of widening the applications of Geomatics and providing a methodological workflow for future Geomatics research, this framework will also strengthen the collaboration between Geosimulation and the other spatial science disciplines.

*6.2.2. Observing the past dynamics of land cover changes*

The goal of Chapter 3 was to observe the past land cover changes in the study area in five-year periods from 1990 to 2020. This chapter particularly focused on explaining the dynamics of rapid land cover transitions and permanent agricultural abandonment in the Ifugao rice terraces. The chapter utilized Google Earth Engine (GEE) to implement time-series land cover mapping, transition analysis, and analysis of paddy field dynamics. The chapter also used regression analysis to analyze the correlation between vegetation abundance and agricultural abandonment.

The first key finding of this chapter is that low vegetation cover intermediates agricultural abandonment and afforestation. Transition analysis showed that a two-step process involving low vegetation as an intermediary land cover typically occurs in between agricultural

abandonment and afforestation. This adds new information to the land cover dynamics in mountainous agricultural landscapes as previous studies have only indicated that afforestation follows agricultural abandonment. In addition to the land cover transitions involving paddy fields, transitions between low vegetation and forest also regularly occurred at high rates which may be due to tree cutting and swidden farming.

The second key finding is that agricultural abandonment mainly occurred in the 1990s then followed by recultivation in the 2000s. Observed temporal dynamics of paddy fields aligned with historical records such as high rates of permanent abandonment in the period between 1990 and 2000 and recultivation (416% increase) in the period between 2000 and 2010. This indicates that efforts from the government and international organizations have been successful in recultivating the paddy fields. However, after 2010, permanent abandonment has been observed to again continuously increase.

The third key finding is that decreasing low vegetation abundance promotes paddy field permanent abandonment. Regression analysis revealed that there is a significant correlation between low vegetation cover abundance and subsequent paddy field permanent abandonment (P=0.0498), which confirms that afforestation in the landscape decreased the water yield and promoted agricultural abandonment. This finding coincides with previous studies showing that decreasing water yield from afforestation contributes to the abandonment of paddy fields (Soriano & Herath, 2018).

This chapter has the novel contribution of developing a framework for analyzing paddy field dynamics involving first-time cultivations, fallowing, recultivation, and permanent abandonment. To the best of the author's knowledge, this is the first study to observe temporal dynamics in paddy fields based on time-series land cover maps. The developed framework can be used to elucidate the patterns of cultivation of farmers which will bring informed decisions for policy making.

*6.2.3. Identifying the drivers of agricultural abandonment*

The goal of Chapter 4 was to analyze the significant spatial and non-spatial driving factors of agricultural abandonment in the Ifugao rice terraces. This chapter particularly focused on using spatial statistical modeling to analyze the drivers of agricultural abandonment observed in Chapter 3.

A key aspect of this chapter is that it proposes a novel statistical LUCC modeling that integrates a logistic model for spatial LUCC drivers and a linear model for non-spatial drivers. The logistic sub-model produces a probability map representing the local probabilities of LUCC, while the linear sub-model produces a probability threshold representing the global LUCC probability. Comparisons between every pixel in the probability map and the global probability threshold generates the LUCC map. The developed spatial statistical model can thus simulate scenarios of future LUCC by using maps and non-spatial values representing respective scenarios as inputs in the model.

The first key finding of this chapter is the identification of the significant spatial drivers of agricultural abandonment. Results showed that slope, cosine aspect, quickflow, distance to town center, distance to road, world heritage site status, forest density, low vegetation density, and paddy field density were significant determinants of the local probabilities of agricultural abandonment. This finding implies that altering the values of these spatial explanatory variables (for example building new roads) will then change the probability of occurrence of agricultural abandonment for a given location.

The second key finding is the identification of the significant non-spatial drivers of agricultural abandonment. Results show that total forest area, five-year average precipitation, and average daily maximum temperature were significant determinants of the global probabilities of agricultural abandonment. Like the first key finding, the change of values in these non-spatial explanatory variables (for example the increase in daily maximum temperature due to climate change) will alter the global probability of agricultural abandonment in the whole Ifugao rice terraces.

The third key finding is that the accuracy assessment of the simulated maps showed satisfactory accuracies, confirming that the developed spatial statistical model is suitable for LUCC simulation. This then shows that research in this chapter was able to provide a novel contribution of developing a spatial statistical model that can be utilized for simulating future LUCC based on spatial and non-spatial explanatory variables.

*6.2.4. Simulating the future status of the cultural landscape*

The goal of Chapter 5 was to develop an ABM that simulates the impact of combinations of socio-environmental policies on the spatial patterns of agricultural lands in a

farm succession-based agricultural landscape. Using expert knowledge, GIS raster files, and a spatial logistic model (developed in the previous chapter), the ABM simulates the interaction between the environment, government, and farm households composed of farm owners, farmlands, and children. To calibrate the model, pattern-oriented modeling was utilized to match simulated temporal patterns of the number of farms and area of paddy fields with observed patterns.

The first key finding of this chapter is that the validation of the model showed that the accuracy of simulated spatial patterns of paddy fields were of acceptable accuracies. Thus, it can be deemed that the simulations generated by the developed ABM can be used for predictions of future scenarios.

The second key finding is that the simulation of policies showed that the provision of aid in restoring eroded terraces is effective in mitigating agricultural abandonment, preventing almost half of the agricultural abandonment compared to the BAU scenario. Meanwhile, promoting the heritage value of the terraces to the youth and provision of monthly subsidies to farm owners do not have significant mitigation effects to the rice terraces, preventing only 3% of the total abandonment compared to the BAU scenario. Thus, it is recommended that the focus on the local government of Banaue should be to just provide aid in restoring eroded terraces.

The third key finding is an implication of the simulation results which is that the environmental driver erosion has a significantly higher impact on agricultural abandonment than the social driver lack of successors. This suggests that policies directly affecting the environment will have a quicker and intensive effect on the environment than social policies that may take time to manifest.

This chapter contributes to the field of Agent-Based Modeling by adopting a modeling framework that can generate accurate land cover maps as an emergent phenomenon of the actions of non-spatial agents. This framework can be adopted in other agent-based modeling studies where actors in a socio-environmental system lack geospatial data but spatially-varying environmental variables such as land cover need to be simulated.

## 6.3. Implications for managing the Ifugao rice terraces

In the past three decades, the Ifugao rice terraces have faced severe agricultural

abandonment and need intervention to mitigate this phenomenon. A major problem in facing this problem is the lack of accurate maps and quantification of the amount of abandonment that occurred in the past decades. This thesis addresses this lack of information. By mapping the rapid land cover changes in five-year intervals from 1990 to 2020, the thesis was able to observe the changes that occurred in the landscape, which can be used as basis for future analysis and planning. It is worth noting in these observations that recultivations of the paddy fields were successful achieved through combined efforts of the government units and organizations. This can be used as an inspiration for goal-setting future management plans; restoring a significant part of the terraces is definitely achievable.

The existence of a feedback loop between the abundance of vegetation cover (low vegetation and forest cover) and permanent abandonment of the paddy fields stresses the importance of mitigating the agricultural abandonment as increasing abandoned paddy fields lead to more abandonment. This should also be used as motivation for large-scale actors to take initiative about this problem. Although difficult to address, the solving of the problem of water scarcity should be addressed by the national government as this is one of the main factors for the feedback loop. As was shown in both chapters 3 and 4, increasing forest cover also agricultural abandonment brought by decreasing water yield. Thus, it is also recommended that the trade-offs in ecosystem services brought by changing land cover should be implemented to show how much ecosystem services such as water yield, carbon sequestration, and habitat quality can change.

As with other mountainous agricultural landscapes, the agricultural abandonment in the Ifugao rice terraces is a multi-faceted phenomenon brought by a variety of social and environmental drivers. Before addressing any environmental problem, it is of significance to first identify drivers so that policies can be drafted to address them. The results of the thesis identified the significant spatial and non-spatial drivers of agricultural abandonment in the Ifugao rice terraces. Some of these factors are difficult or impossible to alter by human actions such as mountain topography or meteorological variables. However, some can provide insights about the social conditions that drive abandonment such as distance to town center and distance to road. It is most probable that improving the access of farmers to services and transportation can reduce abandonment due to improvement in quality of life. It may be improbable to develop new town centers but the government can look into ways of setting up more services in the more rural parts of the Ifugao province to improve the quality of life of farmers. Building new

roads may be a straightforward solution but also improving pathways to roads may improve the accessibility to roads.

Given this variety of drivers of agricultural abandonment, implementing the optimum combination of policies to address the problem can be a daunting task. Knowing the effect of policy implementation beforehand can inform stakeholders of the appropriate set of actions to carry out. The thesis was able to identify the appropriate policies to implement by simulating its impacts on the conservation of the Ifugao rice terraces. Based on the simulation results from the developed ABM, providing aid to farmers in restoring eroded terraces is the most effective policy for mitigating agricultural abandonment. It also showed a synergistic effect when paired with another policy such as increasing the heritage valuation of the rice terraces among the youth and provision of subsidy to farm owners. Thus, it is recommended the government unit should implement a policy of aiding in restoring eroded terraces to farmers who need it. Another policy can also be implemented alongside this but given the limited budget of the provincial government of Ifugao, focusing just on restoring eroded terraces may be the best course of action.

## 6.4. Contributions to research on mountainous agricultural landscape

In the global context, the thesis contributes to studies of mountainous agricultural landscapes. Previous studies of land cover changes in mountainous agricultural landscapes observed the occurrence of afforestation after agricultural abandonment. However, it was revealed in the thesis that typically a two-step transition process occurs between agricultural abandonment and afforestation. Low vegetation acts as an intermediary land cover type for transitions between paddy field and forest. Hence, paddy fields typically first transition into low vegetation before transitioning into forests.

As mountainous agricultural landscapes around the world are part of one of multiple watersheds, water yield is highly dependent on the land cover in the highlands. It is then most likely that the land-transition feedback loop that further promotes agricultural abandonment in the Ifugao rice terraces also exist in other such landscapes. The findings suggest that planning of mountainous agricultural landscapes should address social and environmental driving factors to mitigate this feedback loop to prevent further agricultural abandonment. Specifically, planning of these landscapes should also consider the abundance of other vegetation cover

types aside from only addressing social issues.

The driving factors of agricultural abandonment in the Ifugao rice terraces can also be compared with the drivers of agricultural abandonment in other landscapes. From here, inferences can then be made as to what are the common global drivers of agricultural abandonment. The findings on the set of spatial and non-spatial drivers of abandonment can then be especially useful for synthesis of global research on agricultural abandonment.

The thesis also provides information on the magnitude of impacts of the social and environmental policies for a farm succession-based agricultural landscape, which is typically the case for mountainous agricultural landscapes. Findings from ABM simulations imply that policies which directly affect agricultural lands have much higher mitigating impacts on agricultural abandonment than policies that affect the social aspects of farm households. This may be attributed to the quickness of the manifestation of effects to the paddy fields. The effect of social policies aiming to promote farm succession takes time to manifest as the effect of a lack of successor only manifests on the rice paddy fields once the farm owner starts to age. Meanwhile, environmental policies directly affect the paddy fields, hence its effect in increasing paddy field area instantly manifests.

## 6.5. Methodological novelties

The thesis advances the usage of Geomatics for environmental applications by proposing and adopting a Geomatics framework that aims to holistically inform decision-making for environmental management. The framework is composed of the three main tasks: acquisition, spatial analysis, and Geosimulation. This proposed framework can also be treated as an approach for utilizing spatial data for "predicting the future through observations of the past". It is posited that the adoption of this framework leads to the widening of the environmental application of Geomatics, the establishment of a methodological workflow for informing environmental management, and the enhancement of the collaboration between Geosimulation and other spatial science fields.

A methodological framework for analyzing paddy dynamics was developed for providing an in-depth analysis of spatio-temporal patterns of fallowing and recultivation in paddy fields based on land cover maps. These paddy field dynamics are represented by permanent abandonment, fallowing, first-time cultivations, and recultivation. This analytical

framework can be applied in other agricultural lands, especially in mountainous agricultural landscapes which experience frequent permanent abandonment. With that being said, information derived from this framework can elucidate farmer actions and how cultivation patterns can cause changes in land cover.

The thesis also developed a statistical model of LUCC that integrates a logistic model based on spatial drivers and a linear model based on non-spatial drivers. The logistic model produces a probability map that represents local probabilities of LUCC while the linear model produces a global probability threshold that represents a global probability of LUCC, and by comparing the two variables, LUCC is mapped. Accuracy assessment showed that simulated maps achieved accuracies suitable for LUCC simulation, demonstrating that the statistical model can be a potential tool for prediction of future LUCC.

Lastly, an ABM was developed that adopted two novel methods. First, the ABM employed a modeling framework that was able to generate accurate land cover maps even with the use of non-spatial agents. In the future, Agent-based modeling research which does not have location-data of actors can adopt this framework to simulate spatial patterns of emergent environmental changes. Second, the ABM employed a calibration routine of using GA to implement pattern-oriented modeling. Future calibration for ABMs can also adopt this routine to find the set of parameters that best fit observed patterns of socio-ecological systems.

## 6.6. Conclusions

This study presents key information for the conservation of the Ifugao rice terraces by characterizing the dynamics of the agricultural abandonment. This comprises the observation of past changes, identification of driving factors, and simulation of the future status. The results show that the Ifugao rice terraces have experienced severe agricultural abandonment from 1990 to 2020 due to a combination of environmental and social drivers. Nine spatial factors and three non-spatial factors were found to significantly cause the occurrence of agricultural abandonment. Based on simulations, it is suggested that the local government should focus on providing aid in restoring eroded terraces to mitigate as much agricultural abandonment as possible. The findings of this study provide key information for informing the environmental management of not only the Ifugao rice terraces but also of other mountainous agricultural landscapes. The methodological frameworks implemented in this study, especially the

Geomatics framework for "simulating the future through observations of the past", can be adopted by future researchers in their studies of bringing solutions to environmental issues.

# References

Acabado, S. (2012). The Ifugao agricultural landscapes: Agro-cultural complexes and the intensification debate. *Journal of Southeast Asian Studies*, *43*(3), 500–522. http://www.jstor.org/stable/23321099

Agoot, L. (2018, August 27). *Ifugaos' handiwork sustains famed Banaue Rice Terraces*. Philippine News Agency. https://www.pna.gov.ph/articles/1045981

Aguilar, C. H. M., Altoveros, N. C., Borromeo, T. H., Dayo, M. H. F., & Koohafkan, P. (2021). Traditional rice-based agroecosystem in Kiangan, Ifugao, Philippines: drivers of change, resilience, and potential trajectories. *Agroecology and Sustainable Food Systems*, *45*(2), 296–316. https://doi.org/10.1080/21683565.2020.1813861

Aguirre-Gutiérrez, J., Seijmonsbergen, A. C., & Duivenvoorden, J. F. (2012). Optimizing land cover classification accuracy for change detection, a combined pixel-based and object-based approach in a mountainous area in Mexico. *Applied Geography*, *34*, 29–37. https://doi.org/10.1016/j.apgeog.2011.10.010

Ahmed, B., Ahmed, R., & Zhu, X. (2013). Evaluation of Model Validation Techniques in Land Cover Dynamics. *ISPRS International Journal of Geo-Information 2013, Vol. 2, Pages 577-597*, *2*(3), 577–597. https://doi.org/10.3390/IJGI2030577

Alencar, A., Z. Shimbo, J., Lenti, F., Balzani Marques, C., Zimbres, B., Rosa, M., Arruda, V., Castro, I., Fernandes Márcico Ribeiro, J., Varela, V., Alencar, I., Piontekowski, V., Ribeiro, V., M. C. Bustamante, M., Eyji Sano, E., & Barroso, M. (2020). Mapping Three Decades of Changes in the Brazilian Savanna Native Vegetation Using Landsat Data Processed in the Google Earth Engine Platform. *Remote Sensing*, *12*(6), 924. https://doi.org/10.3390/rs12060924

Arnáez, J., Lana-Renault, N., Lasanta, T., Ruiz-Flaño, P., & Castroviejo, J. (2015). Effects of farming terraces on hydrological and geomorphological processes. A review. In *Catena* (Vol. 128, pp. 122–134). Elsevier. https://doi.org/10.1016/j.catena.2015.01.021

Avtar, R., Tsusaka, K., & Herath, S. (2019). REDD+ Implementation in community-based muyong forest management in Ifugao, Philippines. *Land*. https://doi.org/10.3390/land8110164

Bantayan, N., Calderon, M., Dizon, J., Sajise, A., & Salvador, M. (2012). Estimating the Extent and Damage of the UNESCO World Heritage Sites of the Ifugao Rice Terraces, Philippines. *Journal of Environmental Science and Management*, *15*, 1–5.

Benenson, I., & Torrens, P. M. (2004). Geosimulation: object-based modeling of urban phenomena. *Computers, Environment and Urban Systems*, *28*(1–2), 1–8.

https://doi.org/10.1016/S0198-9715(02)00067-4

Benenson, I., & Torrens, P. M. (2006). Front Matter. In *Geosimulation* (pp. i–xxiii). John Wiley & Sons, Ltd. https://doi.org/10.1002/0470020997.FMATTER

Benra, F., De Frutos, A., Gaglio, M., Álvarez-Garretón, C., Felipe-Lucia, M., & Bonn, A. (2021). Mapping water ecosystem services: Evaluating InVEST model predictions in data scarce regions. *Environmental Modelling & Software*, *138*, 104982. https://doi.org/10.1016/J.ENVSOFT.2021.104982

Biau, G., & Scornet, E. (2016). A random forest guided tour. *Test*, *25*(2), 197–227. https://doi.org/10.1007/S11749-016-0481-7/METRICS

Boavida-Portugal, I., Rocha, J., & Ferreira, C. C. (2016). Exploring the impacts of future tourism development on land use/cover changes. *Applied Geography*, *77*, 82–91. https://doi.org/10.1016/J.APGEOG.2016.10.009

Bolliger, J., Schmatz, D., Pazúr, R., Ostapowicz, K., & Psomas, A. (2017). Reconstructing forest-cover change in the Swiss Alps between 1880 and 2010 using ensemble modelling. *Regional Environmental Change*, *17*(8), 2265–2277. https://doi.org/10.1007/S10113-016-1090-4/FIGURES/7

Bonabeau, E. (2002). Agent-based modeling: Methods and techniques for simulating human systems. *Proceedings of the National Academy of Sciences of the United States of America*, *99*(SUPPL. 3), 7280–7287. https://doi.org/10.1073/PNAS.082080899/ASSET/15AB2074-4729-491A-B9E6-292A9C40AE31/ASSETS/GRAPHIC/PQ0820808004.JPEG

Bonnesoeur, V., Locatelli, B., Guariguata, M. R., Ochoa-Tocachi, B. F., Vanacker, V., Mao, Z., Stokes, A., & Mathez-Stiefel, S.-L. (2019). Impacts of forests and forestation on hydrological services in the Andes: A systematic review. *Forest Ecology and Management*, *433*, 569–584. https://doi.org/https://doi.org/10.1016/j.foreco.2018.11.033

Breiman, L. (2001). Random Forests. *Machine Learning 2001 45:1*, *45*(1), 5–32. https://doi.org/10.1023/A:1010933404324

Burkhard, B., Müller, A., Müller, F., Grescho, V., Anh, Q., Arida, G., Bustamante, J. V. J., Van Chien, H., Heong, K. L., Escalada, M., Marquez, L., Thanh Truong, D., Villareal, S. B., & Settele, J. (2015). Land cover-based ecosystem service assessment of irrigated rice cropping systems in southeast Asia-An explorative study. *Ecosystem Services*, *14*, 76–87. https://doi.org/10.1016/j.ecoser.2015.05.005

Butt, E. W., Conibear, L., Knote, C., & Spracklen, D. V. (2021). Large Air Quality and Public Health Impacts due to Amazonian Deforestation Fires in 2019. *GeoHealth*, *5*(7), e2021GH000429. https://doi.org/10.1029/2021GH000429

Cagat, K. A. D. (2018). Mixed views on the Philippines' Ifugao Rice Terraces: "Good" versus "beautiful" in the management of a UNESCO World Heritage site. In *Journal of Southeast Asian Studies*. https://doi.org/10.1017/S0022463417000704

Calderon, M., Bantayan, N., Dizon, J., Sajise, A. J., Codilan, A., & Canceran, M. (2015). Community-Based Resource Assessment and Management Planning for the Rice Terraces of Hungduan, Ifugao, Philippines. *Journal of Environmental Science and Management*, *18*(1), 47–53.

Calderon, M., Dizon, J., Sajise, A., Andrada II, R., Bantayan, N., & Salvador, M. (2009). Towards the Development of a Sustainable Financing Mechanism for the Conservation of the Ifugao Rice Terraces in the Philippines. In *Economy and Environment Program for Southeast Asia (EEPSEA)*. https://ideas.repec.org/p/eep/report/rr2009071.html

Camacho, L. D., Gevaña, D. T., Carandang, †Antonio P., & Camacho, S. C. (2016). Indigenous knowledge and practices for the sustainable management of Ifugao forests in Cordillera, Philippines. *International Journal of Biodiversity Science, Ecosystem Services & Management*, *12*(1–2), 5–13. https://doi.org/10.1080/21513732.2015.1124453

Cao, W., Zhou, Y., Li, R., Li, X., & Zhang, H. (2021). Monitoring long-term annual urban expansion (1986–2017) in the largest archipelago of China. *Science of The Total Environment*, *776*, 146015. https://doi.org/10.1016/j.scitotenv.2021.146015

Cao, Y., Wu, Y., Zhang, Y., & Tian, J. (2013). Landscape pattern and sustainability of a 1300-year-old agricultural landscape in subtropical mountain areas, Southwestern China. *International Journal of Sustainable Development and World Ecology*, *20*(4), 349–357. https://doi.org/10.1080/13504509.2013.773266

Castonguay, A. C., Burkhard, B., Müller, F., Horgan, F. G., & Settele, J. (2016). Resilience and adaptability of rice terrace social-ecological systems: A case study of a local community's perception in Banaue, Philippines. *Ecology and Society*. https://doi.org/10.5751/ES-08348-210215

Cerdà, A., Rodrigo-Comino, J., Novara, A., Brevik, E. C., Vaezi, A. R., Pulido, M., Giménez-Morera, A., & Keesstra, S. D. (2018). Long-term impact of rainfed agricultural land abandonment on soil erosion in the Western Mediterranean basin: *Https://Doi.Org/10.1177/0309133318758521*, *42*(2), 202–219. https://doi.org/10.1177/0309133318758521

Chen, B., Xiao, X., Li, X., Pan, L., Doughty, R., Ma, J., Dong, J., Qin, Y., Zhao, B., Wu, Z., Sun, R., Lan, G., Xie, G., Clinton, N., & Giri, C. (2017). A mangrove forest map of China in 2015: Analysis of time series Landsat 7/8 and Sentinel-1A imagery in Google Earth Engine cloud computing platform. *ISPRS Journal of Photogrammetry and Remote Sensing*, *131*, 104–120. https://doi.org/10.1016/J.ISPRSJPRS.2017.07.011

Cheng, J., & Masser, I. (2003). Urban growth pattern modeling: a case study of Wuhan city, PR China. *Landscape and Urban Planning*, *62*(4), 199–217. https://doi.org/10.1016/S0169-2046(02)00150-0

Clarke, K. C. (1986). Advances in Geographic Information Systems. *Computers, Environment and Urban Systems*, *10*(3–4), 175–184. https://doi.org/10.1016/0198-9715(86)90006-2

Corbelle-Rico, E., Crecente-Maseda, R., & Santé-Riveira, I. (2012). Multi-scale assessment and spatial modelling of agricultural land abandonment in a European peripheral region: Galicia (Spain), 1956–2004. *Land Use Policy*, *29*(3), 493–501. https://doi.org/10.1016/J.LANDUSEPOL.2011.08.008

Dang, A. N., & Kawasaki, A. (2017). Integrating biophysical and socio-economic factors for land-use and land-cover change projection in agricultural economic regions. *Ecological Modelling*, *344*, 29–37. https://doi.org/10.1016/J.ECOLMODEL.2016.11.004

De Luna Habito, C., & Ealdama, S. J. G. (2019). Identity Construction, Social Media, and Ifugao Rice Terraces Conservation of Indigenous People's Youth Through Appreciative Inquiry. *International Journal of Social Ecology and Sustainable Development*, *10*(4), 47–59. https://doi.org/10.4018/IJSESD.2019100104

Dizon, J. T., Calderon, M. M., Sajise, A. J. U., Andrada, R. T., & Salvador, M. G. (2012). Youths' perceptions of and attitudes towards the Ifugao rice terraces. *Journal of Environmental Science and Management*.

Djokic, D., Ye, Z., & Dartiguenave, C. (2011). *Arc Hydro Tools Overview*.

Dong, J., Xiao, X., Kou, W., Qin, Y., Zhang, G., Li, L., Jin, C., Zhou, Y., Wang, J., Biradar, C., Liu, J., & Moore, B. (2015). Tracking the dynamics of paddy rice planting area in 1986-2010 through time series Landsat images and phenology-based algorithms. *Remote Sensing of Environment*, *160*, 99–113. https://doi.org/10.1016/j.rse.2015.01.004

Drogoul, A., Huynh, N. Q., & Truong, Q. C. (2016). Coupling environmental, social and economic models to understand land-use change dynamics in the Mekong Delta. *Frontiers in Environmental Science*. https://doi.org/10.3389/fenvs.2016.00019

Ducusin, R. J. C., Espaldon, M. V. O., Rebancos, C. M., & De Guzman, L. E. P. (2019). Vulnerability assessment of climate change impacts on a Globally Important Agricultural Heritage System (GIAHS) in the Philippines: the case of Batad Rice Terraces, Banaue, Ifugao, Philippines. *Climatic Change*, *153*(3), 395–421. https://doi.org/10.1007/s10584-019-02397-7

Dulnuan, E. D. (2014). The Ifugao Rice Terraces Tourism: Status, Problems and Concerns. *IAMURE International Journal of Ecology and Conservation*. https://doi.org/10.7718/ijec.v10i1.772

Estacio, I., Basu, M., Sianipar, C. P. M., Onitsuka, K., & Hoshino, S. (2022). Dynamics of land cover transitions and agricultural abandonment in a mountainous agricultural landscape: Case of Ifugao rice terraces, Philippines. *Landscape and Urban Planning*, *222*, 104394. https://doi.org/10.1016/J.LANDURBPLAN.2022.104394

FAO. (2018). *Ifugao Rice Terraces, Philippines*. Food and Agriculture Organization of the United Nations. http://www.fao.org/giahs/giahsaroundtheworld/designated-sites/asia-and-the-pacific/ifugao-rice-terraces/en/

FAO. (2021). *Agricultural heritage around the world*. Food and Agriculture Organization of

the United Nations. https://www.fao.org/giahs/

Foga, S., Scaramuzza, P. L., Guo, S., Zhu, Z., Dilley, R. D., Beckmann, T., Schmidt, G. L., Dwyer, J. L., Joseph Hughes, M., & Laue, B. (2017). Cloud detection algorithm comparison and validation for operational Landsat data products. *Remote Sensing of Environment*, *194*, 379–390. https://doi.org/10.1016/j.rse.2017.03.026

García-Ruiz, J. M., & Lana-Renault, N. (2011). Hydrological and erosive consequences of farmland abandonment in Europe, with special reference to the Mediterranean region - A review. In *Agriculture, Ecosystems and Environment* (Vol. 140, Issues 3–4, pp. 317–338). Elsevier. https://doi.org/10.1016/j.agee.2011.01.003

Geist, H., McConnell, W., Lambin, E. F., Moran, E., Alves, D., & Rudel, T. (2006). Causes and Trajectories of Land-Use/Cover Change. *Land-Use and Land-Cover Change*, 41–70. https://doi.org/10.1007/3-540-32202-7_3

Gellrich, M., Baur, P., Koch, B., & Zimmermann, N. E. (2007). Agricultural land abandonment and natural forest re-growth in the Swiss mountains: A spatially explicit economic analysis. *Agriculture, Ecosystems and Environment*, *118*(1–4), 93–108. https://doi.org/10.1016/j.agee.2006.05.001

Gellrich, M., Baur, P., & Zimmermann, N. E. (2007). Natural forest regrowth as a proxy variable for agricultural land abandonment in the Swiss mountains: A spatial statistical model based on geophysical and socio-economic variables. *Environmental Modeling and Assessment*, *12*(4), 269–278. https://doi.org/10.1007/S10666-006-9062-6/FIGURES/2

Gellrich, M., & Zimmermann, N. E. (2007). Investigating the regional-scale pattern of agricultural land abandonment in the Swiss mountains: A spatial statistical modelling approach. *Landscape and Urban Planning*, *79*(1), 65–76. https://doi.org/10.1016/j.landurbplan.2006.03.004

Gislason, P. O., Benediktsson, J. A., & Sveinsson, J. R. (2006). Random Forests for land cover classification. *Pattern Recognition Letters*, *27*(4), 294–300. https://doi.org/10.1016/J.PATREC.2005.08.011

Gomarasca, M. A. (2009). Geomatics. In *Basics of Geomatics* (pp. 1–17). Springer Netherlands. https://doi.org/10.1007/978-1-4020-9014-1_1

Goodchild, M. F., & Longley, P. A. (1999). The future of GIS and spatial analysis. In *Geographical information systems: principles, techniques, management and applications* (Vol. 1, pp. 567–580). John Wiley New York.

Gorelick, N., Hancher, M., Dixon, M., Ilyushchenko, S., Thau, D., & Moore, R. (2017). Google Earth Engine: Planetary-scale geospatial analysis for everyone. *Remote Sensing of Environment*, *202*, 18–27. https://doi.org/10.1016/j.rse.2017.06.031

Grimm, V., Berger, U., DeAngelis, D. L., Polhill, J. G., Giske, J., & Railsback, S. F. (2010). The ODD protocol: A review and first update. *Ecological Modelling*, *221*(23), 2760–2768. https://doi.org/10.1016/J.ECOLMODEL.2010.08.019

Grimm, V., Railsback, S. F., Vincenot, C. E., Berger, U., Gallagher, C., DeAngelis, D. L., Edmonds, B., Ge, J., Giske, J., Groeneveld, J., Johnston, A. S. A., Milles, A., Nabe-Nielsen, J., Polhill, J. G., Radchuk, V., Rohwäder, M.-S., Stillman, R. A., Thiele, J. C., & Ayllón, D. (2020). The ODD Protocol for Describing Agent-Based and Other Simulation Models: A Second Update to Improve Clarity, Replication, and Structural Realism. *Journal of Artificial Societies and Social Simulation*, *23*(2), 7. https://doi.org/10.18564/jasss.4259

Grimm, V., Revilla, E., Berger, U., Jeltsch, F., Mooij, W. M., Railsback, S. F., Thulke, H. H., Weiner, J., Wiegand, T., & DeAngelis, D. L. (2005). Pattern-oriented modeling of agent-based complex systems: Lessons from ecology. *Science*, *310*(5750), 987–991. https://doi.org/10.1126/SCIENCE.1116681/SUPPL_FILE/GRIMM.SOM.PDF

Groeneveld, J., Müller, B., Buchmann, C. M., Dressler, G., Guo, C., Hase, N., Hoffmann, F., John, F., Klassert, C., Lauf, T., Liebelt, V., Nolzen, H., Pannicke, N., Schulze, J., Weise, H., & Schwarz, N. (2017). Theoretical foundations of human decision-making in agent-based land use models – A review. In *Environmental Modelling and Software* (Vol. 87, pp. 39–48). Elsevier Ltd. https://doi.org/10.1016/j.envsoft.2016.10.008

Güneralp, B., & Seto, K. C. (2013). Futures of global urban expansion: uncertainties and implications for biodiversity conservation. *Environmental Research Letters*, *8*(1), 014025. https://doi.org/10.1088/1748-9326/8/1/014025

He, C., Zhang, J., Liu, Z., & Huang, Q. (2022). Characteristics and progress of land use/cover change research during 1990–2018. *Journal of Geographical Sciences 2022 32:3*, *32*(3), 537–559. https://doi.org/10.1007/S11442-022-1960-2

Herath, S., Tsusaka, K., & Diwa, J. (2015). *Assessment on the feasibility of REDD+ in Nagacadan Rice Terraces of Ifugao and its muyong forest*. https://collections.unu.edu/view/UNU:3335#viewMetadata

Herzmann, S., Jost, A., Korbun, T., Willerding, C., Settele, J., & Plachter, H. (1998). Ifugao Rice Terraces - Landuse changes in a traditional agroecosystem from 1963 to 1997. In *Rice Terraces of Ifugao (Northern-Luzon, Philippines) - Conflicts of Landuse and Environmental Conservation* (pp. 77–89). UFZ-Bericht.

Hou, D., Meng, F., & Prishchepov, A. V. (2021). How is urbanization shaping agricultural land-use? Unraveling the nexus between farmland abandonment and urbanization in China. *Landscape and Urban Planning*, *214*, 104170. https://doi.org/10.1016/J.LANDURBPLAN.2021.104170

Hu, Z., & Lo, C. P. (2007). Modeling urban growth in Atlanta using logistic regression. *Computers, Environment and Urban Systems*, *31*(6), 667–688. https://doi.org/10.1016/J.COMPENVURBSYS.2006.11.001

ICAO. (2018). *Annex 10 to the Convention of International Civil Aviation* (7th ed.).

Katoch, S., Chauhan, S. S., & Kumar, V. (2021). A review on genetic algorithm: past, present,

and future. *Multimedia Tools and Applications*, *80*(5), 8091–8126. https://doi.org/10.1007/S11042-020-10139-6/FIGURES/8

Kim, I., Martins, R. J., Jang, J., Badloe, T., Khadir, S., Jung, H. Y., Kim, H., Kim, J., Genevet, P., & Rho, J. (2021). Nanophotonics for light detection and ranging technology. *Nature Nanotechnology 2021 16:5*, *16*(5), 508–524. https://doi.org/10.1038/S41565-021-00895-3

Kobler, A., Cunder, T., & Pirnat, J. (2005). Modelling spontaneous afforestation in Postojna area, Slovenia. *Journal for Nature Conservation*, *13*(2), 127–135. https://doi.org/https://doi.org/10.1016/j.jnc.2005.01.003

Kollert, A., Bremer, M., Löw, M., & Rutzinger, M. (2021). Exploring the potential of land surface phenology and seasonal cloud free composites of one year of Sentinel-2 imagery for tree species mapping in a mountainous region. *International Journal of Applied Earth Observation and Geoinformation*, *94*, 102208. https://doi.org/10.1016/J.JAG.2020.102208

Kremmydas, D., Athanasiadis, I. N., & Rozakis, S. (2018). A review of Agent Based Modeling for agricultural policy evaluation. *Agricultural Systems*, *164*, 95–106. https://doi.org/10.1016/J.AGSY.2018.03.010

Lawrence, D., & Vandecar, K. (2014). Effects of tropical deforestation on climate and agriculture. *Nature Climate Change 2015 5:1*, *5*(1), 27–36. https://doi.org/10.1038/nclimate2430

Le Page, C., Bazile, D., Becu, N., Bommel, P., Bousquet, F., Etienne, M., Mathevet, R., Souchère, V., Trébuil, G., & Weber, J. (2017). Agent-Based Modelling and Simulation Applied to Environmental Management. In B. Edmonds & R. Meyer (Eds.), *Simulating Social Complexity: A Handbook* (pp. 569–613). Springer International Publishing. https://doi.org/10.1007/978-3-319-66948-9_22

Lei, T. C., Wan, S., & Chou, T. Y. (2008). The comparison of PCA and discrete rough set for feature extraction of remote sensing image classification - A case study on rice classification, Taiwan. *Computational Geosciences*, *12*(1), 1–14. https://doi.org/10.1007/s10596-007-9057-7

Li, B., Chen, D., Wu, S., Zhou, S., Wang, T., & Chen, H. (2016). Spatio-temporal assessment of urbanization impacts on ecosystem services: Case study of Nanjing City, China. *Ecological Indicators*, *71*, 416–427. https://doi.org/10.1016/J.ECOLIND.2016.07.017

Li, H., Zheng, G., Sun, K., Jiang, Z., Li, Y., & Jia, H. (2020). A Logistic Chaotic Barnacles Mating Optimizer with Masi Entropy for Color Image Multilevel Thresholding Segmentation. *IEEE Access*, *8*, 213130–213153. https://doi.org/10.1109/ACCESS.2020.3040177

Li, X., Chen, G., Liu, X., Liang, X., Wang, S., Chen, Y., Pei, F., & Xu, X. (2017). A New Global Land-Use and Land-Cover Change Product at a 1-km Resolution for 2010 to 2100

Based on Human–Environment Interactions. *Https://Doi.Org/10.1080/24694452.2017.1303357*, *107*(5), 1040–1059. https://doi.org/10.1080/24694452.2017.1303357

Liang, X., Li, Y., Shao, J., & Ran, C. (2020). Traditional agroecosystem transition in mountainous area of Three Gorges Reservoir Area. *Journal of Geographical Sciences*, *30*(2), 281–296. https://doi.org/10.1007/s11442-020-1728-5

Liu, D., Zheng, X., & Wang, H. (2020). Land-use Simulation and Decision-Support system (LandSDS): Seamlessly integrating system dynamics, agent-based model, and cellular automata. *Ecological Modelling*, *417*, 108924. https://doi.org/10.1016/j.ecolmodel.2019.108924

Liu, T., & Yang, X. (2015). *Land Change Modeling: Status and Challenges*. 3–16. https://doi.org/10.1007/978-94-017-9813-6_1

Liu, Y., Hou, X., Li, X., Song, B., & Wang, C. (2020). Assessing and predicting changes in ecosystem service values based on land use/cover change in the Bohai Rim coastal zone. *Ecological Indicators*, *111*, 106004. https://doi.org/10.1016/J.ECOLIND.2019.106004

Locatelli, B., Lavorel, S., Sloan, S., Tappeiner, U., & Geneletti, D. (2017). Characteristic trajectories of ecosystem services in mountains. *Frontiers in Ecology and the Environment*, *15*(3), 150–159. https://doi.org/10.1002/fee.1470

Londoño, A. C., Williams, P. R., & Hart, M. L. (2017). A change in landscape: Lessons learned from abandonment of ancient Wari agricultural terraces in Southern Peru. *Journal of Environmental Management*, *202*, 532–542. https://doi.org/10.1016/j.jenvman.2017.01.012

MacDonald, D., Crabtree, J. R., Wiesinger, G., Dax, T., Stamou, N., Fleury, P., Gutierrez Lazpita, J., & Gibon, A. (2000). Agricultural abandonment in mountain areas of Europe: Environmental consequences and policy response. *Journal of Environmental Management*, *59*(1), 47–69. https://doi.org/10.1006/JEMA.1999.0335

Mao, X., Meng, J., & Wang, Q. (2014). Modeling the effects of tourism and land regulation on land-use change in tourist regions: A case study of the Lijiang River Basin in Guilin, China. *Land Use Policy*, *41*, 368–377. https://doi.org/10.1016/J.LANDUSEPOL.2014.06.018

Mapulanga, A. M., & Naito, H. (2019). Effect of deforestation on access to clean drinking water. *Proceedings of the National Academy of Sciences of the United States of America*, *116*(17), 8249–8254. https://doi.org/10.1073/PNAS.1814970116

Mas, J. F., Kolb, M., Paegelow, M., Camacho Olmedo, M. T., & Houet, T. (2014). Inductive pattern-based land use/cover change models: A comparison of four software packages. *Environmental Modelling & Software*, *51*, 94–111. https://doi.org/10.1016/J.ENVSOFT.2013.09.010

McDonald, R. I., Mansur, A. V., Ascensão, F., Colbert, M., Crossman, K., Elmqvist, T.,

Gonzalez, A., Güneralp, B., Haase, D., Hamann, M., Hillel, O., Huang, K., Kahnt, B., Maddox, D., Pacheco, A., Pereira, H. M., Seto, K. C., Simkin, R., Walsh, B., … Ziter, C. (2019). Research gaps in knowledge of the impact of urban growth on biodiversity. *Nature Sustainability 2019 3:1*, *3*(1), 16–24. https://doi.org/10.1038/s41893-019-0436-6

McKay, D. (2003). Cultivating New Local Futures: Remittance Economies and Land-Use Patterns in Ifugao, Philippines. *Journal of Southeast Asian Studies*, *34*(2), 285–306. http://www.jstor.org/stable/20072508

Minta, M., Kibret, K., Thorne, P., Nigussie, T., & Nigatu, L. (2018). Land use and land cover dynamics in Dendi-Jeldu hilly-mountainous areas in the central Ethiopian highlands. *Geoderma*, *314*, 27–36. https://doi.org/10.1016/j.geoderma.2017.10.035

Mirjalili, S. (2019). Genetic Algorithm. *Studies in Computational Intelligence*, *780*, 43–55. https://doi.org/10.1007/978-3-319-93025-1_4

Mitsuda, Y., & Ito, S. (2011). A review of spatial-explicit factors determining spatial distribution of land use/land-use change. *Landscape and Ecological Engineering*, *7*(1), 117–125. https://doi.org/10.1007/S11355-010-0113-4/TABLES/1

Modica, G., Praticò, S., & Di Fazio, S. (2017). Abandonment of traditional terraced landscape: A change detection approach (a case study in Costa Viola, Calabria, Italy). *Land Degradation & Development*, *28*(8), 2608–2622. https://doi.org/10.1002/ldr.2824

Munroe, D. K., & Müller, D. (2007). Issues in spatially explicit statistical land-use/cover change (LUCC) models: Examples from western Honduras and the Central Highlands of Vietnam. *Land Use Policy*, *24*(3), 521–530. https://doi.org/10.1016/J.LANDUSEPOL.2005.09.007

Munyati, C. (2004). Use of Principal Component Analysis (PCA) of remote sensing images in wetland change detection on the Kafue Flats, Zambia. *Geocarto International*, *19*(3), 11–22. https://doi.org/10.1080/10106040408542313

Mustafa, A., Cools, M., Saadi, I., & Teller, J. (2017). Coupling agent-based, cellular automata and logistic regression into a hybrid urban expansion model (HUEM). *Land Use Policy*, *69*, 529–540. https://doi.org/10.1016/j.landusepol.2017.10.009

Nainggolan, D., de Vente, J., Boix-Fayos, C., Termansen, M., Hubacek, K., & Reed, M. S. (2012). Afforestation, agricultural abandonment and intensification: Competing trajectories in semi-arid Mediterranean agro-ecosystems. *Agriculture, Ecosystems & Environment*, *159*, 90–104. https://doi.org/10.1016/J.AGEE.2012.06.023

Okunlola, O. A., Alobid, M., Olubusoye, O. E., Ayinde, K., Lukman, A. F., & Szűcs, I. (2021). Spatial regression and geostatistics discourse with empirical application to precipitation data in Nigeria. *Scientific Reports 2021 11:1*, *11*(1), 1–14. https://doi.org/10.1038/s41598-021-96124-x

Osawa, T., Kohyama, K., & Mitsuhashi, H. (2016). Multiple factors drive regional agricultural abandonment. *Science of The Total Environment*, *542*, 478–483.

https://doi.org/10.1016/J.SCITOTENV.2015.10.067

PAGASA. (n.d.). *Climate of the Philippines*. Philippine Atmospheric, Geophysical and Astronomical Services Administration. Retrieved March 8, 2021, from http://bagong.pagasa.dost.gov.ph/information/climate-philippines

Pazúr, R., Lieskovský, J., Bürgi, M., Müller, D., Lieskovský, T., Zhang, Z., & Prischchepov, A. V. (2020). Abandonment and Recultivation of Agricultural Lands in Slovakia— Patterns and Determinants from the Past to the Future. *Land 2020, Vol. 9, Page 316*, *9*(9), 316. https://doi.org/10.3390/LAND9090316

Pazúr, R., Lieskovský, J., Feranec, J., & Oťaheľ, J. (2014). Spatial determinants of abandonment of large-scale arable lands and managed grasslands in Slovakia during the periods of post-socialist transition and European Union accession. *Applied Geography*, *54*, 118–128. https://doi.org/10.1016/J.APGEOG.2014.07.014

PCIEERD. (n.d.). *Geospatial Assessment and Modelling of Urban Heat Islands in Philippine Cities (GUHeat)*. PCIEERD Innovations. Retrieved May 21, 2023, from https://projects.pcieerd.dost.gov.ph/project/7965

Pe'er, G., Heinz, S. K., & Frank, K. (2006). Connectivity in Heterogeneous Landscapes: Analyzing the Effect of Topography. *Landscape Ecology 2006 21:1*, *21*(1), 47–61. https://doi.org/10.1007/S10980-005-1622-7

Peng, J., Hu, X., Qiu, S., Hu, Y., Meersmans, J., & Liu, Y. (2019). Multifunctional landscapes identification and associated development zoning in mountainous area. *Science of the Total Environment*, *660*, 765–775. https://doi.org/10.1016/j.scitotenv.2019.01.023

Perpiña Castillo, C., Jacobs-Crisioni, C., Diogo, V., & Lavalle, C. (2021). Modelling agricultural land abandonment in a fine spatial resolution multi-level land-use model: An application for the EU. *Environmental Modelling & Software*, *136*, 104946. https://doi.org/10.1016/J.ENVSOFT.2020.104946

Phiri, D., Morgenroth, J., & Xu, C. (2019). Long-term land cover change in Zambia: An assessment of driving factors. *Science of The Total Environment*, *697*, 134206. https://doi.org/10.1016/J.SCITOTENV.2019.134206

Piras, S., & Botnarenco, S. (2019). Problems of farm succession in the post-Soviet space: insights from the Republic of Moldova. *Journal of Land Use Science*, *13*(6), 631–644. https://doi.org/10.1080/1747423X.2019.1603332

Pôças, I., Cunha, M., Marcal, A. R. S., & Pereira, L. S. (2011). An evaluation of changes in a mountainous rural landscape of Northeast Portugal using remotely sensed data. *Landscape and Urban Planning*, *101*(3), 253–261. https://doi.org/10.1016/j.landurbplan.2011.02.030

Praticò, S., Solano, F., Di Fazio, S., & Modica, G. (2021). Machine Learning Classification of Mediterranean Forest Habitats in Google Earth Engine Based on Seasonal Sentinel-2 Time-Series and Input Image Composition Optimisation. *Remote Sensing 2021, Vol. 13,*

*Page 586*, *13*(4), 586. https://doi.org/10.3390/RS13040586

Qiu, Z., Chen, B., & Takemoto, K. (2014). Conservation of terraced paddy fields engaged with multiple stakeholders: The case of the Noto GIAHS site in Japan. *Paddy and Water Environment*, *12*(2), 275–283. https://doi.org/10.1007/S10333-013-0387-X/FIGURES/4

Ren, Y., Lü, Y., Comber, A., Fu, B., Harris, P., & Wu, L. (2019). Spatially explicit simulation of land use/land cover changes: Current coverage and future prospects. In *Earth-Science Reviews* (Vol. 190, pp. 398–415). Elsevier B.V. https://doi.org/10.1016/j.earscirev.2019.01.001

Sandnes, F. E. (2011). Determining the geographical location of image scenes based on object shadow lengths. *Journal of Signal Processing Systems*, *65*(1), 35–47. https://doi.org/10.1007/S11265-010-0538-X/FIGURES/14

Schowengerdt, R. A. (2007). The Nature of Remote Sensing. *Remote Sensing*, 1–X. https://doi.org/10.1016/B978-012369407-2/50004-8

Serrano, R., & Cadaweng, E. (2005). The Ifugao Muyong: Sustaining water, culture and life. In P. Durst, C. Brown, H. Tacio, & M. Ishikawa (Eds.), *In search of excellence: Exemplary forest management in Asia and the Pacific* (pp. 103–112). Regional Community Forestry Training Center for Asia and the Pacific, Food and Agriculture Organization.

Seto, K. C., Fragkias, M., Güneralp, B., & Reilly, M. K. (2011). A Meta-Analysis of Global Urban Land Expansion. *PLOS ONE*, *6*(8), e23777. https://doi.org/10.1371/JOURNAL.PONE.0023777

Shu, B., Zhu, S., Qu, Y., Zhang, H., Li, X., & Carsjens, G. J. (2020). Modelling multi-regional urban growth with multilevel logistic cellular automata. *Computers, Environment and Urban Systems*, *80*, 101457. https://doi.org/10.1016/J.COMPENVURBSYS.2019.101457

SITMo. (2008). *IMPACT - The effects of Tourism on Culture and Environment in Asia and the Pacific: Sustainable Tourism and the Preservation of the World Heritage Site of the IFUGAO Rice Terraces, Philippines*. https://unesdoc.unesco.org/ark:/48223/pf0000182647

Smajgl, A., & Barreteau, O. (2017). Framing options for characterising and parameterising human agents in empirical ABM. *Environmental Modelling & Software*, *93*, 29–41. https://doi.org/10.1016/J.ENVSOFT.2017.02.011

Smajgl, A., Barreteau, O., Smajgl, A., & Barreteau, O. (2014). Empiricism and Agent-Based Modelling. *Empirical Agent-Based Modelling - Challenges and Solutions*, 1–26. https://doi.org/10.1007/978-1-4614-6134-0_1

Soriano, M. A., & Herath, S. (2018). Quantifying the role of traditional rice terraces in regulating water resources: implications for management and conservation efforts. *Agroecology and Sustainable Food Systems*.

https://doi.org/10.1080/21683565.2018.1437497

Srinivasan, S. (2015). Spatial Regression Models. *Encyclopedia of GIS*, 1–6. https://doi.org/10.1007/978-3-319-23519-6_1294-2

Sun, Z., Lorscheid, I., Millington, J. D., Lauf, S., Magliocca, N. R., Groeneveld, J., Balbi, S., Nolzen, H., Müller, B., Schulze, J., & Buchmann, C. M. (2016). Simple or complicated agent-based models? A complicated issue. *Environmental Modelling & Software*, *86*, 56–67. https://doi.org/10.1016/J.ENVSOFT.2016.09.006

Synes, N. W., Brown, C., Palmer, S. C. F., Bocedi, G., Osborne, P. E., Watts, K., Franklin, J., & Travis, J. M. J. (2019). Coupled land use and ecological models reveal emergence and feedbacks in socio-ecological systems. *Ecography*, *42*(4), 814–825. https://doi.org/10.1111/ECOG.04039

Taillandier, P., Gaudou, B., Grignard, A., Huynh, Q. N., Marilleau, N., Caillou, P., Philippon, D., & Drogoul, A. (2019). Building, composing and experimenting complex spatial models with the GAMA platform. *GeoInformatica*, *23*(2), 299–322. https://doi.org/10.1007/S10707-018-00339-6/FIGURES/6

Tang, W., & Yang, J. (2020). Agent-Based Land Change Modeling of a Large Watershed: Space-Time Locations of Critical Threshold. *Journal of Artificial Societies and Social Simulation*, *23*(1), 15. https://doi.org/10.18564/jasss.4226

Tarolli, P., Preti, F., & Romano, N. (2014). Terraced landscapes: From an old best practice to a potential hazard for soil degradation due to land abandonment. In *Anthropocene* (Vol. 6, pp. 10–25). Elsevier Ltd. https://doi.org/10.1016/j.ancene.2014.03.002

Tarolli, P., & Straffelini, E. (2020). Agriculture in Hilly and Mountainous Landscapes: Threats, Monitoring and Sustainable Management. *Geography and Sustainability*, *1*(1), 70–76. https://doi.org/10.1016/j.geosus.2020.03.003

Terkenli, T. S., Castiglioni, B., & Cisani, M. (2019). *The Challenge of Tourism in Terraced Landscapes* (pp. 295–309). Springer, Cham. https://doi.org/10.1007/978-3-319-96815-5_18

Tian, M., Min, Q. wen, Jiao, W. jun, Yuan, Z., Fuller, A. M., Yang, L., Zhang, Y. xun, Zhou, J., & Cheng, B. (2016). Agricultural Heritage Systems Tourism: definition, characteristics and development framework. *Journal of Mountain Science*, *13*(3), 440–454. https://doi.org/10.1007/s11629-015-3724-2

Tilliger, B., Rodríguez-Labajos, B., Bustamante, J. V., & Settele, J. (2015). Disentangling values in the interrelations between cultural ecosystem services and landscape conservation - A case study of the Ifugao Rice Terraces in the Philippines. *Land*. https://doi.org/10.3390/land4030888

Torrens, P. M. (2006). Geosimulation and its application to urban growth modeling. *Complex Artificial Environments*, 119–136. https://doi.org/10.1007/3-540-29710-3_8/COVER

Truong, Q. C., Taillandier, P., Gaudou, B., Vo, M. Q., Nguyen, T. H., & Drogoul, A. (2016).

Exploring Agent Architectures for Farmer Behavior in Land-Use Change. A Case Study in Coastal Area of the Vietnamese Mekong Delta. In B. Gaudou & J. S. Sichman (Eds.), *Multi-Agent Based Simulation XVI* (pp. 146–158). Springer International Publishing.

UNESCO. (n.d.). *Rice Terraces of the Philippine Cordilleras*. UNESCO WHC. Retrieved April 20, 2020, from https://whc.unesco.org/en/list/722/

UNESCO. (2005). Examination of the State of conservation of World Heritage properties. *Convention Concerning the Protection of the World Cultural and Natural Heritage*.

United Nations ESCAP. (n.d.). *Mangrove Monitoring and Conservation: Philippines*. SDG Help Desk. Retrieved May 21, 2023, from https://sdghelpdesk.unescap.org/technical-assistance/best-practices/mangrove-monitoring-and-conservation-philippines

van der Zanden, E. H., Verburg, P. H., Schulp, C. J. E., & Verkerk, P. J. (2017). Trade-offs of European agricultural abandonment. *Land Use Policy*, *62*, 290–301. https://doi.org/10.1016/J.LANDUSEPOL.2017.01.003

van Vliet, J. (2019). Direct and indirect loss of natural area from urban expansion. *Nature Sustainability 2019 2:8*, *2*(8), 755–763. https://doi.org/10.1038/s41893-019-0340-0

Verburg, P. H., Alexander, P., Evans, T., Magliocca, N. R., Malek, Z., Rounsevell, M. DA, & van Vliet, J. (2019). Beyond land cover change: towards a new generation of land use models. *Current Opinion in Environmental Sustainability*, *38*, 77–85. https://doi.org/10.1016/J.COSUST.2019.05.002

Vidal-Legaz, B., Martínez-Fernández, J., Picón, A. S., & Pugnaire, F. I. (2013). Trade-offs between maintenance of ecosystem services and socio-economic development in rural mountainous communities in southern Spain: A dynamic simulation approach. *Journal of Environmental Management*, *131*, 280–297. https://doi.org/10.1016/j.jenvman.2013.09.036

Vinayak, B., Lee, H. S., Gedam, S., & Latha, R. (2022). Impacts of future urbanization on urban microclimate and thermal comfort over the Mumbai metropolitan region, India. *Sustainable Cities and Society*, *79*, 103703. https://doi.org/10.1016/J.SCS.2022.103703

Visser, H., & De Nijs, T. (2006). The Map Comparison Kit. *Environmental Modelling & Software*, *21*(3), 346–358. https://doi.org/10.1016/J.ENVSOFT.2004.11.013

Wang, Y., Dai, E., Yin, L., & Ma, L. (2018). Land use/land cover change and the effects on ecosystem services in the Hengduan Mountain region, China. *Ecosystem Services*, *34*, 55–67. https://doi.org/10.1016/J.ECOSER.2018.09.008

Wu, Y., Li, S., & Yu, S. (2016). Monitoring urban expansion and its effects on land use and land cover changes in Guangzhou city, China. *Environmental Monitoring and Assessment*, *188*(1), 1–15. https://doi.org/10.1007/S10661-015-5069-2/FIGURES/5

Wulder, M. A., White, J. C., Loveland, T. R., Woodcock, C. E., Belward, A. S., Cohen, W. B., Fosnight, E. A., Shaw, J., Masek, J. G., & Roy, D. P. (2016). The global Landsat archive: Status, consolidation, and direction. *Remote Sensing of Environment*, *185*, 271–283.

https://doi.org/10.1016/j.rse.2015.11.032

Xiao, R., Su, S., Mai, G., Zhang, Z., & Yang, C. (2015). Quantifying determinants of cash crop expansion and their relative effects using logistic regression modeling and variance partitioning. *International Journal of Applied Earth Observation and Geoinformation*, *34*(1), 258–263. https://doi.org/10.1016/J.JAG.2014.08.015

Xu, X., Du, Z., & Zhang, H. (2016). Integrating the system dynamic and cellular automata models to predict land use and land cover change. *International Journal of Applied Earth Observation and Geoinformation*, *52*, 568–579. https://doi.org/10.1016/J.JAG.2016.07.022

Xystrakis, F., Psarras, T., & Koutsias, N. (2017). A process-based land use/land cover change assessment on a mountainous area of Greece during 1945–2009: Signs of socio-economic drivers. *Science of the Total Environment*, *587–588*, 360–370. https://doi.org/10.1016/j.scitotenv.2017.02.161

Yang, B., Yang, X., Leung, L. R., Zhong, S., Qian, Y., Zhao, C., Chen, F., Zhang, Y., & Qi, J. (2019). Modeling the Impacts of Urbanization on Summer Thermal Comfort: The Role of Urban Land Use and Anthropogenic Heat. *Journal of Geophysical Research: Atmospheres*, *124*(13), 6681–6697. https://doi.org/10.1029/2018JD029829

Yang, S., Zhao, W., Liu, Y., Wang, S., Wang, J., & Zhai, R. (2018). Influence of land use change on the ecosystem service trade-offs in the ecological restoration area: Dynamics and scenarios in the Yanhe watershed, China. *Science of the Total Environment*, *644*, 556–566. https://doi.org/10.1016/j.scitotenv.2018.06.348

Zhang, F., Yushanjiang, A., & Jing, Y. (2019). Assessing and predicting changes of the ecosystem service values based on land use/cover change in Ebinur Lake Wetland National Nature Reserve, Xinjiang, China. *Science of The Total Environment*, *656*, 1133–1144. https://doi.org/10.1016/J.SCITOTENV.2018.11.444

Zhou, Y., Dong, J., Xiao, X., Liu, R., Zou, Z., Zhao, G., & Ge, Q. (2019). Continuous monitoring of lake dynamics on the Mongolian Plateau using all available Landsat imagery and Google Earth Engine. *Science of the Total Environment*, *689*, 366–380. https://doi.org/10.1016/j.scitotenv.2019.06.341

Zhu, Z., & Woodcock, C. E. (2014). Continuous change detection and classification of land cover using all available Landsat data. *Remote Sensing of Environment*, *144*, 152–171. https://doi.org/10.1016/j.rse.2014.01.011

Ziegler, A. D., Giambelluca, T. W., Tran, L. T., Vana, T. T., Nullet, M. A., Fox, J., Vien, T. D., Pinthong, J., Maxwell, J. F., & Evett, S. (2004). Hydrological consequences of landscape fragmentation in mountainous northern Vietnam: Evidence of accelerated overland flow generation. *Journal of Hydrology*, *287*(1–4), 124–146. https://doi.org/10.1016/j.jhydrol.2003.09.027

Zlatanova, S., & Krawczyk, A. (2022). Proposal of Redefinition of the Terms Geomatics and

Geoinformatics on the Basis of Terminological Postulates. *ISPRS International Journal of Geo-Information 2022, Vol. 11, Page 557*, *11*(11), 557. https://doi.org/10.3390/IJGI11110557

# Appendix

## A1. The Google Earth Engine code

The following lines were the JavaScript code executed in Google Earth Engine to implement the methodological framework. The link of the code can also be accessed in this link: https://code.earthengine.google.com/a0fc0e8278dd7d73e621007d03cbca78

```
//----------Dates----------
var SD88 = ee.Date('1987-12-01');var ED88 = ee.Date('1988-05-31');
var SD89 = ee.Date('1988-12-01');var ED89 = ee.Date('1989-05-31');
var SD90 = ee.Date('1989-12-01');var ED90 = ee.Date('1990-05-31');
var SD91 = ee.Date('1990-12-01');var ED91 = ee.Date('1991-05-31');
var SD92 = ee.Date('1991-12-01');var ED92 = ee.Date('1992-05-31');
var SD93 = ee.Date('1992-12-01');var ED93 = ee.Date('1993-05-31');
var SD94 = ee.Date('1993-12-01');var ED94 = ee.Date('1994-05-31');
var SD95 = ee.Date('1994-12-01');var ED95 = ee.Date('1995-05-31');
var SD96 = ee.Date('1995-12-01');var ED96 = ee.Date('1996-05-31');
var SD97 = ee.Date('1996-12-01');var ED97 = ee.Date('1997-05-31');
var SD98 = ee.Date('1997-12-01');var ED98 = ee.Date('1998-05-31');
var SD99 = ee.Date('1998-12-01');var ED99 = ee.Date('1999-05-31');
var SD00 = ee.Date('1999-12-01');var ED00 = ee.Date('2000-05-31');
var SD01 = ee.Date('2000-12-01');var ED01 = ee.Date('2001-05-31');
var SD02 = ee.Date('2001-12-01');var ED02 = ee.Date('2002-05-31');
var SD03 = ee.Date('2002-12-01');var ED03 = ee.Date('2003-05-31');
var SD04 = ee.Date('2003-12-01');var ED04 = ee.Date('2004-05-31');
var SD05 = ee.Date('2004-12-01');var ED05 = ee.Date('2005-05-31');
var SD06 = ee.Date('2005-12-01');var ED06 = ee.Date('2006-05-31');
var SD07 = ee.Date('2006-12-01');var ED07 = ee.Date('2007-05-31');
var SD08 = ee.Date('2007-12-01');var ED08 = ee.Date('2008-05-31');
var SD09 = ee.Date('2008-12-01');var ED09 = ee.Date('2009-05-31');
var SD10 = ee.Date('2009-12-01');var ED10 = ee.Date('2010-05-31');
var SD11 = ee.Date('2010-12-01');var ED11 = ee.Date('2011-05-31');
var SD12 = ee.Date('2011-12-01');var ED12 = ee.Date('2012-05-31');
var SD13 = ee.Date('2012-12-01');var ED13 = ee.Date('2013-05-31');
var SD14 = ee.Date('2013-12-01');var ED14 = ee.Date('2014-05-31');
var SD15 = ee.Date('2014-12-01');var ED15 = ee.Date('2015-05-31');
var SD16 = ee.Date('2015-12-01');var ED16 = ee.Date('2016-05-31');
var SD17 = ee.Date('2016-12-01');var ED17 = ee.Date('2017-05-31');
var SD18 = ee.Date('2017-12-01');var ED18 = ee.Date('2018-05-31');
var SD19 = ee.Date('2018-12-01');var ED19 = ee.Date('2019-05-31');
var SD20 = ee.Date('2019-12-01');var ED20 = ee.Date('2020-05-31');
var SD21 = ee.Date('2020-12-01');var ED21 = ee.Date('2021-05-31');
//-------------------------------------Start-------------------------------------
//1. Filter collection to study area
var L5_Ifugao = L5_SR.filterBounds(Catchment);
var L8_Ifugao = L8_SR.filterBounds(Catchment);
Map.centerObject(Catchment, 13);

//2. Filter collections to plus/minus two years (Planting Season)
function plusminus2years(imgcol,SDm2,EDm2,SDm1,EDm1,
                SD00,ED00,SDp1,EDp1,SDp2,EDp2){
  var Ifugao_m2 = imgcol.filterDate(SDm2, EDm2);
  var Ifugao_m1 = imgcol.filterDate(SDm1, EDm1);
```

```
    var Ifugao_00 = imgcol.filterDate(SD00, ED00);
    var Ifugao_p1 = imgcol.filterDate(SDp1, EDp1);
    var Ifugao_p2 = imgcol.filterDate(SDp2, EDp2);
    var Ifugao_TP = Ifugao_m2.merge(Ifugao_m1)
            .merge(Ifugao_00).merge(Ifugao_p1)
            .merge(Ifugao_p2);
    return Ifugao_TP;
}
function plusminus1year2020(imgcol,SDm1,EDm1,
                SD00,ED00,SDp1,EDp1){
    var Ifugao_m1 = imgcol.filterDate(SDm1, EDm1);
    var Ifugao_00 = imgcol.filterDate(SD00, ED00);
    var Ifugao_p1 = imgcol.filterDate(SDp1, EDp1);
    var Ifugao_TP = Ifugao_m1.merge(Ifugao_00)
            .merge(Ifugao_p1);
    return Ifugao_TP;
}
var L5_Ifugao1990_TP = plusminus2years(L5_Ifugao,SD88,ED88,SD89,ED89,
                SD90,ED90,SD91,ED91,SD92,ED92);
var L5_Ifugao1995_TP = plusminus2years(L5_Ifugao,SD93,ED93,SD94,ED94,
                SD95,ED95,SD96,ED96,SD97,ED97);
var L5_Ifugao2000_TP = plusminus2years(L5_Ifugao,SD98,ED98,SD99,ED99,
                SD00,ED00,SD01,ED01,SD02,ED02);
var L5_Ifugao2005_TP = plusminus2years(L5_Ifugao,SD03,ED03,SD04,ED04,
                SD05,ED05,SD06,ED06,SD07,ED07);
var L5_Ifugao2010_TP = plusminus2years(L5_Ifugao,SD08,ED08,SD09,ED09,
                SD10,ED10,SD11,ED11,SD12,ED12);
var L8_Ifugao2015_TP = plusminus2years(L8_Ifugao,SD13,ED13,SD14,ED14,
                SD15,ED15,SD16,ED16,SD17,ED17);
var L8_Ifugao2020_TP = plusminus1year2020(L8_Ifugao,SD19,ED19,
                SD20,ED20,SD21,ED21);


//3. Clip collections to catchment, mask cloud and cloud shadows, and rename bands
function watershedclip(img){
    return img.clip(Catchment);
}
function maskLSR(image) {
    var qaMask = image.select('QA_PIXEL').bitwiseAnd(parseInt('11111', 2)).eq(0);
    var saturationMask = image.select('QA_RADSAT').eq(0);
    var opticalBands = image.select('SR_B.').multiply(0.0000275).add(-0.2);
    var thermalBands = image.select('ST_B.*').multiply(0.00341802).add(149.0);
    return image.addBands(opticalBands, null, true)
        .addBands(thermalBands, null, true)
        .updateMask(qaMask)
        .updateMask(saturationMask);
}
function renamebands5(img){
    var blue = img.select('SR_B1').rename('blue');
    var green = img.select('SR_B2').rename('green');
    var red = img.select('SR_B3').rename('red');
    var nir = img.select('SR_B4').rename('nir');
    var swir1 = img.select('SR_B5').rename('swir1');
    var swir2 = img.select('SR_B7').rename('swir2');
    return img.addBands(blue).addBands(green).addBands(red)
            .addBands(nir).addBands(swir1).addBands(swir2);
}
function renamebands8(img){
    var blue = img.select('SR_B2').rename('blue');
    var green = img.select('SR_B3').rename('green');
    var red = img.select('SR_B4').rename('red');
    var nir = img.select('SR_B5').rename('nir');
    var swir1 = img.select('SR_B6').rename('swir1');
    var swir2 = img.select('SR_B7').rename('swir2');
    return img.addBands(blue).addBands(green).addBands(red)
            .addBands(nir).addBands(swir1).addBands(swir2);
}
var Ifugao1990_TP_masked = L5_Ifugao1990_TP.map(watershedclip).map(maskLSR).map(renamebands5);
```

```
var Ifugao1995_TP_masked = L5_Ifugao1995_TP.map(watershedclip).map(maskLSR).map(renamebands5);
var Ifugao2000_TP_masked = L5_Ifugao2000_TP.map(watershedclip).map(maskLSR).map(renamebands5);
var Ifugao2005_TP_masked = L5_Ifugao2005_TP.map(watershedclip).map(maskLSR).map(renamebands5);
var Ifugao2010_TP_masked = L5_Ifugao2010_TP.map(watershedclip).map(maskLSR).map(renamebands5);
var Ifugao2015_TP_masked = L8_Ifugao2015_TP.map(watershedclip).map(maskLSR).map(renamebands8);
var Ifugao2020_TP_masked = L8_Ifugao2020_TP.map(watershedclip).map(maskLSR).map(renamebands8);


//4. Spatial patterns of good observation
var I1990goodobservation = Ifugao1990_TP_masked.reduce(ee.Reducer.count());
var I1995goodobservation = Ifugao1995_TP_masked.reduce(ee.Reducer.count());
var I2000goodobservation = Ifugao2000_TP_masked.reduce(ee.Reducer.count());
var I2005goodobservation = Ifugao2005_TP_masked.reduce(ee.Reducer.count());
var I2010goodobservation = Ifugao2010_TP_masked.reduce(ee.Reducer.count());
var I2015goodobservation = Ifugao2015_TP_masked.reduce(ee.Reducer.count());
var I2020goodobservation = Ifugao2020_TP_masked.reduce(ee.Reducer.count());


//5. Create composite for Principal Components Analysis
var bandsI = ['blue', 'green', 'red', 'nir', 'swir1', 'swir2'];
var PCAcomposite1990 = Ifugao1990_TP_masked.median().select(bandsI);
var PCAcomposite1995 = Ifugao1995_TP_masked.median().select(bandsI);
var PCAcomposite2000 = Ifugao2000_TP_masked.median().select(bandsI);
var PCAcomposite2005 = Ifugao2005_TP_masked.median().select(bandsI);
var PCAcomposite2010 = Ifugao2010_TP_masked.median().select(bandsI);
var PCAcomposite2015 = Ifugao2015_TP_masked.median().select(bandsI);
var PCAcomposite2020 = Ifugao2020_TP_masked.median().select(bandsI);

//6. Train with Principal Component Analysis (in ArcGIS)
function getNewBandNames(prefix, bNames){
  var seq = ee.List.sequence(1, bNames.length());
  return seq.map(function(b){
    return ee.String(prefix).cat(ee.Number(b).int());
  });
}
function DoCentered(composite, region){
  var bandNames = composite.bandNames();
  var meanDict = composite.reduceRegion({
    reducer: ee.Reducer.mean(),
    geometry: region,
    scale: 30,
    maxPixels: 1e9
  });
  var means = ee.Image.constant(meanDict.values(bandNames));
  var centered = composite.subtract(means);
  return centered;
}
function getPrincipalComponents(centered, region){
  var bandNames = centered.bandNames();
  var arrays = centered.toArray();
  var covar = arrays.reduceRegion({
    reducer: ee.Reducer.centeredCovariance(),
    geometry: region,
    scale: 30,
    maxPixels: 1e9
  });
  var covarArray = ee.Array(covar.get('array'));
  var eigens = covarArray.eigen();
  var eigenValues = eigens.slice(1, 0, 1);
  var eigenVectors = eigens.slice(1, 1);
  var arrayImage = arrays.toArray(1);
  var principalComponents = ee.Image(eigenVectors).matrixMultiply(arrayImage);
  var sdImage = ee.Image(eigenValues.sqrt())
    .arrayProject([0]).arrayFlatten([getNewBandNames('sd', bandNames)]);
  return principalComponents
    .arrayProject([0])
    .arrayFlatten([getNewBandNames('pc', bandNames)])
    .divide(sdImage);
}
```

```
var pcImage1990 = getPrincipalComponents(DoCentered(PCAcomposite1990,Catchment),Catchment);
var pcImage1995 = getPrincipalComponents(DoCentered(PCAcomposite1995,Catchment),Catchment);
var pcImage2000 = getPrincipalComponents(DoCentered(PCAcomposite2000,Catchment),Catchment);
var pcImage2005 = getPrincipalComponents(DoCentered(PCAcomposite2005,Catchment),Catchment);
var pcImage2010 = getPrincipalComponents(DoCentered(PCAcomposite2010,Catchment),Catchment);
var pcImage2015 = getPrincipalComponents(DoCentered(PCAcomposite2015,Catchment),Catchment);
var pcImage2020 = getPrincipalComponents(DoCentered(PCAcomposite2020,Catchment),Catchment);

//7. Include elevation as band
var bandsL = ['blue', 'green', 'red', 'nir', 'swir1', 'swir2','elev'];
var elev = ee.Image(watershedclip(DEM)).select('elevation').rename('elev');
var composite1990 = Ifugao1990_TP_masked.median().addBands(elev).select(bandsL);
var composite1995 = Ifugao1995_TP_masked.median().addBands(elev).select(bandsL);
var composite2000 = Ifugao2000_TP_masked.median().addBands(elev).select(bandsL);
var composite2005 = Ifugao2005_TP_masked.median().addBands(elev).select(bandsL);
var composite2010 = Ifugao2010_TP_masked.median().addBands(elev).select(bandsL);
var composite2015 = Ifugao2015_TP_masked.median().addBands(elev).select(bandsL);
var composite2020 = Ifugao2020_TP_masked.median().addBands(elev).select(bandsL);

//8. Classification through Random Forest (Part 1)
function doTrainAndClassify_1(composite,bb,PCtrain){
 var training_1 = composite.select(bb).sampleRegions({
   collection: PCtrain,
   properties: ['LC'],
   scale: 30
 });
 var classifier_1 = ee.Classifier.smileRandomForest(100)
   .train({
     features: training_1,
     classProperty: 'LC',
     inputProperties: bb
   });
 var classified = composite.classify(classifier_1);
 return classified;
}
var classified1990 = doTrainAndClassify_1(composite1990,bandsL,Train1990);
var classified1995 = doTrainAndClassify_1(composite1995,bandsL,Train1995);
var classified2000 = doTrainAndClassify_1(composite2000,bandsL,Train2000);
var classified2005 = doTrainAndClassify_1(composite2005,bandsL,Train2005);
var classified2010 = doTrainAndClassify_1(composite2010,bandsL,Train2010);
var classified2015 = doTrainAndClassify_1(composite2015,bandsL,Train2015);
var classified2020 = doTrainAndClassify_1(composite2020,bandsL,Train2020);

//9. Create Frequency Map
var lc_col = ee.ImageCollection(classified1990)
       .merge(ee.ImageCollection(classified1995))
       .merge(ee.ImageCollection(classified2000))
       .merge(ee.ImageCollection(classified2005))
       .merge(ee.ImageCollection(classified2010))
       .merge(ee.ImageCollection(classified2015))
       .merge(ee.ImageCollection(classified2010));
function MaskFrequentLC(img){
 var frequent = img.gte(5);
 return frequent.updateMask(frequent);
}
var freq_ricefield = MaskFrequentLC(lc_col
         .map(function(img){return img.updateMask(img.eq(1))})
         .reduce(ee.Reducer.count()));
var freq_builtup = MaskFrequentLC(lc_col
         .map(function(img){return img.updateMask(img.eq(2))})
         .reduce(ee.Reducer.count()));
var freq_forest = MaskFrequentLC(lc_col
         .map(function(img){return img.updateMask(img.eq(3))})
         .reduce(ee.Reducer.count()));
var freq_lowplants = MaskFrequentLC(lc_col
         .map(function(img){return img.updateMask(img.eq(4))})
         .reduce(ee.Reducer.count()));
```

```
var ricefieldvector = freq_ricefield.reduceToVectors({geometry: Catchment,scale: 30});
var builtupvector = freq_builtup.reduceToVectors({geometry: Catchment,scale: 30});
var forestvector = freq_forest.reduceToVectors({geometry: Catchment,scale: 30});
var lowplantsvector = freq_lowplants.reduceToVectors({geometry: Catchment,scale: 30});


//10. Create new training samples
function GetTrainingSamples(classified,vector){
  var trainingfeat = classified.sample({
    region: vector,
    scale: 30,
    numPixels: 5000,
    geometries: true
  });
  return trainingfeat;
}
function GetTrainingSamples(classified,code,vector){
  var trainingfeat = classified.updateMask(classified.eq(code)).sample({
    region: vector,
    scale: 30,
    numPixels: 5000,
    geometries: true
  });
  return trainingfeat;
}

function GetTrainFeat(classified,v1,v2,v3,v4){
  var train_ricefield = GetTrainingSamples(classified,1,v1);
  var train_builtup = GetTrainingSamples(classified,2,v2);
  var train_forest = GetTrainingSamples(classified,3,v3);
  var train_lowplants = GetTrainingSamples(classified,4,v4);
  var train_features = train_ricefield.merge(train_builtup)
                   .merge(train_forest).merge(train_lowplants);
  return train_features;
}
var Trainfeat_2020 = GetTrainFeat(classified2020,ricefieldvector,
              builtupvector,forestvector,lowplantsvector);
var Trainfeat_2015 = GetTrainFeat(classified2015,ricefieldvector,
              builtupvector,forestvector,lowplantsvector);
var Trainfeat_2010 = GetTrainFeat(classified2010,ricefieldvector,
              builtupvector,forestvector,lowplantsvector);
var Trainfeat_2005 = GetTrainFeat(classified2005,ricefieldvector,
              builtupvector,forestvector,lowplantsvector);
var Trainfeat_2000 = GetTrainFeat(classified2000,ricefieldvector,
              builtupvector,forestvector,lowplantsvector);
var Trainfeat_1995 = GetTrainFeat(classified1995,ricefieldvector,
              builtupvector,forestvector,lowplantsvector);
var Trainfeat_1990 = GetTrainFeat(classified1995,ricefieldvector,
              builtupvector,forestvector,lowplantsvector);

//11. Classification through Random Forest (Part 2)
function doTrainAndClassify_2(composite,bb,train){
  var training_2 = composite.select(bb).sampleRegions({
    collection: train,
    properties: ['classification'],
    scale: 30
  });
  var classifier_2 = ee.Classifier.smileRandomForest(100)
    .train({
      features: training_2,
      classProperty: 'classification',
      inputProperties: bb
    });
  var classified = composite.classify(classifier_2);
  return classified;
}
var classified_2_1990 = doTrainAndClassify_2(composite1990,bandsL,Trainfeat_1990);
var classified_2_1995 = doTrainAndClassify_2(composite1995,bandsL,Trainfeat_1995);
```

```
var classified_2_2000 = doTrainAndClassify_2(composite2000,bandsL,Trainfeat_2000);
var classified_2_2005 = doTrainAndClassify_2(composite2005,bandsL,Trainfeat_2005);
var classified_2_2010 = doTrainAndClassify_2(composite2010,bandsL,Trainfeat_2010);
var classified_2_2015 = doTrainAndClassify_2(composite2015,bandsL,Trainfeat_2015);
var classified_2_2020 = doTrainAndClassify_2(composite2020,bandsL,Trainfeat_2020);


//12. Transition rules
var lc_col2 = ee.ImageCollection(classified_2_1990)
        .merge(ee.ImageCollection(classified_2_1995))
        .merge(ee.ImageCollection(classified_2_2000))
        .merge(ee.ImageCollection(classified_2_2005))
        .merge(ee.ImageCollection(classified_2_2010))
        .merge(ee.ImageCollection(classified_2_2015))
        .merge(ee.ImageCollection(classified_2_2020));
function transitionfirstyear(img1,img2,img3,c1,c2){
 var img1rule = img1.updateMask(img1.eq(c1));
 var img2rule = img2.updateMask(img2.eq(c2));
 var img3rule = img3.updateMask(img3.eq(c2));
 var finalrule = img1rule.and(img2rule).and(img3rule);
 var img1filtered = img1.where(finalrule.eq(1),c2);
 return img1filtered;
}
function transitionbetween(img1,img2,img3,c1,c2){
 var img1rule = img1.updateMask(img1.eq(c1));
 var img2rule = img2.updateMask(img2.eq(c2));
 var img3rule = img3.updateMask(img3.eq(c1));
 var finalrule = img1rule.and(img2rule).and(img3rule);
 var img2filtered = img2.where(finalrule.eq(1),c1);
 return img2filtered;
}
function transitionlastyear(img1,img2,img3,c1,c2){
 var img1rule = img1.updateMask(img1.eq(c1));
 var img2rule = img2.updateMask(img2.eq(c1));
 var img3rule = img3.updateMask(img3.eq(c2));
 var finalrule = img1rule.and(img2rule).and(img3rule);
 var img3filtered = img3.where(finalrule.eq(1),c1);
 return img3filtered;
}
function Filtertransitionfirstyear(lclist,accfilcol){
 accfilcol = ee.ImageCollection(accfilcol);
 lclist = ee.List(lclist);
 var img1 = ee.Image(lclist.get(0));
 var img2 = ee.Image(lclist.get(1));
 var img3 = ee.Image(lclist.get(2));
 var rule9 = transitionfirstyear(img1,img2,img3,2,1); //BRR
 var rule10 = transitionfirstyear(rule9,img2,img3,2,3); //BFF
 var resultimage = ee.Image(rule10);
 var accfilcol_update = accfilcol.merge(ee.ImageCollection(resultimage));
 return accfilcol_update;
}
function Filtertransitionbetween(currentno,startdic){
 startdic = ee.Dictionary(startdic);
 var accfilcol = ee.ImageCollection(startdic.get('accfilcol'));
 var lclist = ee.List(startdic.get('lclist'));
 currentno = ee.Number(currentno);
 var img1 = ee.Image(lclist.get(currentno.subtract(1)));
 var img2 = ee.Image(lclist.get(currentno));
 var img3 = ee.Image(lclist.get(currentno.add(1)));
 var rule1 = transitionbetween(img1,img2,img3,1,2); //RBR
 var rule2 = transitionbetween(img1,rule1,img3,1,3); //RFR
 var rule3 = transitionbetween(img1,rule2,img3,2,1); //BRB
 var rule4 = transitionbetween(img1,rule3,img3,2,3); //BFB
 var rule5 = transitionbetween(img1,rule4,img3,2,4); //BLB
 var rule6 = transitionbetween(img1,rule5,img3,3,1); //FRF
 var rule7 = transitionbetween(img1,rule6,img3,3,2); //FBF
 var rule8 = transitionbetween(img1,rule7,img3,4,2); //LBL
 var resultimage = ee.Image(rule8);
```

```
  var coldictionary = ee.Dictionary({
    accfilcol: accfilcol.merge(ee.ImageCollection(resultimage)),
    lclist: lclist
  });
  return coldictionary;
}
function Filtertransitionlastyear(lclist,accfilcol){
  accfilcol = ee.ImageCollection(accfilcol);
  lclist = ee.List(lclist);
  var img1 = ee.Image(lclist.get(-3));
  var img2 = ee.Image(lclist.get(-2));
  var img3 = ee.Image(lclist.get(-1));
  var rule11 = transitionlastyear(img1,img2,img3,2,1); //BBR
  var rule12 = transitionlastyear(img1,img2,rule11,2,3); //BBF
  var resultimage = ee.Image(rule12);
  var accfilcol_update = accfilcol.merge(ee.ImageCollection(resultimage));
  return accfilcol_update;
}
function IterateTemporalFilter(curno, lccol){
  lccol = ee.ImageCollection(lccol);
  var landcoverlist = ee.List(lccol.toList(7));
  var accfiltercol = ee.ImageCollection([]);
  var filfirst_accfilcol = Filtertransitionfirstyear(landcoverlist,accfiltercol);
  var bet_list = ee.List([1,2,3,4,5]);
  var bet_dic = ee.Dictionary({
      accfilcol: filfirst_accfilcol,
      lclist: landcoverlist
    });
  var betweenresdic = ee.Dictionary(bet_list.iterate(Filtertransitionbetween, bet_dic));
  var filbet_accfilcol = ee.ImageCollection(betweenresdic.get('accfilcol'));
  var fillast_accfilcol = Filtertransitionlastyear(landcoverlist,filbet_accfilcol);
  return fillast_accfilcol;
}
var iter_list = ee.List([1,2,3]);
var fil_lc_col = ee.ImageCollection(iter_list.iterate(IterateTemporalFilter, lc_col2));
var prefinalclassified1990 = ee.Image(fil_lc_col.toList(7).get(0));
var prefinalclassified1995 = ee.Image(fil_lc_col.toList(7).get(1));
var prefinalclassified2000 = ee.Image(fil_lc_col.toList(7).get(2));
var prefinalclassified2005 = ee.Image(fil_lc_col.toList(7).get(3));
var prefinalclassified2010 = ee.Image(fil_lc_col.toList(7).get(4));
var prefinalclassified2015 = ee.Image(fil_lc_col.toList(7).get(5));
var prefinalclassified2020 = ee.Image(fil_lc_col.toList(7).get(6));


//13. Masking misclassified paddy fields
function filterclip(img){
  var watermask =  img.where(img.eq(1),1)
              .where(img.eq(2),1)
              .where(img.eq(3),1)
              .where(img.eq(4),1)
              .where(img.eq(5),0);
  var maskedcliped = img.updateMask(watermask).clip(Catchment).rename('classification');
  return maskedcliped;
}
function maskpaddyinstream(prefinalclassified,stream){
  var paddyinwater = prefinalclassified.eq(1).and(stream);
  var prefinalwater = prefinalclassified.where(paddyinwater.eq(1),5);
  var neighbor = prefinalwater.neighborhoodToBands(ee.Kernel.square(1));
  var neighborscollection =
            ee.ImageCollection(filterclip(neighbor.select("classification_-1_-1")))
        .merge(ee.ImageCollection(filterclip(neighbor.select("classification_0_-1"))))
        .merge(ee.ImageCollection(filterclip(neighbor.select("classification_1_-1"))))
        .merge(ee.ImageCollection(filterclip(neighbor.select("classification_-1_0"))))
        .merge(ee.ImageCollection(filterclip(neighbor.select("classification_1_0"))))
        .merge(ee.ImageCollection(filterclip(neighbor.select("classification_-1_1"))))
        .merge(ee.ImageCollection(filterclip(neighbor.select("classification_0_1"))))
        .merge(ee.ImageCollection(filterclip(neighbor.select("classification_1_1"))));
  var majorityneighbor = neighborscollection.reduce(ee.Reducer.mode());
```

```
  var finalclassified = prefinalclassified.where(paddyinwater.eq(1),majorityneighbor);
  return finalclassified;
}
var finalclassified1990 = maskpaddyinstream(prefinalclassified1990,Streamline);
var finalclassified1995 = maskpaddyinstream(prefinalclassified1995,Streamline);
var finalclassified2000 = maskpaddyinstream(prefinalclassified2000,Streamline);
var finalclassified2005 = maskpaddyinstream(prefinalclassified2005,Streamline);
var finalclassified2010 = maskpaddyinstream(prefinalclassified2010,Streamline);
var finalclassified2015 = maskpaddyinstream(prefinalclassified2015,Streamline);
var finalclassified2020 = maskpaddyinstream(prefinalclassified2020,Streamline);
var LCPalette = {
 min: 1,
 max: 4,
 palette: [
  'cdb33b', // rice field
  'c4c4c4', // built-up
  '225129', // forest
  '387242' // low plants
 ]
};
Map.addLayer(finalclassified1990, LCPalette, 'Land Cover 1990');
Map.addLayer(finalclassified1995, LCPalette, 'Land Cover 1995');
Map.addLayer(finalclassified2000, LCPalette, 'Land Cover 2000');
Map.addLayer(finalclassified2005, LCPalette, 'Land Cover 2005');
Map.addLayer(finalclassified2010, LCPalette, 'Land Cover 2010');
Map.addLayer(finalclassified2015, LCPalette, 'Land Cover 2015');
Map.addLayer(finalclassified2020, LCPalette, 'Land Cover 2020');

//14. Accuracy Assessment
function validateImage(finalclassifiedyr, Valyr, yr){
  var validationyr = finalclassifiedyr.sampleRegions({
    collection: Valyr,
    properties: ['actual'],
    scale: 30,
  });
  print("Validation feature:", yr, validationyr);
  var testAccuracyyr = validationyr.errorMatrix('actual', 'classification');
  print('Validation error matrix: ', yr, testAccuracyyr);
  var AccuracyDic = ee.Dictionary({
    Consumers: testAccuracyyr.consumersAccuracy(),
    Producers: testAccuracyyr.producersAccuracy(),
    Overall: testAccuracyyr.accuracy(),
    Kappa: testAccuracyyr.kappa()
  });
  print("Validation Accuracies:", yr, AccuracyDic);
  return testAccuracyyr;
}
var testAccuracy1990 = validateImage(finalclassified1990, Val1990, 1990);
var testAccuracy1995 = validateImage(finalclassified1995, Val1995, 1995);
var testAccuracy2000 = validateImage(finalclassified2000, Val2000, 2000);
var testAccuracy2005 = validateImage(finalclassified2005, Val2005, 2005);
var testAccuracy2010 = validateImage(finalclassified2010, Val2010, 2010);
var testAccuracy2015 = validateImage(finalclassified2015, Val2015, 2015);
var testAccuracy2020 = validateImage(finalclassified2020, Val2020, 2020);

//15. Agriculture Change analysis
function AgriAbandon(classified, code){
  var rice = classified.where(classified.eq(1),code)
                .where(classified.eq(2),0)
                .where(classified.eq(3),0)
                .where(classified.eq(4),0);
  return rice;
}
var riceA1990 = AgriAbandon(finalclassified1990,1);
var riceA1995 = AgriAbandon(finalclassified1995,2);
var riceA2000 = AgriAbandon(finalclassified2000,3);
var riceA2005 = AgriAbandon(finalclassified2005,4);
```

```
var riceA2010 = AgriAbandon(finalclassified2010,5);
var riceA2015 = AgriAbandon(finalclassified2015,6);
var riceA2020 = AgriAbandon(finalclassified2020,7);
var rice_last = ee.ImageCollection(riceA1990)
        .merge(ee.ImageCollection(riceA1995))
        .merge(ee.ImageCollection(riceA2000))
        .merge(ee.ImageCollection(riceA2005))
        .merge(ee.ImageCollection(riceA2010))
        .merge(ee.ImageCollection(riceA2015))
        .merge(ee.ImageCollection(riceA2020)).max();
function AgriExpansion(classified, code){
  var rice = classified.where(classified.eq(1),code)
                .where(classified.eq(2),8)
                .where(classified.eq(3),8)
                .where(classified.eq(4),8);
  return rice;
}
var riceE1990 = AgriExpansion(finalclassified1990,1);
var riceE1995 = AgriExpansion(finalclassified1995,2);
var riceE2000 = AgriExpansion(finalclassified2000,3);
var riceE2005 = AgriExpansion(finalclassified2005,4);
var riceE2010 = AgriExpansion(finalclassified2010,5);
var riceE2015 = AgriExpansion(finalclassified2015,6);
var riceE2020 = AgriExpansion(finalclassified2020,7);
var rice_first = ee.ImageCollection(riceE1990)
        .merge(ee.ImageCollection(riceE1995))
        .merge(ee.ImageCollection(riceE2000))
        .merge(ee.ImageCollection(riceE2005))
        .merge(ee.ImageCollection(riceE2010))
        .merge(ee.ImageCollection(riceE2015))
        .merge(ee.ImageCollection(riceE2020)).min()
        .remap([1,2,3,4,5,6,7,8],[1,2,3,4,5,6,7,0]);

//16. Expansion and reduction of land cover types
function Reclass(classified,classcode,code){
  var reclass = classified.where(classified.eq(1),0)
                .where(classified.eq(2),0)
                .where(classified.eq(3),0)
                .where(classified.eq(4),0)
                .where(classified.eq(classcode),code);
  return reclass;
}
function RedandExp(finalc1990,finalc2020,classcode){
  var classfirstyr = Reclass(finalc1990,classcode,1);
  var classlastyr = Reclass(finalc2020,classcode,2);
  var classdiff = classlastyr.subtract(classfirstyr);
  var classchange = classfirstyr //if continuous, = 1
            .where(classdiff.eq(-1),2) //if abandoned, = -1
            .where(classdiff.eq(2),3); //if expanded, = 2
  return classchange;
}
var ricechange = RedandExp(finalclassified1990,finalclassified2020,1);
var builtupchange = RedandExp(finalclassified1990,finalclassified2020,2);
var forestchange = RedandExp(finalclassified1990,finalclassified2020,3);
var lowplantschange = RedandExp(finalclassified1990,finalclassified2020,4);

//17. Transition values
function TransitionClass(classifiedfrom,classifiedto,classcodefrom,classcodeto){
  var transtofrom = classifiedfrom.eq(classcodefrom).and(classifiedto.eq(classcodeto));
  return transtofrom;
}
function TransitionsEachPeriod(classifiedfrom,classifiedto){
  var ricTOric = TransitionClass(classifiedfrom,classifiedto,1,1);
  var ricTObui = TransitionClass(classifiedfrom,classifiedto,1,2);
  var ricTOfor = TransitionClass(classifiedfrom,classifiedto,1,3);
  var ricTOlow = TransitionClass(classifiedfrom,classifiedto,1,4);
  var buiTOric = TransitionClass(classifiedfrom,classifiedto,2,1);
```

146

```
    var buiTObui = TransitionClass(classifiedfrom,classifiedto,2,2);
    var buiTOfor = TransitionClass(classifiedfrom,classifiedto,2,3);
    var buiTOlow = TransitionClass(classifiedfrom,classifiedto,2,4);
    var forTOric = TransitionClass(classifiedfrom,classifiedto,3,1);
    var forTObui = TransitionClass(classifiedfrom,classifiedto,3,2);
    var forTOfor = TransitionClass(classifiedfrom,classifiedto,3,3);
    var forTOlow = TransitionClass(classifiedfrom,classifiedto,3,4);
    var lowTOric = TransitionClass(classifiedfrom,classifiedto,4,1);
    var lowTObui = TransitionClass(classifiedfrom,classifiedto,4,2);
    var lowTOfor = TransitionClass(classifiedfrom,classifiedto,4,3);
    var lowTOlow = TransitionClass(classifiedfrom,classifiedto,4,4);
    var transitionmap = classifiedfrom
                .where(ricTOric.eq(1),1).where(ricTObui.eq(1),2)
                .where(ricTOfor.eq(1),3).where(ricTOlow.eq(1),4)
                .where(buiTOric.eq(1),5).where(buiTObui.eq(1),6)
                .where(buiTOfor.eq(1),7).where(buiTOlow.eq(1),8)
                .where(forTOric.eq(1),9).where(forTObui.eq(1),10)
                .where(forTOfor.eq(1),11).where(forTOlow.eq(1),12)
                .where(lowTOric.eq(1),13).where(lowTObui.eq(1),14)
                .where(lowTOfor.eq(1),15).where(lowTOlow.eq(1),16);
    return transitionmap;
}
var transition1990to1995 = TransitionsEachPeriod(finalclassified1990,finalclassified1995);
var transition1995to2000 = TransitionsEachPeriod(finalclassified1995,finalclassified2000);
var transition2000to2005 = TransitionsEachPeriod(finalclassified2000,finalclassified2005);
var transition2005to2010 = TransitionsEachPeriod(finalclassified2005,finalclassified2010);
var transition2010to2015 = TransitionsEachPeriod(finalclassified2010,finalclassified2015);
var transition2015to2020 = TransitionsEachPeriod(finalclassified2015,finalclassified2020);


//18. Agricultural Abandonment and Expansion
function Paddydynamics(transition,ricelast,lastcode,ricefirst,firstcode){
  var abandonment = transition.where(transition.eq(1),0).where(transition.eq(2),1)
                    .where(transition.eq(3),1).where(transition.eq(4),1)
                    .where(transition.eq(5),0).where(transition.eq(6),0)
                    .where(transition.eq(7),0).where(transition.eq(8),0)
                    .where(transition.eq(9),0).where(transition.eq(10),0)
                    .where(transition.eq(11),0).where(transition.eq(12),0)
                    .where(transition.eq(13),0).where(transition.eq(14),0)
                    .where(transition.eq(15),0).where(transition.eq(16),0);
  var expansion = transition.where(transition.eq(1),0).where(transition.eq(2),0)
                    .where(transition.eq(3),0).where(transition.eq(4),0)
                    .where(transition.eq(5),1).where(transition.eq(6),0)
                    .where(transition.eq(7),0).where(transition.eq(8),0)
                    .where(transition.eq(9),1).where(transition.eq(10),0)
                    .where(transition.eq(11),0).where(transition.eq(12),0)
                    .where(transition.eq(13),1).where(transition.eq(14),0)
                    .where(transition.eq(15),0).where(transition.eq(16),0);
  var paddydynamics = abandonment.where(rice_last.eq(lastcode),2)
      .where(expansion.eq(1),3).where(rice_first.eq(firstcode),4);
  return paddydynamics;
}
var PaddyDynamics19901995 = Paddydynamics(transition1990to1995,rice_last,1,rice_first,2);
var PaddyDynamics19952000 = Paddydynamics(transition1995to2000,rice_last,2,rice_first,3);
var PaddyDynamics20002005 = Paddydynamics(transition2000to2005,rice_last,3,rice_first,4);
var PaddyDynamics20052010 = Paddydynamics(transition2005to2010,rice_last,4,rice_first,5);
var PaddyDynamics20102015 = Paddydynamics(transition2010to2015,rice_last,5,rice_first,6);
var PaddyDynamics20152020 = Paddydynamics(transition2015to2020,rice_last,6,rice_first,7);
```

## A2. The R code

The following lines were the R code executed in Rstudio to implement the logistic regression for building the statistical model of LUCC.

```
##0. Set working directory and library
install.packages("pscl")
install.packages("ROCR")
library(pscl)
library(ROCR)
setwd("C:/Users/estac/Documents/(Acads) PhD - Environmental Management/Dissertation/Data/2. Logistic
regression/...Revision/Bivariate analysis/WorkingDIR")
getwd()
##set the personal library
.libPaths("C:/Users/estac/Documents/(Acads) PhD - Environmental Management/Dissertation/Data/2. Logistic
regression/Final regression/WorkingDIR/MyLibrary")
#.libPaths() ## Press tab for options

##1. Add and attach training csv to R
#agriabandon.data <- read.csv("MyData2/Reg20052010.csv")
agriabandon.data <- read.csv("MyData2/Generalregression.csv")
attach(agriabandon.data)
summary(agriabandon.data)

##2. Convert "variablen" to categorical variable (example)
#s_aspect <- ifelse(aspect > 135 & aspect <225, 1, 0)
##add new variable to data
#agriabandon.data <- cbind(agriabandon.data, s_aspect)

##3. Are any of your covariates correlated? Generate a Pearson correlation coefficient matrix
cor.matrix <- cor(agriabandon.data, method = "pearson")
cor.matrix

##4. Standardize continuous variables which allows you to compare the strength of each covariate in model results
#z-score scaling (var-mean/sd, which makes the mean=0, sd=1, var ranges, add to dataframe)
Elevation.std <- scale(dem, center=TRUE, scale=TRUE)
Slope.std <- scale(slope, center=TRUE, scale=TRUE)
SinAspect.std <- scale(SinAspect, center=TRUE, scale=TRUE)
CosAspect.std <- scale(CosAspect, center=TRUE, scale=TRUE)
Soilgroup.std <- scale(Soil_Group, center=TRUE, scale=TRUE)
QF.std <- scale(QF, center=TRUE, scale=TRUE)
Dist_stream.std <- scale(stream, center=TRUE, scale=TRUE)
Dist_townc.std <- scale(Dist_city, center=TRUE, scale=TRUE)
Dist_road.std <- scale(Dist_road, center=TRUE, scale=TRUE)
Dist_viewp.std <- scale(Dist_view, center=TRUE, scale=TRUE)
Heritagesi.std <- scale(Heritage, center=TRUE, scale=TRUE)
Lowveg.std <- scale(Lowveg, center=TRUE, scale=TRUE)
Forest.std <- scale(forest, center=TRUE, scale=TRUE)
Builtup.std <- scale(builtup, center=TRUE, scale=TRUE)
Ricefield.std <- scale(Paddyfield, center=TRUE, scale=TRUE)
agriabandon.data <- cbind(agriabandon.data, Elevation.std, Slope.std, SinAspect.std, CosAspect.std, Soilgroup.std, QF.std,
Dist_stream.std, Dist_townc.std, Dist_road.std, Dist_viewp.std, Heritagesi.std, Lowveg.std, Forest.std, Builtup.std,
Ricefield.std)

###5. Run logistic regression and summarize results
#abandonment_vars.model <- glm(Code ~ Elevation.std + Slope.std + SinAspect.std + CosAspect.std + Soilgroup.std +
QF.std + Dist_stream.std +  Dist_townc.std + Dist_road.std + Dist_viewp.std + Heritagesi.std + Lowveg.std + Forest.std +
Builtup.std +  Ricefield.std, family = binomial, data = agriabandon.data)
abandonment_vars.model <- glm(Code ~ dem + slope + SinAspect + CosAspect + Soil_Group + QF + stream +  Dist_city +
Dist_road + Dist_view + Heritage + Lowveg + forest + builtup + Paddyfield, family = binomial, data = agriabandon.data)
summary(abandonment_vars.model)
pR2(abandonment_vars.model)
```

###9. predicted values
Predicted=predict(abandonment_vars.model, type="response")
write.table(Predicted, "predictedvalues.txt", sep="\t")

###10. Residuals
##residual deviance indicates the response predicted by a model
##on adding independent variables. The lower the values, the better the model
residuals(abandonment_vars.model, type="deviance")

###11. Confusion matrix: a tabular representation of actual vs predicted values
##This helps us to find the accuracy of the model and avoid overfitting
table(agriabandon.data$Code, Predicted > 0.5)

###12. ROC : ROC summarizes the predictive power for all possible values of p > 0.5.
ROCRpred <- prediction(Predicted, agriabandon.data$Code)
ROCRperf <- performance(ROCRpred, 'tpr', 'fpr')
plot(ROCRperf)
#### Find AUC area under curve of ROC: referred to as index of accuracy (A) or
##concordance index, is a perfect performance metrix for ROC curve
auc <- performance(ROCRpred, measure = "auc")
auc <- auc@y.values[[1]]
auc
plot(ROCRperf, main="AUC=0.69", colorize = TRUE, text.adj = c(-0.2,17))

# A3. The GAMA code

The following lines were the GAML code executed in GAMA to develop the Agent-based model of Ifugao rice terraces

```
model Ifugaoriceterraces

global {//
//--Modeling and simulation fundamentals--
//float seedvalue <- 9.0;
float startt <- machine_time;

//--Experiment type--
int by_optimization <- 0;
bool bool_optimization <- by_optimization = 1 ? true:false;
bool stop_currentrun <- false;
bool is_batch <- false;
bool is_calibration <- false;

//--For accuracies--
list<string> categories <- ["Paddyfield", "otherlandcover","NODATA"];
matrix<float> fuzzy_categories;
matrix<float> fuzzy_transitions;
list<float> nb_per_cat_actual;
list<float> nb_per_cat_model;
float accuracy_fuzzykappa;
float accuracy_fuzzykappa_sim;
float accuracy_PAD;
float accuracy_paddyfieldresidual;
int accuracy_numberoffarmsresidual;
list<float> yearlyfuzzykappa;
list<float> yearlyfuzzykappa_sim;
list<float> yearlyPAD;
list<float> yearlypaddyfieldresidual;
list<int> yearlynumberoffarmsresidual;
float model_fuzzykappa;
float model_fuzzykappa_sim;
float model_PAD;
float model_paddyfieldresidual;
float model_numberoffarmsresidual;
float optimizationmeasure;

//--import of files and setting of the environment--
//csv
file csv_file_Tabledata <- csv_file("../includes/Final_Yearlytabledata.csv",",");
matrix matrix_Tabledata <- matrix(csv_file_Tabledata);
file csv_file_paddyfieldarea <- csv_file("../includes/Final_LULCdata.csv",",");
matrix matrix_paddyfieldarea <- matrix(csv_file_paddyfieldarea);
file csv_file_numberoffarms <- csv_file("../includes/Numberoffarms.csv",",");
matrix matrix_numberoffarms <- matrix(csv_file_numberoffarms);

//raster files
grid_file raster_file_LCactual1990 <- file('../includes/lcactual1990.asc'); //0
grid_file raster_file_slope <- file('../includes/slope.asc'); //2
grid_file raster_file_cosaspect <- file('../includes/cosaspect.asc'); //3
grid_file raster_file_disttowncenter <- file('../includes/dist_towncenter.asc'); //4
grid_file raster_file_distroad <- file('../includes/dist_road.asc'); //5
grid_file raster_file_heritage <- file('../includes/heritage.asc'); //6
grid_file raster_file_quickflow1990 <- file('../includes/qf1990.asc'); //7
grid_file raster_file_densforest1990 <- file('../includes/density_forest1990.asc'); //8
grid_file raster_file_denslowveg1990 <- file('../includes/density_lowveg1990.asc'); //9
grid_file raster_file_denspaddy1990 <- file('../includes/density_paddyfield1990.asc'); //10
```

```
grid_file raster_file_quickflow1995 <- file('../includes/qf1995.asc'); //11
grid_file raster_file_densforest1995 <- file('../includes/density_forest1995.asc'); //12
grid_file raster_file_denslowveg1995 <- file('../includes/density_lowveg1995.asc'); //13
grid_file raster_file_denspaddy1995 <- file('../includes/density_paddyfield1995.asc'); //14
grid_file raster_file_LCactual1995 <- file('../includes/lcactual1995.asc'); //15


grid_file raster_file_quickflow2000 <- file('../includes/qf2000.asc'); //17
grid_file raster_file_densforest2000 <- file('../includes/density_forest2000.asc'); //18
grid_file raster_file_denslowveg2000 <- file('../includes/density_lowveg2000.asc'); //19
grid_file raster_file_denspaddy2000 <- file('../includes/density_paddyfield2000.asc'); //20
grid_file raster_file_LCactual2000 <- file('../includes/lcactual2000.asc'); //21

/*
grid_file raster_file_quickflow2005 <- file('../includes/qf2005.asc'); //23
grid_file raster_file_densforest2005 <- file('../includes/density_forest2005.asc'); //24
grid_file raster_file_denslowveg2005 <- file('../includes/density_lowveg2005.asc'); //25
grid_file raster_file_denspaddy2005 <- file('../includes/density_paddyfield2005.asc'); //26
//grid_file raster_file_LCactual2005 <- file('../includes/lcactual2005.asc'); //27


grid_file raster_file_quickflow2010 <- file('../includes/qf2010.asc'); //29
grid_file raster_file_densforest2010 <- file('../includes/density_forest2010.asc'); //30
grid_file raster_file_denslowveg2010 <- file('../includes/density_lowveg2010.asc'); //31
grid_file raster_file_denspaddy2010 <- file('../includes/density_paddyfield2010.asc'); //32
//grid_file raster_file_LCactual2010 <- file('../includes/lcactual2010.asc'); //33
*/

grid_file raster_file_quickflow2015 <- file('../includes/qf2015.asc');
grid_file raster_file_densforest2015 <- file('../includes/density_forest2015.asc'); //30
grid_file raster_file_denslowveg2015 <- file('../includes/density_lowveg2015.asc'); //31
grid_file raster_file_denspaddy2015 <- file('../includes/density_paddyfield2015.asc'); //32
grid_file raster_file_LCactual2015 <- file('../includes/lcactual2015.asc');

grid_file raster_file_LCactual2020 <- file('../includes/lcactual2020.asc');

//boundary
geometry shape <- envelope(raster_file_LCactual1990);

//--Constant parameters through all scenarios (based on data)--
//Time-constant
int startingyear <- 1990;
int endingyear <- 2020;
float coef_slope <- 0.0499;
float coef_cosaspect <- -0.303;
float coef_quickflow <- 0.000360;
float coef_disttowncenter <- 0.000198;
float coef_distroad <- -0.000281;
float coef_heritage <- -0.841;
float coef_densforest <- 1.210;
float coef_denslowveg <- 2.010;
float coef_denspaddy <- -2.540;
int init_nb_farmers <- 1746;
float Valuesheritage_rate <- 0.25;
//Time-changing
float precipitation  <- 20.0;
float max_temp <- 20.0;
float familysize <- 4.87;
float lifeexpectancy <- 65.0;
float actual_paddyfieldarea <- 0.0;
//--Constant parameters through all scenarios (based on calibration)--
float parameter_precip_effect_on_erosion <- 10.0;
float parameter_maxtemp_effect_on_watersupply <- 69.0;
float parameter_threshold_succesorincome <- 19000.0;
int initialoldestfarmer <- 60;
int initialyoungestfarmer <- 29;

//--Changing parameters through scenarios--
```

```
int govfixeserosion_number <- 0;
bool governmentfixeserodedareas <- govfixeserosion_number = 1 ? true:false;
float subsidyperfamilyhead <- 0.0;

//--Temporal variables--
//year
    int current_year;
    //Environment
float erosion_rate <- 0.9;
float watersupply_rate <- 0.10;
    //Agents
    int nb_farmerhouseholds;
float ave_farmarea;
list yearlynb_farmerhouseholds;
//LUCC
float Permanentlyabandonedarea;
int Permanentlyabandonedcount;
float PeriodicPermanentlyabandonedarea;
int PeriodicPermanentlyabandonedcount;
float Paddyfieldarea;
    int Paddyfieldcount;
    list yearlypaddyfieldarea;

    //--initialization setting--
    init{
        write startingyear;
        current_year <- startingyear;
        erosion_rate <- 0.1;
        watersupply_rate <- 0.9;

        list<float> areafactorlist;
        loop times: init_nb_farmers{
            float areafactor <- rnd(1.0,3.0);
            add areafactor to: areafactorlist;
        }
        float areafactorsum <- sum(areafactorlist);
        list init_yearcolumn <- matrix_paddyfieldarea column_at 0;
        int init_index <- init_yearcolumn index_of current_year;
        float currenttotalpaddyarea <- float(matrix_paddyfieldarea[1,init_index]);
        list<float> parameterinit_farmerareas;
        loop areafactor over: areafactorlist{
            float farmerarea <- areafactor*currenttotalpaddyarea/areafactorsum;
            add farmerarea to: parameterinit_farmerareas;
        }
        int initializedfarmowner <- 0;
        create farmowner number: init_nb_farmers{
            farmarea <- parameterinit_farmerareas at initializedfarmowner;
            farmarea_stillpaddy <- farmarea;
            farmarea_temporarilyabandoned <- [0.0,0.0,0.0];
            farmowner_age <- rnd(initialyoungestfarmer, initialoldestfarmer);
            convertedfrompaddy <- 0.0;
            newowner <- true;
            do createsuccesors;
            initializedfarmowner <- initializedfarmowner + 1;
        }
        nb_farmerhouseholds <- length(farmowner);
        ave_farmarea <- farmowner mean_of each.farmarea;
        Permanentlyabandonedarea <- farmowner sum_of (each.convertedfrompaddy);
        Permanentlyabandonedcount <- int(Permanentlyabandonedarea/900.0);
        Paddyfieldarea <- farmowner sum_of each.farmarea_stillpaddy;
        Paddyfieldcount <- int(Paddyfieldarea/900.0);

        ask grid_cell {
            neighbours  <- self neighbors_at 1;
            LCtype  <- bands[0];
            paddyfield <- LCtype = 1.0 ? true:false;
            paddyfieldactual <- -1.0;
```

```
                paddyfieldmodel <- -1.0;
                grid_value <- -1.0;
                paddyLUCCprob <- -1.0;
                if LCtype > 1.0{
                        paddyfieldactual <- 0.0;
                        paddyfieldmodel <- 0.0;
                        grid_value <- 0.0;
                }
                if paddyfield{
                        paddyfieldactual <- 1.0;
                        paddyfieldmodel <- 1.0;
                        grid_value <- 1.0;
                        paddyLUCCprob <- 0.0;
                }
                if grid_value >= 0{
                        color <- rgb(255, 255*(grid_value),0);
                } else{
                        color <- #black;
                }

                if paddyfieldactual = 1.0{
                        cat_init <- "Paddyfield";
                        cat_actual <- "Paddyfield";
                } else if paddyfieldactual = 0.0{
                        cat_init <- "Paddyfield";
                        cat_actual <- "otherlandcover";
                } else{
                        cat_init <- "Paddyfield";
                        cat_actual <- "NODATA";
                }
                realdata <- cat_actual = "NODATA" ? false: true;
        }
        ask factorsnondens {
                slope <- bands[1];
                cosaspect <- bands[2];
                disttowncenter <- bands[3];
                distroad <- bands[4];
                heritage <- bands[5];
                quickflow <- bands[6];
                color <- rgb(255, 40*slope,0);
        }
        ask factorsdens {
                densforest <- bands[1];
                denslowveg <- bands[2];
                denspaddy <- bands[3];
                color <- rgb(255, 255*densforest,0);
        }
    }

reflex sequenceswithinayear when: (current_year != endingyear){
        if is_calibration{
                if current_year = 1995 or current_year = 2000
                or current_year = 2015{
                        do Updaterasterbandsandactualabandonment;
                        write "updated";
                }
        }
        do Effectofenvironmenttolivingconditions;
        do Agentsactions;
        do Changesbasedonsmallscaleprocesses;
        current_year <- cycle + startingyear + 1;
        write current_year;
        if is_calibration{
                if current_year = 1995 or current_year = 2000
                or current_year = 2015 or current_year = 2020{
                        do Generationofnewlandusemap;
                }
```

```
            }
            if is_calibration{
                if current_year = 2002 or current_year = 2012{
                    do Computeaccuracy_familysize;
                }
                if current_year = 1995 or current_year = 2000 or current_year = 2015
                or current_year = 2020{
                    do Computeaccuracy_LUCC;
                }
            }
}

reflex stop_simulation when: current_year = endingyear{
        if is_calibration{
            list yearlyfuzzykappasquared <- yearlyfuzzykappa collect (each^2);
            list yearlyfuzzykappa_simsquared <- yearlyfuzzykappa_sim collect (each^2);
            list yearlyPADsquared <- yearlyPAD collect (each^2);
            list yearlypaddyfieldresidualsquared <- yearlypaddyfieldresidual collect (each^2);
            list yearlynumberoffarmsresidualsquared <- yearlynumberoffarmsresidual collect (each^2);
            model_fuzzykappa <- sqrt(yearlyfuzzykappasquared mean_of (each));
            model_fuzzykappa_sim <- sqrt(yearlyfuzzykappa_simsquared mean_of (each));
            model_PAD <- sqrt(yearlyPADsquared mean_of (each));
            model_paddyfieldresidual <- sqrt(yearlypaddyfieldresidualsquared mean_of (each));
            model_numberoffarmsresidual <- sqrt(yearlynumberoffarmsresidualsquared mean_of (each));
            optimizationmeasure <- model_paddyfieldresidual*model_numberoffarmsresidual;
            write "model_fuzzykappa: " + model_fuzzykappa;
            write "model_fuzzykappa_sim: " + model_fuzzykappa_sim;
            write "model_PAD: " + model_PAD;
            write "model_paddyfieldresidual: " + model_paddyfieldresidual;
            write "model_numberoffarmsresidual: " + model_numberoffarmsresidual;
            write "optimization measure: " + optimizationmeasure;
        }
      write "End of simulation. Duration: " + (machine_time - startt)/1000;
      stop_currentrun <- true;
      if !is_batch{
            //save grid_cell to:"../results/LCasc_calib.asc" type:"asc";
            //save grid_cell to:"../results/LCtif_calib.tif" type:"geotiff";
        save [nb_farmerhouseholds, ave_farmarea, Permanentlyabandonedarea, Paddyfieldarea
          ] to: "../results/Simulationresults.csv" type: "csv" rewrite: true header: true;
            do pause;
      }
   }

    action Updaterasterbandsandactualabandonment{
        int rindex <- int((current_year-startingyear)/5);
        if current_year = 2015{
            rindex <- 3;
        }
        int quickflowindex <- rindex + 6;
        int densforestindex <- 3*rindex + 1;
        int denslowvegindex <- 3*rindex + 2;
        int denspaddyindex <- 3*rindex + 3;
        ask factorsnondens{
            quickflow <- bands[quickflowindex];
        }
        ask factorsdens{
            densforest <- bands[densforestindex];
            denslowveg <- bands[denslowvegindex];
            denspaddy <- bands[denspaddyindex];
        }
}

action Effectofenvironmenttolivingconditions{
        list yearcolumn <- matrix_Tabledata column_at 0;
        int index <- yearcolumn index_of float(current_year);
        precipitation <- float(matrix_Tabledata[1,index]);
        max_temp <- float(matrix_Tabledata[2,index]);
```

```
        familysize <- float(matrix_Tabledata[3,index]);
        lifeexpectancy <- float(matrix_Tabledata[4,index]);
        erosion_rate <- parameter_precip_effect_on_erosion*(10.0^-10)*(precipitation^2);
        watersupply_rate <- (100.0*parameter_maxtemp_effect_on_watersupply)/(max_temp^2);
}


action Agentsactions{
        int nooffarmer <- 1;
        ask farmowner{
                do tillland;
                nooffarmer <- nooffarmer + 1;
        }
        ask farmowner where !each.newowner{
                do seeksuccesors;
                nooffarmer <- nooffarmer + 1;
        }
}


action Changesbasedonsmallscaleprocesses{
        nb_farmerhouseholds <- length(farmowner);
        ave_farmarea <- farmowner mean_of (each.farmarea);
        float formerpaddyfieldarea <- Paddyfieldarea;
        int formerpaddyfieldcount <- Paddyfieldcount;
        Paddyfieldarea <- farmowner sum_of (each.farmarea_stillpaddy);
        Paddyfieldcount <- int(Paddyfieldarea/900.0);
        Permanentlyabandonedarea <-  formerpaddyfieldarea - Paddyfieldarea;
        Permanentlyabandonedcount <- int(Permanentlyabandonedarea/900.0);
        PeriodicPermanentlyabandonedarea <-  PeriodicPermanentlyabandonedarea + Permanentlyabandonedarea;
        PeriodicPermanentlyabandonedcount <- int(PeriodicPermanentlyabandonedarea/900.0);
        add nb_farmerhouseholds to: yearlynb_farmerhouseholds;
        add Paddyfieldarea to: yearlypaddyfieldarea;
}

action Generationofnewlandusemap{
        ask grid_cell{
                if paddyfield{
                        paddyLUCCprob <- 1.0/(1.0+exp(-1.0*((coef_slope*factorsnondens(location).slope)+
                                (coef_cosaspect*factorsnondens(location).cosaspect)+
                                (coef_quickflow*factorsnondens(location).quickflow)+
                                (coef_disttowncenter*factorsnondens(location).disttowncenter)+
                                (coef_distroad*factorsnondens(location).distroad)+
                                (coef_heritage*factorsnondens(location).heritage)+
                                (coef_densforest*factorsdens(location).densforest)+
                                (coef_denslowveg*factorsdens(location).denslowveg)+
                                (coef_denspaddy*factorsdens(location).denspaddy))));
                }
        }
        float allocatedPermanentlyabandonedcount <- 0.0;
        write "PeriodicPermanentlyabandonedcount"+PeriodicPermanentlyabandonedcount;
        loop while: PeriodicPermanentlyabandonedcount != allocatedPermanentlyabandonedcount{
                float highestprob <- grid_cell
                                        where (each.paddyfield and each.paddyLUCCprob <= 1 and
each.paddyLUCCprob >= 0)
                                        max_of each.paddyLUCCprob;
                grid_cell highestprobcell <- (grid_cell where (each.paddyfield and each.paddyLUCCprob=highestprob))[0];
                highestprobcell.LCtype <- 4.0;
                highestprobcell.paddyfield <- false;
                highestprobcell.paddyfieldmodel <- 0.0;
                highestprobcell.grid_value <- 0.0;
                allocatedPermanentlyabandonedcount <- allocatedPermanentlyabandonedcount + 1;
        }
        PeriodicPermanentlyabandonedarea <- 0.0;
        PeriodicPermanentlyabandonedcount <- 0;
        ask grid_cell{
                if grid_value >= 0{
                        color <- rgb(255, 255*(grid_value),0);
                } else{
```

```
                color <- #black;
            }
        }
}

action Computeaccuracy_familysize{
        //compute numberoffarmers residual
        list yearcolumn <- matrix_numberoffarms column_at 0;
        int index <- yearcolumn index_of current_year;
        int actualnumberoffarms <- int(matrix_numberoffarms[1,index]);
        accuracy_numberoffarmsresidual <- actualnumberoffarms - nb_farmerhouseholds;
        write "Number of farms residual: " + accuracy_numberoffarmsresidual;
        add accuracy_numberoffarmsresidual to: yearlynumberoffarmsresidual;
}

action Computeaccuracy_LUCC{
        //compute fuzzy kappa value
        //int rindex <- int((current_year-startingyear)/5);
        int LCactualindex <- 0;
        if current_year = 1995{
                LCactualindex <- 1;
        } else if current_year = 2000{
                LCactualindex <- 2;
        } else if current_year = 2015{
                LCactualindex <- 3;
        } else if current_year = 2020{
                LCactualindex <- 4;
        }

        ask grid_cell{
                LCtype  <- bands[LCactualindex];
                paddyfield <- LCtype = 1 ? true:false;
                paddyfieldactual <- -1.0;
                if LCtype > 1.0{
                        paddyfieldactual <- 0.0;
                }
                if paddyfield{
                        paddyfieldactual <- 1.0;
                }
                if paddyfieldactual = 1.0{
                        cat_actual <- "Paddyfield";
                } else if paddyfieldactual = 0.0{
                        cat_actual <- "otherlandcover";
                } else{
                        cat_actual <- "NODATA";
                }
                realdata <- cat_actual = "NODATA" ? false: true;

                if paddyfieldmodel = 1.0{
                        cat_model <- "Paddyfield";
                } else if paddyfieldmodel = 0.0{
                        cat_model <- "otherlandcover";
                } else{
                        cat_model <- "NODATA";
                }
                if cat_model = "NODATA"{
                        realdata <- false;
                }
        }
        fuzzy_categories <- 0.0 as_matrix {length(categories),length(categories)};
        loop i from: 0 to: length(categories) - 1 {
                fuzzy_categories[i,i] <- 1.0;
        }
        fuzzy_transitions <- 0.0 as_matrix {length(categories)*length(categories),length(categories)*length(categories)};
        loop i from: 0 to: (length(categories) * length(categories)) - 1 {
                fuzzy_transitions[i,i] <- 1.0;
        }
```

```
list<float> similarity_per_agents ;
using topology(grid_cell) {
      accuracy_fuzzykappa <- fuzzy_kappa(grid_cell where each.realdata,
                                          grid_cell where each.realdata collect (each.cat_actual),
                                          grid_cell where each.realdata collect (each.cat_model),
                                          similarity_per_agents,
                                          categories,
                                          fuzzy_categories,
                                          60);
      accuracy_fuzzykappa_sim <- fuzzy_kappa_sim(grid_cell where each.realdata,
                                          grid_cell where each.realdata collect (each.cat_init),
                                          grid_cell where each.realdata collect (each.cat_actual),
                                          grid_cell where each.realdata collect (each.cat_model),
                                          similarity_per_agents,
                                          categories,
                                          fuzzy_transitions,
                                          60);

                                          /*
                                          fuzzy_kappa(list(cell),
                                          cell collect (each.cat_observed),
                                          cell collect (each.cat),
                                          similarity_per_agents,
                                          categories,
                                          fuzzy_categories,
                                          10);
                                          fuzzy_kappa_sim(list(cell),
                                          cell collect (each.cat_init),
                                          cell collect (each.cat_observed),
                                          cell collect (each.cat),
                                          similarity_per_agents,
                                          categories,
                                          fuzzy_transitions,
                                          10);
                                          *
                                          *
                                          *
                                          * */



}
list realcell <- grid_cell where each.realdata;
loop i from: 0 to: length(grid_cell where each.realdata) - 1 {
      int val <- int(255 * similarity_per_agents[i]);
      ask realcell[i]{
            color_fuzzy <- rgb(val, val, val);
      }
}

//compute PAD
loop c over: categories {
      nb_per_cat_actual << grid_cell count (each.cat_actual = c);
      nb_per_cat_model << grid_cell count (each.cat_model = c);
}
accuracy_PAD <- percent_absolute_deviation(nb_per_cat_actual,nb_per_cat_model);
//compute paddy field area residual
list fiveyearcolumn <- matrix_paddyfieldarea column_at 0;
int yindex <- fiveyearcolumn index_of current_year;
actual_paddyfieldarea <- float(matrix_paddyfieldarea[1,yindex]);
accuracy_paddyfieldresidual <- actual_paddyfieldarea - Paddyfieldarea;

//Add to accuracy lists
write "Fuzzy Kappa: " + accuracy_fuzzykappa;
write "Fuzzy Kappa simulation: " + accuracy_fuzzykappa_sim;
write "PAD: " + accuracy_PAD;
write "Paddy field residual: " + accuracy_paddyfieldresidual;
add accuracy_fuzzykappa to: yearlyfuzzykappa;
```

```
        add accuracy_fuzzykappa_sim to: yearlyfuzzykappa_sim;
        add accuracy_PAD to: yearlyPAD;
        add accuracy_paddyfieldresidual to: yearlypaddyfieldresidual;
}


}

species farmowner{
float farmarea;
float farmarea_stillpaddy;
list<float> farmarea_temporarilyabandoned;
int farmowner_age;
float convertedfrompaddy;
bool newowner;

        action createsuccesors{
        float childrennumber <- familysize - 2;
        create succesor number: int(rnd(childrennumber-0.5,childrennumber+0.5)){
                succesor_age <- farmowner_age - rnd(26, 35);
                totalincome <- rnd(8167.0,28167.0);
                decided <- false;
                migrated <- false;
                valuesheritage <- false;
                caninherit <- false;
        }
    }

    action tillland{
        list<float> cultivationdiff <- [0.0,0.0,0.0];
        float farmarea_eroded <- 0.0;
        float abandonedarea <- 0.0;
        if !governmentfixeserodedareas{
                float erodedland <- erosion_rate*abs(farmarea_stillpaddy);
                farmarea_eroded <- erodedland > abs(farmarea_stillpaddy) ? abs(farmarea_stillpaddy): erodedland;
                farmarea_stillpaddy <-  farmarea_stillpaddy - farmarea_eroded;
        }
        float wateredfield <- watersupply_rate*abs(farmarea);
        float maxareathatcanbetilled <- abs(farmarea);
        if farmowner_age >= 60 and farmowner_age <= 80{
                float fieldpercentagethatcanbetilled <- (80.0 - farmowner_age)/20.0;
                maxareathatcanbetilled <- fieldpercentagethatcanbetilled*abs(farmarea);
        }
        float harvestableland <- min([wateredfield,maxareathatcanbetilled,farmarea - farmarea_eroded]);
        if harvestableland <= abs(farmarea_stillpaddy){
                abandonedarea <- abs(farmarea_stillpaddy) - harvestableland;
                farmarea_temporarilyabandoned[2] <- abandonedarea;
                farmarea_stillpaddy <-  harvestableland;
        } else if harvestableland > abs(farmarea_stillpaddy){
                float recultivatedarea <- harvestableland - abs(farmarea_stillpaddy);
                cultivationdiff[0] <- farmarea_temporarilyabandoned[0] - recultivatedarea;
                if cultivationdiff[0] < 0{
                        cultivationdiff[1] <- farmarea_temporarilyabandoned[1] + cultivationdiff[0];
                        cultivationdiff[0] <- 0;
                }
                farmarea_temporarilyabandoned[0] <- cultivationdiff[0];
                farmarea_temporarilyabandoned[1] <- cultivationdiff[1];
                farmarea_stillpaddy <-  harvestableland;
        }
        farmarea <- farmarea - farmarea_eroded - farmarea_temporarilyabandoned[0];
        remove from: farmarea_temporarilyabandoned index: 0;
        add 0 to: farmarea_temporarilyabandoned;
        newowner <- false;
    }

  action seeksuccesors{
        farmowner_age <- farmowner_age + 1;
        bool hasinheritor <- false;
```

```
        ask succesor{
                succesor_age <- succesor_age + 1;
                if !decided{
                        if succesor_age >= 18{
                                totalincome <- totalincome + subsidyperfamilyhead;
                                valuesheritage <- flip(Valuesheritage_rate);
                                if (totalincome < parameter_threshold_succesorincome) and !valuesheritage{
                                        decided <- true;
                                        migrated <- true;
                                        caninherit <- false;
                                } else {
                                        decided <- true;
                                        migrated <- false;
                                        caninherit <- true;
                                }
                        }
                }
                if succesor_age >= 25 and caninherit{
                        hasinheritor <- true;
                }
        }
        if hasinheritor{
                int num_possibleinheritors <- succesor count each.caninherit;
                int num_inheritors <- num_possibleinheritors > 3 ? 3: num_possibleinheritors;
                list oldesttoyoungest <- reverse(succesor where each.caninherit sort_by each.succesor_age);
                loop inherittimes from: 0 to: num_inheritors-1{
                        create farmowner number: 1{
                                farmarea <- myself.farmarea/num_inheritors;
                                farmarea_stillpaddy  <- myself.farmarea_stillpaddy/num_inheritors;
                                farmarea_temporarilyabandoned <- [myself.farmarea_temporarilyabandoned[0]/num_inheritors,

        myself.farmarea_temporarilyabandoned[1]/num_inheritors,
                                                                        0];
                                farmowner_age <- oldesttoyoungest[inherittimes].succesor_age;
                                convertedfrompaddy <- myself.convertedfrompaddy/num_inheritors;
                                newowner <- true;
                                do createsuccesors;
                        }
                }
                do die;
        } else{
                if farmowner_age >= lifeexpectancy{
                        do die;
                }
        }
    }

species succesor {
        int succesor_age;
        float totalincome;
        bool decided;
        bool migrated;
        bool valuesheritage;
        bool caninherit;
}
}

grid grid_cell use_regular_agents: false files: [raster_file_LCactual1990,
                        raster_file_LCactual1995,
                        raster_file_LCactual2000,
                        raster_file_LCactual2015,
                        raster_file_LCactual2020
                        ]{
list<grid_cell> neighbours;
float LCtype;
bool paddyfield;
float paddyfieldactual;
```

```
float paddyfieldmodel;
float paddyLUCCprob;

//For accuracy
string cat_init;
string cat_actual;
string cat_model;
bool realdata;

//Visualization
rgb color_actual;
rgb color_modelled;
rgb color_fuzzy;
aspect actual{
        draw shape color: color_actual;
}
aspect modelled{
        draw shape color: color_modelled;
}
aspect fuzzy{
        draw shape color:color_fuzzy;
}
}

grid factorsnondens use_regular_agents: false files: [raster_file_LCactual1990, raster_file_slope,raster_file_cosaspect,
                        raster_file_disttowncenter, raster_file_distroad, raster_file_heritage,
                        raster_file_quickflow1990, raster_file_quickflow1995,
                        raster_file_quickflow2000, /*raster_file_quickflow2005,
                        raster_file_quickflow2010,*/ raster_file_quickflow2015
                        ]{
//abandonment probability factors
//constant
float slope;
float cosaspect;
float disttowncenter;
float distroad;
float heritage;
//changing
float quickflow;
}

grid factorsdens use_regular_agents: false files: [raster_file_LCactual1990, raster_file_densforest1990,
raster_file_denslowveg1990, raster_file_denspaddy1990,
                        raster_file_densforest1995, raster_file_denslowveg1995, raster_file_denspaddy1995,

                        raster_file_densforest2000, raster_file_denslowveg2000, raster_file_denspaddy2000,

                        //raster_file_densforest2005, raster_file_denslowveg2005, raster_file_denspaddy2005,
                        //raster_file_densforest2010, raster_file_denslowveg2010, raster_file_denspaddy2010,
                        raster_file_densforest2015, raster_file_denslowveg2015, raster_file_denspaddy2015
                        ]{
float densforest;
float denslowveg;
float denspaddy;
}

experiment Validation type: batch repeat: 15 keep_seed: true until: stop_currentrun{
parameter "Batch mode:" var: is_batch <- true;
parameter "Calibration mode:" var: is_calibration <- true;

int runnumber <- 1;
    reflex save_results_explo{
        write "Run"+runnumber+"ended";
        float mean_model_fuzzykappa <- mean(simulations collect each.model_fuzzykappa);
        float mean_model_fuzzykappa_sim <- mean(simulations collect each.model_fuzzykappa_sim);
        float mean_model_model_PAD <- mean(simulations collect each.model_PAD);
        float mean_model_model_paddyfieldresidual <- mean(simulations collect each.model_paddyfieldresidual);
```

160

```
        float mean_model_model_numberoffarmsresidual <- mean(simulations collect each.model_numberoffarmsresidual);
        float mean_model_optimizationmeasure <- mean(simulations collect each.optimizationmeasure);
        float mean_nb_farmerhouseholds <- mean(simulations collect each.nb_farmerhouseholds);
        float mean_ave_farmarea <- mean(simulations collect each.ave_farmarea);
        float mean_Paddyfieldarea <- mean(simulations collect each.Paddyfieldarea);
        float mean_Paddyfieldcount <- mean(simulations collect each.Paddyfieldcount);
        save [runnumber, parameter_precip_effect_on_erosion,parameter_maxtemp_effect_on_watersupply,
parameter_threshold_succesorincome, initialoldestfarmer,

        mean_model_fuzzykappa,mean_model_fuzzykappa_sim,mean_model_model_PAD,mean_model_model_paddyfieldre
sidual,mean_model_model_numberoffarmsresidual,mean_model_optimizationmeasure,
                nb_farmerhouseholds,mean_ave_farmarea,mean_Paddyfieldarea,mean_Paddyfieldcount
        ] to: "../results/Validation/Revised_Validation_fuzzysim_aggre2.csv" type: "csv" rewrite: false header: true;
        //save grid_cell to:"../results/Validation8_map2_asc_calib.asc" type:"asc";
        //save grid_cell to:"../results/Validation8_map2_tif_calib.tif" type:"geotiff";
    int simnumber <- 1;
    ask simulations {
        save [myself.runnumber, simnumber, self.model_fuzzykappa, self.model_fuzzykappa_sim, self.model_PAD,
self.model_paddyfieldresidual, self.model_numberoffarmsresidual, self.optimizationmeasure,
                self.nb_farmerhouseholds, self.ave_farmarea, self.Permanentlyabandonedarea, self.Permanentlyabandonedcount,
self.Paddyfieldarea, self.Paddyfieldcount,
                self.yearlyfuzzykappa, self.yearlyfuzzykappa_sim, self.yearlyPAD, self.yearlypaddyfieldresidual,
self.yearlynumberoffarmsresidual,
                self.yearlypaddyfieldarea, self.yearlynb_farmerhouseholds
         ] to: "../results/Validation/Revised_Validation_fuzzysim_ind2.csv" type: "csv" rewrite: false header: true;
        simnumber <- simnumber + 1;
    }
     runnumber <- runnumber + 1;
    }
}
```

# Dedication

I read once that in making decisions,

a foolproof way to know if we should do an action

is to think if our future self will thank us for doing it.

*Too shy to leave the party?* The tomorrow you will thank you if

you let him have enough social rest.

*Stuck in an unhappy relationship?* You six months from now will

be grateful if you give him a chance to find happiness again.

*Having doubts in taking a PhD?* Three-years-after you will give

you his deepest gratitude if you stand up to the challenge.

One night in 2022, I made a list of adjectives and nouns

that I want my future self to embody

I wrote down an oddly specific line:

*Highly cited professor in spatial modeling*

To my future self,

probably too far from now but one I have high hopes for,

I dedicate this dissertation to you.